Functional characterization of the basic helix-loop-helix transcription factor LeFER essential for upregulation of iron responses in tomato roots

Dissertation

zur Erlangung des Grades

der Doktorin der Naturwissenschaften

der Naturwissenschaftlich-Technischen Fakultät III

Chemie, Pharmazie, Bio- und Werkstoffwissenschaften

der Universität des Saarlandes

-Dr. rer. nat.-

von Frau Tzvetina Krassimirova Brumbarova

geboren am 05. 04. 1979

in Sofia, Bulgarien

Saarbrücken

Tag des Kolloquiums: 07.02.2007

Dekan: Univ.-Prof. Dr. rer.nat. Kaspar Hegetschweiler

Berichterstatter: Jun.-Prof. Dr. Petra Bauer

Prof. Dr. Rita Bernhardt

Dr. Hans-Peter Mock

Abstract

Iron (Fe) deficiency in humans is the most prevalent nutritional disorder in the world. Since plants serve as the primary source of dietary Fe, improving the Fe content of crops represents an important step towards a better public health. Tomato responds to low Fe availability by an enhanced proton extrusion from the root and upregulation of the genes encoding FeIII-chelate reductase (*LeFRO1*) and FeII transporter (*LeIRT1*). As a result, more Fe is rendered soluble and thus accessible for the plant. Previously, we identified the tomato gene *LeFER* as one of the major regulators of Fe uptake in the root under Fe-deficiency conditions. *LeFER* encodes a bHLH transcription factor that is responsible for the induction of Fe-mobilization genes. The aim of the presented work was to study upstream regulatory events of LeFER action, and the effects of LeFER function on the network of metabolic pathways in the cell under Fe-deficiency conditions. First, we examined the control of *LeFER* gene and LeFER protein expression in response to Fe-nutritional status in wild type, mutant plants with defects in Fe-uptake regulation, and 35S transgenic plants overexpressing *LeFER*. Both *LeFER* gene and LeFER protein were found consistently downregulated in roots after generous (100 µM, physiologically optimal) compared to low (0.1 µM) and sufficient (10 µM) Fe supply, and occasionally downregulated at sufficient compared to low Fe supply. Second, downregulation of LeFER by high Fe was found additionally controlled at posttranscriptional level. LeFER showed nuclear localisation and transcriptional activation in yeast. Third, LeFER protein regulation in the Fe-accumulation mutant *chloronerva* indicated that LeFER protein expression was not directly controlled by signals derived from Fe transport. Thus, we concluded that LeFER is able to affect transcription in the nucleus and its action is controlled by Fe supply at multiple regulatory levels. Fourth, we investigated the changes in the tomato root proteome when different plant genotypes were grown under different Fe-supply conditions (as indicated above). Using proteomics tools, differentially expressed proteins have been identified – dependent and independent on LeFER protein expression. Our data show major changes in the proteome as a result of exposure to low Fe in the medium, affecting an array of metabolic pathways ultimately involved in, among others, energy balance, stress response, and phytohormone signaling.

2

Abstrakt

Eisenmangel ist die häufigste Ernährungskrankheit von Menschen. Da Pflanzen die primäre Quelle von Eisen (Fe) in unserer Ernährung sind, sind Kulturpflanzen mit verbessertem Eisengehalt ein wichtiger Schritt in Richtung einer besseren Gesundheit der Bevölkerung. Tomatenpflanzen reagieren auf niedrige Eisenverfügbarkeit mit Erhöhung der FeII Konzentration in der Wurzelumgebung aufgrund der erhöhten Protonenausscheidung und der Induktion der FeIII-Chelatreduktase (LeFRO1) und des FeII Transporters (LeIRT1). Infolgedessen wird mehr Fe lösbar gemacht und steht der Pflanze zur Verfügung. Vorangegangene Arbeiten der Arbeitsgruppe haben *LeFER* als hauptsächliches Regulatorgen identifziert, welches die Eisenaufnahme in Wurzeln bei Eisenmangel kontrolliert. *LeFER* kodiert für einen Transkriptionsfaktor der basischen Helix-Loop-Helix Familie, welcher für die Induktion von Eisenmangelantworten verantwortlich ist. Ziel der vorliegenden Arbeit war es, oberhalb liegende Regulationsmechanismen von *LeFER* näher zu untersuchen, und die Auswirkungen der LeFER Funktion auf das Netzwerk von metabolischen Wegen in der Zelle unter Eisenmangel zu untersuchen. Zuerst untersuchten wir die Kontrolle der Expression des *LeFER* Gens und LeFER Proteins als Antwort auf den Eisenhaushalt in Wildtyp, Mutanten mit Defekten der Eisenaufnahmeregulation, und in 35S transgenen Pflanzen, welche *LeFER* überexprimieren. *LeFER* mRNA und LeFER Protein waren herunterreguliert in Wurzeln, die großzügig mit Fe versorgt waren (100 µM, physiologisch optimal) verglichen mit Wurzeln, die normal oder unterversorgt waren mit Fe (10 µM, 0.1 µM). Gelegentlich war eine niedrige Expression auch bei normaler Eisenversorgung zu sehen. Zweitens, wir haben gefunden, dass LeFER zusätzlich auf posttranskriptioneller Ebene herunterreguliert war durch viel Fe. LeFER zeigte Zellkernlokalisation und transkriptionelle Aktivierung in Hefe. Drittens, die LeFER Proteinregulation in der Eisenakkumulationsmutante *chloronerva* zeigte, dass LeFER Proteinexpression nicht direkt durch Signale des Eisentransports reguliert war. Wir schlussfolgerten, dass LeFER die Transkription im Zellkern beeinflusst, und seine Aktivität durch die Eisenversorgung auf verschiedenen Ebenen reguliert wird. Viertens, wir untersuchten Veränderungen im Tomate Wurzelproteom, wenn Pflanzen mit

unterschiedlichen Genotypen verschiedenen Eisenbedingungen ausgesetzt waren. Mit Proteomics Werkzeugen haben wir Proteine identifiziert, welche abhängig oder unabhängig von LeFER differentiell durch Fe exprimiert waren. Unsere Daten zeigten, dass große Veränderungen im Wurzelproteom als Antwort auf Eisenmangel auftreten, welche eine Reihe von metabolischen Wegen beeinflussten, die mit Energieversorgung, Stressantworten und Phytohormonsignalwegen in Verbindung stehen.

Contents

Contents

Contents

Contents

Contents

1. Introduction

Iron (Fe) is an essential nutrient for every organism. As a component of many vital enzymes, it is required for a wide range of biological functions, such as electron transport in the respiratory chain (e.g. cytochromes), DNA synthesis (e.g. ribonucleotide reductase), photosynthesis (e.g. chlorophyll synthesis and chloroplast structure/ function), nitrogen fixation (e.g. symbiotic root nodules establishment/ function) and hormone synthesis (e.g. lipoxygenase, ethylene precursor) (Briat and Lobreaux, 1997).

Fe deficiency is the world's most prevalent human nutritional disorder (WHO: http://www.who.int/nut/ida.htm). Although vegetables, for example spinach, are regarded as Fe rich, plant (nonheme) Fe is poorly absorbed – only 1.4 - 7% of the Fe from spinach can be taken into the body, compared to 20% from red meet (Scrimshaw, 1991). In many developing countries, the use of staple crops with naturally low Fe content can cause nutritional problems, especially when vegetables are the predominant food source. This effect can also be caused in plants with high Fe content such as legumes in the presence of antinutrients, such as oxalic acid or phytate that decrease the bioavailability of Fe (Hell and Stephan, 2003).

The foliar application of Fe chelators such as Fe-EDTA or Fe-EDDHA has been recommended to cure "Fe-chlorosis" – the yellowing of leaves as a result of Fe deficiency (Chen, 1997). These chemicals are, however, very expensive for extensive use. Fe deficiency of crops growing on calcareous soils can be cured to some extent with fertilizers. However, such treatments are costly and cannot be precisely targeted to the deficient parts of the plant, causing, in some cases, Fe excess followed by yield reduction.

To have significant impact on the Fe nutrition of humans, improvement strategies are under way to fortify crops with Fe. That is, to develop new varieties of major crops with increased amounts of bioavailable Fe.

In this respect, understanding the control of Fe-uptake mechanisms in plants is of vital importance for efficient Fe fortification efforts. It would help to address the Fe-deficiency problem in a better way leading to a specific and more effective solution.

1. Introduction

1.1. Bioavailability of Fe

Despite being generally present in high quantities in soils (the forth most abundant element in the lithosphere), Fe has a very limited bioavailability in aerobic and neutral pH environments. In aerobic soils, Fe is found predominantly in the form of FeIII, mainly as a constituent of oxyhydroxide polymers with extremely low solubility. Due to that, the equilibrium concentration of free FeIII in such environments is limited to approximately 10^{-17} M. Such a value is far below that required for the optimal growth of plants and microbes – 10^{-9} to 10^{-4} and 10^{-7} to 10^{-5}, respectively (Guerinot and Yi, 1994). The insufficient Fe availability can be particularly pronounced in plants grown on calcareous soils, which cover approximately one-third of Earth's surface. Therefore, without active mechanisms for extracting Fe from the soil, most plants would exhibit Fe-deficiency symptoms, such as chlorotic (yellowed) interveinal areas in young leaves and stunted root growth, which leads to reduced crop yields or even complete crop failure.

In contrast, in acidic, waterlogged soils, excess FeII can be toxic for the plants. It promotes the formation of reactive oxygen-based radicals that are able to damage vital cellular components (notably membranes, by lipid peroxidation), leading to a loss of integrity and possible cell death. Plants exposed to excessive levels of Fe show bronzing (coalesced tissue necrosis), flaccidity and/ or blackening of the roots (Schmidt, 1999).

As a consequence of these properties of solubility and toxicity, Fe homeostasis in the whole organism, as well as in the cells, must be balanced to supply enough Fe for cell metabolism and to avoid excessive, toxic levels. In this way, plants have evolved different mechanisms to control Fe uptake.

1.2. Strategies for Fe Uptake in Plants

As a strategy for restricting excessive uptake of Fe, wetland species have evolved mechanisms for oxidizing ferrous Fe (FeII) in the rhizosphere (Schmidt, 1999).

Plants, living under aerobic soil conditions, have developed two phylogenetically distinct strategies to cope with the extremely low availability of soluble Fe compounds (Marschner and Römheld, 1994). Dicots and nongraminaceous monocots employ an Fe-acquisition mechanism termed Strategy I based on the reductive detachment of Fe from its ligand. Under Fe-deficient conditions, such plants exhibit enhanced proton extrusion

1. Introduction

in the rhizosphere, increased FeIII-reduction capacity at the root surface, followed by an uptake of FeII via a ferrous transporter on the root plasma membrane (Römheld and Marschner, 1983). As a result, plants elevate the Fe availability in the rhizosphere and enhance its uptake.

In response to Fe deficiency, graminaceous monocots release high-affinity Fe-chelating substances from the mugineic acid family, called phytosiderophores (PS). These substances solubilize the inorganic FeIII compounds from the soil and the resulting FeIII-PS complexes are taken up by the root cells via a specific plasma membrane transport system without reduction of the FeIII ion. This mechanism is termed Strategy II (Römheld and Marschner, 1986) and it resembles the microbial siderophore system (Neilands, 1981).

1.3. Strategy I

Strategy I-type plants respond to Fe deficiency with both morphological and physiological changes (Römheld, 1987), which lead to an increased root surface area for reduction and transport of Fe. The changes in morphology include formation of root hairs, swelling of root tips, enhanced lateral root development and reduced lateral root growth (Schmidt, 1999) (Fig. 1).

1.3.1. Rhizosphere Acidification

A main physiological response to Fe deficiency is the increased acidification of the rhizosphere due to activation of a specific H^+-ATPase, which leads to extrusion of protons from the roots and aids in rendering more Fe soluble. This process can be quite fast – within a few hours the roots may lower the pH in the soil solution to values of 3 or lower. At the same time, a pH decrease of 1 releases 10^3 times more FeIII ions into the rhizosphere (Bienfait, 1985). This not only helps to acidify the extracellular space but it also has a pivotal role in establishing the electrochemical gradient (a proton moving force) that drives the uptake of solutes through their respective carriers and channels (Sussman, 1999). The capacity of a plant to acidify the rhizosphere in response to Fe deficiency depends to some extent on the cation/anion uptake balance and the nitrogen (N) nutrition of the plant. One member of the family of P-type H^+-ATPases, *AHA2*

1. Introduction

('*Arabidopsis* H$^+$-ATPase'), is most abundantly expressed in root hairs (Sussman, 1994) and may encode an isoform involved in the uptake of mineral nutrients (Fox and Guerinot, 1998).
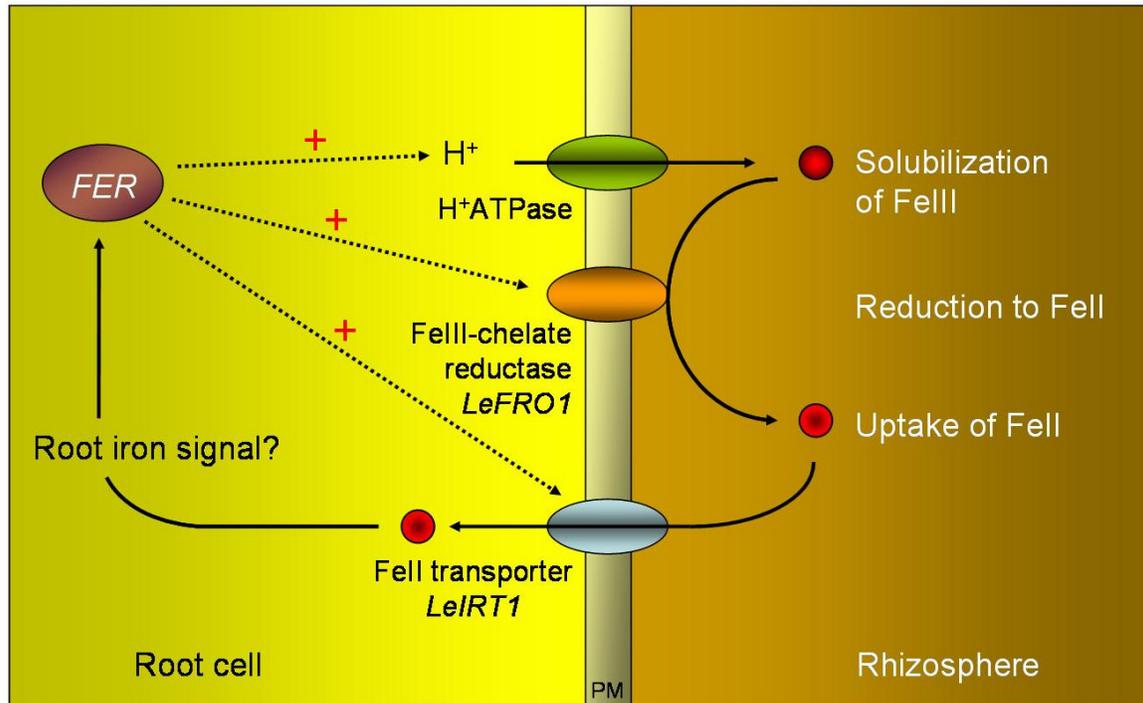
Figure 1: Strategy I for Fe uptake in plants.

The uptake of Fe in roots of dicots and nongraminaceous monocots is based on FeIII reduction and involves three distinct processes: (i) acidification of the rhizosphere through an H$^+$-ATPase activity, which solubilizes FeIII; (ii) reduction of FeIII to FeII through a plasma membrane-bound FeIII-chelate reductase (LeFRO1 in tomato); and (iii) uptake of FeII into the root epidermal cells through an FeII transporter (LeIRT1 in tomato). Fe deficiency is sensed by the roots and an yet unknown Fe signal triggers the expression of the bHLH transcription factor LeFER, which acts as a positive regulator of the above-described Strategy I components.

1.3.2. FeIII Reduction

The second and most typical physiological strategy I response to Fe deficiency is an enhanced FeIII reduction. It is thought to be the primary factor in making Fe available for absorption (Guerinot and Yi, 1994). Ferric reduction takes place at the plasma membrane

1. Introduction

of root epidermal cells. It catalyses transmembrane electron transport from cytosolic reduced pyridine nucleotides to extracellular Fe compounds serving as electron acceptors. This process is an obligatory prerequisite for Fe uptake in Strategy I plants and it is activated at insufficient Fe supply (Buckhout et al., 1989). Plasma membranes isolated from roots of Fe-deficient plants contained 2- to 3-fold higher specific activities for FeIII-chelate reductase than plasma membranes isolated from plants grown under Fe-sufficient conditions (Buckhout et al., 1989). The enzymatic activity of FeIII reductase in the root epidermal cells is additionally optimized by the pH decrease on the root surface, as a result of the H^+-ATPase activity, since the optimum pH of the plant membrane reductase is generally around 6 (Chaney et al., 1972).

1.3.3. Uptake of FeII

Fe is transported across the root plasma membrane as free FeII via a separate transporter acting downstream of the FeIII-chelate reductase. The capacity of uptake and translocation of Fe is greatly enhanced upon Fe starvation (Yi and Guerinot, 1996). In *Arabidopsis*, AtIRT1 functions as the major root transporter responsible for the uptake of FeII from the soil solution following the reduction of FeIII chelates by the plasma membrane reductase in response to Fe deficiency (Eide et al., 1996).

1.3.4. Genes Involved in the Mobilization of Fe in Strategy I Plants
1.3.4.1. Reductase Genes

AtFRO2 - The characterization of three allelic *Arabidopsis* mutants (*frd1-1*, *frd1-2* and *frd1-3*) which do not show induction of FeIII-chelate reductase under Fe-deficient conditions, confirms that Fe must be reduced prior to its transport and that FeIII reduction can be uncoupled from proton release (Yi and Guerinot, 1996). The reductive mechanism of Fe uptake by Strategy I plants shares many similarities with the high-affinity Fe-uptake system of yeast. This property has been successfully used to characterize the reductase/ FeII-transport system of plants at a molecular level.

The FeIII-chelate reductase gene *AtFRO2* has been cloned by Robinson *et al.* (1999) from Fe-deficient *Arabidopsis* roots, based on sequence similarity with the yeast *FRE*

1. Introduction

genes, and it was shown to map to *frd1-1*. When expressed in *frd1-1* mutant lines, it restores FeIII-reductase activity.

AtFRO2 is upregulated in roots under Fe-deficiency conditions (Robinson et al., 1999). *AtFRO2* mRNA was detected in root epidermal cells, similarly to observations for *AtIRT1* localization (see below). Additionally, a posttranscriptional level of control on *AtFRO2* gene expression was revealed by analysis on transgenic 35S::AtFRO2 plants, which failed to induce FeIII-reductase activity under sufficient Fe-supply conditions regardless of the constitutive expression of the gene (Connolly et al., 2003).

AtFRO2 shares similarities with human phagocytic NADPH gp91^{phox} oxidoreductase and with the yeast FeIII-chelate reductases, specifically in the heme- and nucleotide cofactor-binding sites. This is consistent with its function in electron transfer from cytosolic NADPH to extracellular FeIII. Therefore, AtFRO2 belongs to the superfamily of flavocytochromes that transport electrons across membranes (Robinson et al., 1999).

AtFRO2 belongs to an eight-member gene family in *Arabidopsis*. *AtFRO3* is also strongly induced upon Fe deficiency in roots, which suggests it has a similar function as *AtFRO2* (Wu et al., 2005). However, *AtFRO3* is predominantly expressed in the vascular cylinder, whereas *AtFRO2* is expressed at high levels in the outer layers of Fe-deficient roots, suggesting that FRO family members function in a variety of locations in the plant (Mukherjee et al., 2006).

In pea, **PsFRO1** represents the reductase involved in root Fe acquisition (Waters et al., 2002), supported by the observation that *PsFro1* mRNA levels in plants correlated with FeIII-chelate reductase activity. In contrast to *AtFRO2*, *PsFRO1* is expressed in both root and shoot (upregulated by Fe deficiency), suggesting an additional role in Fe distribution throughout the plant.

In tomato, the main FeIII-chelate reductase is encoded by *LeFRO1*, which is expressed in roots, leaves, cotyledons, flowers, and young fruits. The transcription intensity of *LeFRO1* in roots is dependent on the Fe status whereas it is constitutively expressed in leaves (Li et al., 2004). Two more genes, termed LeFRO-TC124302 and LeFRO-TC129233, were identified in tomato due to their sequence similarity to *AtFRO2*. LeFRO-TC124302 was expressed in a root-specific manner, slightly Fe regulated and dependent on a functional *LeFER* gene, but it was found to be specific to the *L.*

esculentum genome. A *L. esculentum* introgression line devoid of LeFRO-TC124302 had similar levels of FeIII-reductase activity as the wild type, indicating that LeFRO-TC124302 is not essential for FeIII reduction. All LeFRO-TC129233 EST sequences were derived from flower libraries, the gene was not detected in roots or shoots (Bauer et al., 2004b). This data additionally suggests that *LeFRO1* is the main gene responsible for FeIII-chelate reduction under Fe deficiency in tomato roots.

1.3.4.2. Transporter Genes

AtIRT1 – Expression of an *Arabidopsis* cDNA library into the yeast *fet3fet4* (*FERROUS TRANSPORTER*) double mutant strain, impaired in both low- and high-affinity Fe transport, enabled cloning of a plant FeII transporter by screening for complementation of the mutant phenotype (Eide et al., 1996). It was designated *AtIRT1* (*IRON-REGULATED TRANSPORTER*). The *AtIRT1* gene is not the equivalent of the *FET3* or *FET4* genes of *S. cerevisiae*. Instead, it encodes the founding member of a different class of eukaryotic metal ion transporters, referred to as the ZIP (ZRT, IRT-LIKE TRANSPORTERS) family (Guerinot, 2000), with related sequences in rice, yeast, nematodes and humans. It encodes a protein with eight transmembrane (TM) domains. Four histidine-glycine repeats constitute potential metal-binding sites between TM domains 3 and 4 (Eng et al., 1998).

In addition, AtIRT1 mediates uptake of MnII and ZnII in the yeast *smf1* and *zrt1zrt2* mutants, respectively defective in Mn and Zn transport, but cannot restore growth of the Cu uptake-deficient yeast mutant *ctr1*, implying that this transporter is not involved in the uptake of Cu (Korshunova et al., 1999). Inhibition of Fe uptake in AtIRT1-expressing yeast by excess of several transition metals such as Cd, Co, Mn and Zn was observed, showing that AtIRT1 is also able to transport CdII and CoII. The determinants for this broad substrate specificity of AtIRT1 have been investigated by site-directed mutagenesis (Rogers et al., 2000).

AtIRT1 expression is induced in roots of plants grown under Fe-deficiency (Eide et al., 1996; Connolly et al., 2002; Vert et al., 2002), suggesting a role of AtIRT1 in Fe uptake in planta. Such role has been demonstrated by the characterization of an *Arabidopsis irt1* knock-out mutant (Vert et al., 2002). The *irt1* mutant plant is chlorotic

1. Introduction

and has a severe growth defect in soil, leading to death, which can be rescued by the application of exogenous Fe, probably through the activity of not yet characterized low-affinity Fe transporters. Additionally, roots of the *irt1* mutant are defective in Fe uptake, and do not accumulate Zn, Cd, Mn, and Co under Fe-deficient conditions. This is in agreement with the observation that Fe-deficient plants have increased levels of root-associated Mn, Zn, Cd and Co, suggesting that, in addition to Fe, AtIRT1 mediates uptake of these metals into plant cells (Korshunova et al., 1999). The fact the AtIRT1 has plasma membrane localization in root epidermal cells supports a transporter function in Fe uptake from the soil. These lines of evidence for the function of AtIRT1 in planta have been confirmed by two other independently obtained *irt1* mutant lines (Henriques et al., 2002; Varotto et al., 2002). Thus, AtIRT1 is considered as the major Fe transporter at the root surface in *A. thaliana* (Vert et al., 2002).

AtIRT1 production is further regulated at the protein level as AtIRT1 protein accumulation is repressed by sufficient Fe and Zn. 35S::AtIRT1 transgenic plants express *AtIRT1* mRNA constitutively, but are unable, under Fe-deficient conditions, to produce AtIRT1 protein in any plant tissue except the root (Connolly et al., 2002). This additional level of control of *AtIRT1* expression provides the plant with an effective mechanism to switch off Fe-uptake activity when not needed.

AtIRT1 homologues have also been characterized in pea and tomato (Cohen et al., 1998; Eckhardt et al., 2001). The pea gene, called **PsRIT1**, is upregulated under Fe deficiency and complements both the *fet3fet4* and *zrt1zrt2* yeast mutants, thus potentially mediating high-affinity Fe and Zn uptake in plants.

In tomato, **LeIRT1** and **LeIRT2** are both expressed in roots but only *LeIRT1* appears to be strongly upregulated in response to Fe deficiency (Eckhardt et al., 2001). Both genes restore the growth defect of the *fet3fet4*, *zrt1zrt2*, and *smf1* yeast mutants (Eckhardt et al., 2001). However, the tomato genes are able to complement the Cu transport-deficient yeast strain *ctr1* whereas *AtIRT1* does not (Eide et al., 1996).

AtIRT2 – AtIRT2 is a gene belonging to the ZIP family and closely related to *AtIRT1*. AtIRT2 is able to transport Fe and Zn, but, unlike AtIRT1, it cannot transport Mn and Cd, when expressed in yeast (Vert et al., 2001). *AtIRT2* is expressed only in roots, in the same

1. Introduction

territories as *AtIRT1*, and is upregulated by Fe deficiency. However, both the level of expression of *AtIRT2* and its induction by Fe deficiency are much lower compared to *AtIRT1*. A null *irt2* mutant has no apparent phenotype, and overexpression of *AtIRT2* in *irt1* mutants does not rescue the *irt1* growth defect, which raises the question of the function of AtIRT2 in planta (Varotto et al., 2002; Vert et al., 2002).

AtNRAMPs – The *NRAMP* (*NATURAL RESISTANCE-ASSOCIATED MACROPHAGE PROTEIN*) gene family of metal transporters in *Arabidopsis* has seven members (Maser et al., 2001). Generally, *NRAMPs* are widely distributed throughout living organisms, functioning in the transport of a broad range of divalent metal cations, including Fe (Gunshin et al., 1997). Their name was derived from phagosomal NRAMP1 which functions as an efflux pump in the membrane and in this way enhances resistance against intracellular bacteria by reducing metal availability (Lafuse et al., 2000).

One of the seven *Arabidopsis* members, *AtEIN2*, is involved in ethylene response and its function in metal transport has not been demonstrated yet.

On the other hand, the role of AtNRAMP1, AtNRAMP3, and AtNRAMP4 in metal transport has been shown both in yeast and in planta (Curie et al., 2000; Thomine et al., 2000). In yeast, expression of *AtNRAMP1*, *AtNRAMP3*, or *AtNRAMP4* complements the phenotype of strains defective in Mn or Fe uptake. In addition, heterologous expression of *AtNRAMP3* or *AtNRAMP4* increases yeast sensitivity to Cd, indicating that these genes encode metal transporters with multiple specificities (Curie et al., 2000; Thomine et al., 2000).

In *Arabidopsis*, *AtNRAMP1*, *AtNRAMP2*, *AtNRAMP3*, and *AtNRAMP4* are expressed in both roots and shoots, but only the accumulation of *AtNRAMP1*, *AtNRAMP3*, and *AtNRAMP4* increases in roots in response to Fe deficiency (Curie et al., 2000).

AtNRAMP1 overexpression in plants confers increased resistance to toxic Fe levels (Curie et al., 2000). The closely related genes *AtNRAMP3* and *AtNRAMP4* share similar tissue-specific expression patterns, transcriptional regulation by Fe, and subcellular localization at the vacuolar membrane (Thomine et al., 2003; Lanquar et al., 2005). Although neither single mutant has a dramatic phenotype, the germination of *nramp3 nramp4* double mutants is arrested under low Fe nutrition and fully rescued by high Fe

supply (Lanquar et al., 2005). Additionally, mutant seeds have wild type Fe content, but fail to retrieve Fe from the vacuolar globoids. These results indicate that AtNRAMP3 and AtNRAMP4 function redundantly in the mobilization of Fe from the vacuole during early seed development. *AtNRAMP3* and *AtNRAMP4* are currently the most likely candidates to control the active (re)mobilization of metals to and from the vacuolar pool.

The tomato homologues of *AtNRAMP1* and *AtNRAMP3*, **LeNRAMP1** and **LeNRAMP3** (Bereczky et al., 2003), respectively, encode functional NRAMP metal transporters in yeast, where they were shown to be Fe regulated and localized mainly to intracellular vesicles. *LeNRAMP1*, in contrast to *LeNRAMP3*, has a root-specific expression and is strongly upregulated by Fe deficiency. Additionally, *LeNRAMP1* was expressed in the vascular root parenchyma. A role for LeNRAMP1 in Fe compartmentalization within the plant but not in Fe uptake from the soil was suggested (Bereczky et al., 2003).

AtYSL – A search for homologues of the maize *YS1* gene in *Arabidopsis* identified eight genes, named *YSL* (*YELLOW STRIPE-LIKE*) (Curie et al., 2001). Since nongraminaceous plants do not synthesize or secrete PS, it was suggested that YSL proteins mediate the uptake of metals that are complexed with plant-derived PS or nicotianamine (NA) (Colangelo and Guerinot, 2006). NA is produced in all plants and has the ability to bind Fe (von Wiren et al., 1999). Based on sequence similarity to ZmYS1, *A. thaliana* has eight predicted AtYSL proteins. Two family members, *AtYSL1* and *AtYSL2* have recently been studied in some detail.

AtYSL1 is a shoot-specific gene, expressed in the xylem parenchyma of leaves, whose transcript levels increase in response to Fe excess (Le Jean et al., 2005). Based on the phenotype of the *ysl1* mutant, a role of AtYSL1 in long-distance circulation of Fe and NA and their delivery to the seed was suggested.

AtYSL2 transports FeII and CuII when these metals are chelated by NA. *AtYSL2* is expressed in many cell types in both shoots and roots, such as the xylem-associated cells within the vasculature of expanded leaves (DiDonato et al., 2004), and in the pericycle and endodermis of the roots (Schaaf et al., 2005), suggesting that diverse cell types obtain metals as metal-NA complexes. *AtYSL2* transcript accumulation increases under conditions of Fe sufficiency or Fe resupply (DiDonato et al., 2004; Schaaf et al., 2005),

and responds also to Cu (DiDonato et al., 2004) and Zn (Schaaf et al., 2005). Based on its expression pattern and its apparent protein localization in lateral membranes (DiDonato et al., 2004), a major function of AtYSL2 might be in the lateral transport of metals in the vasculature, most probably through the plant veins (DiDonato et al., 2004). The *ysl2-1* single mutant does not have an obvious phenotype which may reflect functional redundancy within the *Arabidopsis* YSL family (DiDonato et al., 2004).

AtIREG2 – Another class of transporters involved in the intracellular distribution of Fe might be represented by AtIREG2 (or AtFPN2). AtIREG1, 2, and 3 are related by sequence to the animal IRON-REGULATED PROTEINS (IREGs), also called FERROPORTINS (FPNs) (Schaaf et al., 2006), for which a function in Fe export has been demonstrated, as for example for the mammalian *IREG1* gene (McKie et al., 2000). *AtIREG2* is involved in Fe-dependent Ni detoxification in the roots. Its expression is clearly upregulated under Fe deficiency and localized in the tonoplast in Arabidopsis (Schaaf et al., 2006).

AtFRD3 – The *Arabidosis frd3* mutant, also isolated as *man1* (Delhaize, 1996), is unable to turn off the root FeIII-reductase activity at sufficient Fe supply (Yi and Guerinot, 1996). *frd3* accumulates a variety of metals, such as Fe and Mn, due to the upregulation of *AtIRT1* (Delhaize, 1996).

The *AtFRD3* gene has a root-specific expression, and encodes a transmembrane protein belonging to the MULTIDRUG AND TOXIN EFFLUX TRANSPORTERS (MATE) family (Rogers and Guerinot, 2002). AtFRD3 was shown to function in Fe localization in Arabidopsis by loading of an Fe chelator in the root xylem necessary for efficient Fe uptake out of the xylem or apoplastic space and into leaf cells (Green and Rogers, 2004). It has recently been suggested that the Fe chelator transported by AtFRD3 is citric acid (Durrett et al., 2006).

1.3.4.3. Nicotianamine (NA)

The tomato mutant *chloronerva* accumulates high levels of Fe (Stephan and Scholz, 1993) and behaves as if it is always experiencing Fe deficiency, even when grown under Fe-sufficient conditions. Among the typical symptoms of Fe deficiency is the characteristic interveinal chlorosis in young leaves. On the other hand, the Fe-uptake

1. Introduction

mechanisms in the mutant, including proton extrusion and reductase activity, are constitutively expressed. As a result, it accumulates too much Fe in its shoots, leading to retarded growth and development of necrotic spots on the leaves. Grafting the *chloronerva* mutant onto wild type or vice versa normalizes the mutant phenotype, indicating that it is due to the lack of a transportable substance (Ling et al., 1999).

The observed abnormalities in *chloronerva* have been correlated with a deficiency in NA synthesis (Stephan and Grün, 1989) due to a mutation in the gene *LeNAS* encoding the enzyme NA synthase (NAS) that converts S-adenosyl methionine to NA (Ling et al., 1999). The *LeNAS* gene has been mapped to the long arm of chromosome 1 (Ling et al., 1996) and later isolated by map-based cloning (Ling et al., 1999).

chloronerva is an NA auxotroph – application of NA to the roots or leaves of mutant plants leads to their phenotypic recovery (Stephan and Scholz, 1993). It was thought that in *chloronerva* cells Fe is unable to react with the sensor protein without the aid of NA, leaving the repressor unsaturated and Fe uptake to continue in excess of cellular needs (Scholz et al., 1992). This could explain why the NA-free mutant suffers from apparent Fe deficiency and fails to repress inducible Fe-uptake processes (Stephan and Scholz, 1993).

On the molecular level, lack of NA in the *chloronerva* mutant results in induced expression of *LeIRT1* and *LeNRAMP1*, compared with wild type, despite sufficient Fe supply. This upregulation was found dependent on the presence of a functional *LeFER* gene. Thus, it was concluded that LeNAS is required for the proper Fe-dependent regulation of *LeIRT1* and *LeNRAMP1* (Bereczky et al., 2003).

NA occurs in all plants and chelates metal cations, including Fe. Its role as a mediator of Fe transport in the phloem could also explain the various phenotypes of the *chloronerva* mutant (Stephan et al., 1994; 1996). Evidence for this is that the concentrations of NA in the phloem correlate with those of Fe and other metals, and that the NA-free mutant *chloronerva* has a phenotype indicative of Fe deficiency (Stephan and Scholz, 1993; Pich and Scholz, 1996). It was also shown that NA chelates both FeII and FeIII, and role for NA in scavenging Fe for protecting the cell from oxidative damage, resulting from the Fenton reaction, was proposed (von Wiren et al., 1999). Additional evidence in support of such a role was provided by the cellular distribution of

1. Introduction

NA in response to the Fe status of both pea and tomato plants – while under Fe deficient (0 µM) and normal (10 µM) Fe supply NA was mainly present in the cytoplasm, in Fe-loaded plants (100 µM) most of the NA was present in the vacuole, indicating the possible importance of vacuolar sequestration in the detoxification of excess Fe (Pich et al., 2001).

Additional evidence for the role of NA was obtained from transgenic tobacco plants that constitutively expressed the barley *HvNAAT* gene (Takahashi et al., 2003). In graminaceous plants, NAAT catalyzes the amino group transfer of NA for the biosynthesis of phytosiderophores (see **1.4. Strategy II**). In this way, the transgenic plants experienced NA shortage, which caused disorders in internal metal transport, leading to interveinal chlorosis of young leaves (similar to the *chloronerva* phenotype) and abnormally shaped and sterile flowers. These findings demonstrated the essential role of NA in growth, flower development, and fertility in plants (Takahashi et al., 2003).

1.3.4.4. Other Known Mutants Impaired in Strategy I Response

Several plant mutants are known to exhibit increased rates of Fe uptake irrespective of Fe supply. The genes responsible for these mutant phenotypes could represent important components of the Fe-response pathway, however they are not yet identified.

brz - The pea mutant *brz* (*bronze*) accumulates high levels of Fe (Kneen et al., 1990) (Welch and Kochian, 1992) similar to the tomato mutant *chloronerva*. The *brz* mutant develops bronze necrotic spots on its leaves probably due to the 50-fold increased leaf-Fe content compared to leaves of wild type plants. The basis for the excessive Fe accumulation appears to be the increased FeIII reduction and FeII uptake regardless of plant Fe status (Grusak et al., 1990). The *brz* mutant also accumulates high levels of other divalent cations (MgII, MnII, ZnII). The *brz* mutation is monogenic, recessive and maps to chromosome 4 (Kneen et al., 1990).

dgl - Similar phenotype is observed for the *dgl* (*degenerated leaflets*) mutant in pea (Grusak and Pezeshgi, 1996). It also has an increased capacity to acidify the rhizosphere. Reductase studies using plants with reciprocal shoot:root grafts demonstrated that shoot expression of the *dgl* gene leads to the generation of a transmissible signal that enhances FeIII reductase activity in roots. The *dgl* gene product may alter or interfere with a

1. Introduction

normal component of a signal transduction mechanism regulating Fe homeostasis in plants (Grusak and Pezeshgi, 1996).

1.3.4.5. Ferritin

Due to the potential of free Fe for causing damage in the cell through radical formation, plants need to regulate its uptake and store it in a safe and soluble form. Two important compartments involved in this function are the apoplastic space and the vacuoles (Briat et al., 1995). The ferritins, a class of multimeric proteins, also act as an Fe buffer inside the cell (Harrison and Arosio, 1996). The importance of ferritin function is emphasised by its ubiquitous distribution among living species – plants, animals, fungi and bacteria.

1.4. Strategy II

Strategy II plants are characterized by the release of phytosiderophores (PS) (e.g. mugineic acid (MA) in barley and avenic acid in oat) which efficiently solubilize inorganic FeIII by chelation, and by the induction of a high-affinity uptake system for FeIII-PS complexes that transports the FeIII chelates as intact molecules (Römheld, 1987). Both processes are induced in response to Fe deficiency through upregulation of the underlying genes (Fig. 2).

This strategy is considered to be more efficient than Strategy I; a good illustration for this is the fact that grasses can grow on calcareous soils which do not support the growth of dicots. One reason for this may be that Strategy II is less pH dependent than Strategy I (Guerinot and Yi, 1994).

Knowledge of the Strategy II Fe-acquisition mechanism has increased considerably since the discovery of PS in washings from the roots of Fe-deficient rice and oats (Takagi, 1976; 1993). It was found that PSs are structurally related to NA. Later, it became evident that NA is an intermediate in the biosynthesis of the mugineic acid family of PS. Although NA is produced by both monocots and dicots, the subsequent steps leading to MAs synthesis are specific to grasses. The critical enzyme in this specific pathway is nicotianamine-aminotransferase (NAAT) (Shojima et al., 1990; Ohata et al., 1993; Kanazawa et al., 1994; 1995) that catalyzes the transfer of an amino residue to NA,

1. Introduction

resulting in the production of 2'-deoxymugineic acid (DMA), the precursor of all other MAs (Shojima et al., 1990). Subsequent hydroxylation of DMA results in the formation of other members of the MA family (Nakanishi et al., 1993; Okumura et al., 1994; Nakanishi et al., 2000).
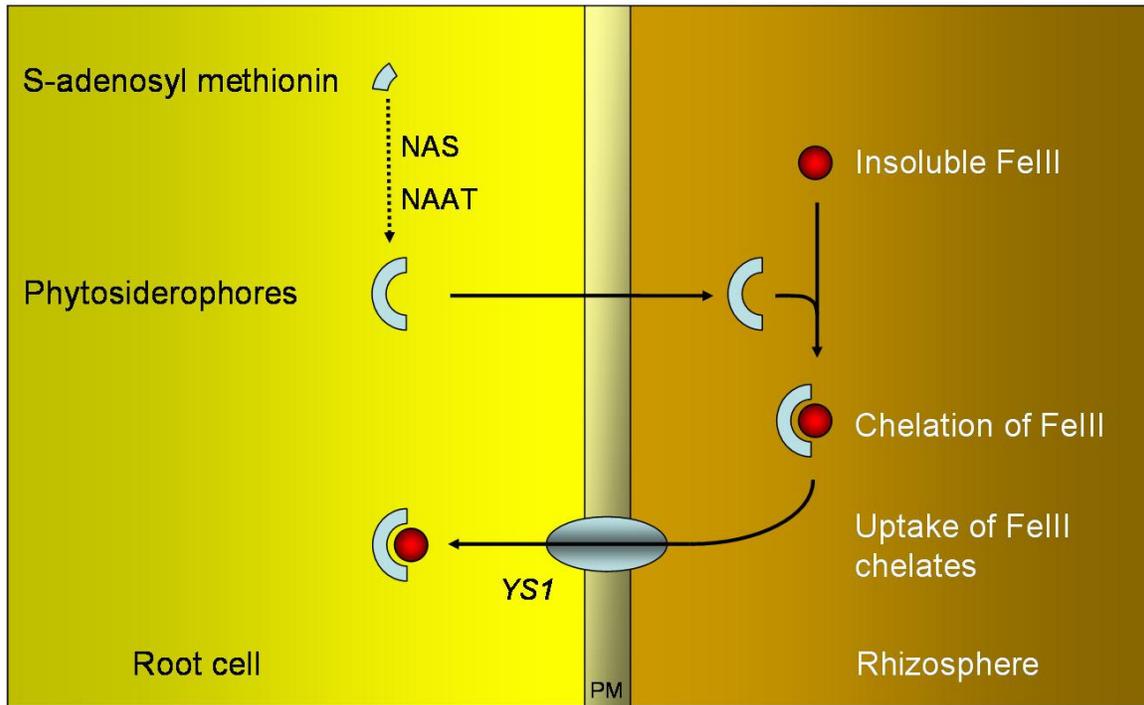
Figure 2: Strategy II for Fe uptake in plants.

The uptake of Fe in roots of graminaceous monocots is based on FeIII chelation and involves two distinct processes: (i) biosynthesis of FeIII-chelating substances – phytosiderophores from S-adensyl methionin through the enzymatic activity of nicotianamine synthase (NAS) and nicotianamine aminotransferase (NAAT), and excretion of PS into the rhizosphere, where they chelate FeIII from insoluble compounds; and (ii) uptake of FeIII-PS complexes into the root epidermal cells through a specific transporter (YS1 in maize).

The uptake of FeIII-PS complexes in Strategy II plants occurs through a specialized transporter. The gene encoding for this transporter was discovered by investigating the *yellow-stripe 1* (*ys1*) mutant of maize, which is unable to respond to Fe deficiency due to a defect in the uptake of FeIII-PS complexes (Von Wiren et al., 1994). The *ZmYS1* gene encodes a plasma membrane protein from the OLIGOPEPTIDE TRANSPORTER (OPT)

1. Introduction

family (Yen et al., 2001). Both *ZmYS1* mRNA and protein are upregulated by Fe deficiency in roots and shoots, where ZmYS1 functions as a proton-coupled symporter to transport FeIII-PS and FeIII-NA (Curie et al., 2001; Roberts et al., 2004; Schaaf et al., 2004).

1.5. Fe Transport Throughout the Plant and Systemic Signaling

Generally speaking, accumulation of a given metal is a function of uptake capacity and intracellular binding sites. In a multicellular organism, the situation is complicated by tissue- and cell-specific differences and also by intercellular transport. The processes that are assumed to influence metal accumulation rates in plants are the following: mobilization and uptake from the soil, compartmentation and sequestration within the root, efficiency of xylem loading and transport, distribution between metal sinks in the aerial parts, sequestration and storage in leaf cells. At every level, concentration and affinities of chelating molecules, as well as the presence and selectivity of transporters, affect metal accumulation rates (Clemens et al., 2002).

The uptake of Fe in the plant starts in the apoplast of the root epidermal cells (Bienfait et al., 1985). Once taken up into the root symplast, Fe has to be shielded from oxygen to prevent precipitation and generation of oxygen radicals. For this purpose, it is assumed to be chelated by NA for several reasons: (i) NA forms stable complexes with both Fe oxidation states at neutral and weakly alkaline pH (Stephan et al., 1996), (ii) NA is ubiquitous in higher plants in all tissues (Scholz et al., 1992), (iii) Fe-NA complexes are relatively poor Fenton reagents (von Wiren et al., 1999), and (iv) NA concentrations correlate with localization and levels of Fe (Pich et al., 2001).

Radial transport of Fe from the root epidermis to the xylem vessels is most probably occurring as an FeII-NA complex on a symplastic route (Stephan et al., 1996).

Fe is loaded in the xylem sap and translocated into the aerial parts of the plant through the transpiration stream. This process is mediated by xylem parenchyma or transfer cells and represents a separate control point for nutrient transport to the shoot (Schurr, 1999). The role of YSL transporters in loading Fe from the cortical cells to the xylem has been suggested (Colangelo and Guerinot, 2006). Organic acids, especially citrate, are the main metal chelators in the xylem (White et al., 1981) and it is generally

1. Introduction

agreed that Fe is oxidized when released into the xylem vessels and then transported as an FeIII-citrate complex (Tiffin, 1966; Lopez-Millan et al., 2000).

Further up in the shoot, Fe is unloaded from the xylem into the apoplastic spaces of leaf mesophyll cells. The uptake of FeIII by leaf mesophyll appears to depend on a reduction step via a plasma membrane-bound FeIII-chelate reductase, which most likely releases FeII from FeIII citrate (Brüggemann et al., 1993). There is also some evidence that FeIII reduction *in vivo* may be aided by intermediate superoxide radical formation or by strong blue light (Brüggemann et al., 1993). In pea and tomato, *PsFRO1* and *LeFRO1*, respectively, are also expressed in leaves and induced by Fe deficiency (Waters et al., 2002; Li et al., 2004), making them good candidates for an FeIII reductase in the leaf.

The distribution of Fe from the cells adjacent to the veins to the leaf lamina is probably again mediated by an Fe-NA complex, because in the NA-deficient mutant *chloronerva* most of the Fe is deposited along the veins. As a result, a characteristic interveinal chlorosis develops (Stephan and Scholz, 1993).

Fe moves from source to sink tissues via the phloem sap. NA is one of the potential phloem metal transporters (Stephan and Scholz, 1993). It binds preferentially FeII, and not FeIII, in the phloem sap (von Wiren et al., 1999). There is a low but significant steady-state concentration of FeII in the phloem (Maas et al., 1988). The bulk of Fe in the phloem is in the form of FeIII and chelated by the IRON TRANSPORT PROTEIN (ITP) (belonging to the Late Embryogenesis Abundant (LEA) family) (Krueger et al., 2002). It is suggested that NA plays a role in loading and unloading Fe in the phloem by chelating FeII in the transition to and from FeIII-ITP complexes. The YSL transporters are good candidates for transporting FeII-NA in and out of the phloem. A reductase should also be involved in the process, oxidizing FeII from NA for binding to ITP, and reducing FeIII from ITP for binding to NA.

For the induction of Fe-deficiency responses, small amounts of extracellular Fe are more favourable than no Fe. For example, increased reductase activity was found in *Glycine max* roots supplied with 0.32 μM Fe relative to those supplied with 0.1 μM (Chaney et al., 1972). Similar results have been reported for various species (Jolley et al., 1986; Miller and Olsen, 1986; Stephan and Grün, 1989). Likewise, in mutants that are

1. Introduction

characterized by increased Fe-deficiency responses (such as *chloronerva*, for example), higher reductase activity is observed with normal amounts of Fe relative to Fe-free grown plants (Stephan and Grün, 1989; Grusak et al., 1990; Grusak and Pezeshgi, 1996). A stimulation of the Fe uptake system by low, non-zero, Fe concentrations may be advantageous in ecological terms.

Besides sensing changes in Fe supply in the rhizosphere, plants are able to monitor the shoot Fe status and to send a signal from the shoot to the root to activate uptake mechanisms. The identity of this signal is still unknown but it is believed to be transmitted by the phloem (Maas et al., 1988). Candidates are plant hormones, Fe-complexes or redistributed Fe (Hell and Stephan, 2003).

When split-root plants were grown continuously with a localized supply of Fe, an increase in reduction rates was evident in the Fe-supplied portion of the root system. Apparently, the reductase activity of the Fe-supplied roots is controlled by the shoot Fe requirement, compensating for the decreased percentage of roots participating in Fe acquisition (Schmidt et al., 1996).

The regulation of the root high-affinity Fe-uptake system by whole-plant signals was investigated in *Arabidopsis*, through monitoring the gene expression of the root FeIII-chelate reductase *AtFRO2* and the high-affinity Fe transporter *AtIRT1* (Vert et al., 2003). Split-root experiments indicated that the expression of *AtFRO2* and *AtIRT1* is controlled by a local induction from the root Fe pool and through a systemic pathway involving a shoot-borne signal, both signals being integrated to tightly control production of the root Fe uptake proteins. Additionally, the expression of *AtFRO2* and *AtIRT1* is diurnally regulated (expressed during the day and downregulated at night) but this level of control can be overruled by Fe starvation (Vert et al., 2003).

In summary, information trafficking between different plant parts appears to be of crucial importance for the regulation of appropriate internal concentrations of Fe in higher plants. Although root cells are capable of sensing intracellular and possibly external Fe concentrations and of inducing Fe-deficiency responses, this control can be overruled by shoot-derived signals. This is most obvious in cases where, despite adequate external Fe concentrations, either the translocation or the uptake of Fe by leaf cells is

inhibited or a high demand for shoot growth is clear (e.g. when Fe supply is locally restricted as in the case of split-root plants) (Schmidt, 1999).

1.6. Regulation of Fe-Uptake Components

Plants have to cope with two problems during acquisition of Fe for their needs. On one hand, it is the low bioavailability of Fe in the soils which often causes Fe deficiency in the plant. On the other hand, Fe can be highly toxic for the cells if it is not properly chelated and compartmentalized. For these reasons, coordination of Fe uptake processes according to the growth requirements of the plant is of vital importance for its survival, and is thus under tight regulation. This regulation occurs at several different levels.

1.6.1. Transcriptional Regulation

Many of the biological processes in a plant are regulated at the level of transcription. Changes in gene expression have been shown to underlie the response to environmental cues and stresses (such as light, temperature, and nutrient availability), the defense response against pathogens, and many more. In plants, as well as in animals, development is based on the cellular capacity for differential gene expression (Benfey and Weigel, 2001). Alterations in gene expression are also emerging as a major source of the diversity and change that underlie the morphological evolution of eukaryotic organisms (Tautz, 2000). In particular, morphological changes that occurred during plant domestication and crop improvement in agriculture have been associated with mutations in transcription factors (Peng et al., 1999), alterations in their expression (Wang et al., 1999), or changes in the expression of other types of regulatory proteins (Frary et al., 2000).

The proteins involved in transcription in eukaryotes can be classified into four different functional groups: (1) the basic transcription apparatus and intrinsic associated factors (also known as general transcription factors); (2) large multi-subunit coactivators and other cofactors; (3) sequence-specific DNA-binding transcription factors; and (4) chromatin-related proteins. In contrast to the components of the basal transcription machinery, which in general are highly conserved, coregulators and transcription factors have diverged largely among eukaryotes (Lemon and Tjian, 2000).

1. Introduction

In plants, the maintenance of Fe homeostasis is so far mainly described on the level of gene expression. A mechanism similar to the IRE/IRP control in animals has not been described yet.

1.6.1.1. *LeFER* Gene

The first identified regulator of Fe nutrition in plants is the *LeFER* gene in tomato (Ling et al., 2002).

The chlorotic tomato Fe-inefficient mutant *fer* (T3238*fer*) (Fig. 3A) is unable to respond to Fe deficiency by switching on Strategy I responses, including the enhanced proton extrusion in the rhizosphere, the increase in FeIII-chelate reductase activity, and the FeII uptake. Thus, the mutant is unable to survive on FeIII in soil. However, if supplied with the Fe complex FeHEDTA at high concentrations, or grafted onto wild-type rootstock, the plant develops normally (Brown et al., 1971; Brown and Ambler, 1974). Reciprocal grafting of the mutant to a wild type indicated that the *LeFER* gene is required in the root but not in the shoot (Brown et al., 1971).

Genetic analysis showed that the *fer* mutation is a monogenic recessive trait, which could be mapped to the center of chromosome 6 (Ling et al., 1996). The *LeFER* gene was isolated by map-based cloning, and was predicted to encode a basic helix-loop-helix (bHLH) protein (Fig. 3B) that is required for induction of Fe-mobilization responses in tomato roots (Ling et al., 2002).
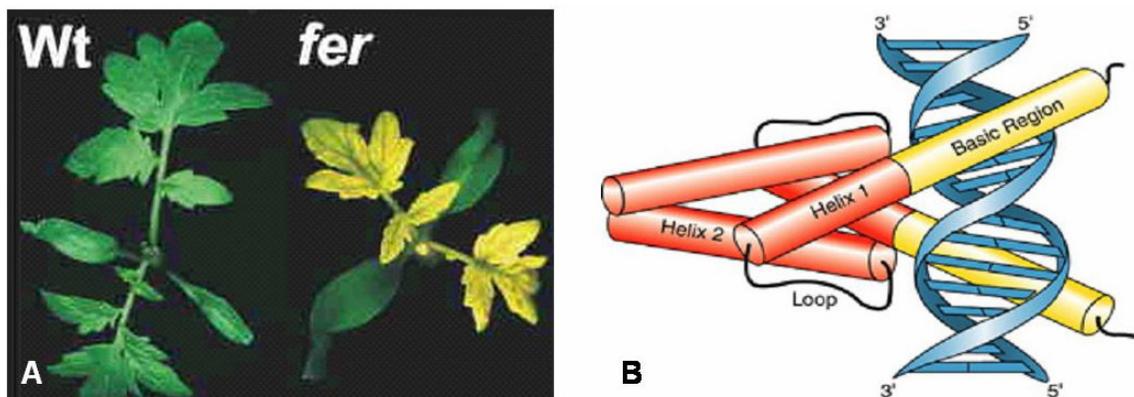
Figure 3: *fer* mutant and the regulator of Fe uptake in tomato, *LeFER*.

1. Introduction

(A) The tomato *fer* mutant exhibits severe leaf chlorosis and retarded growth compared to wild type (Wt) plants, since it is unable to switch on Strategy I responses under Fe-deficient conditions. (B) The gene responsible for the *fer* mutant phenotype, *LeFER*, belongs to the bHLH family of transcription factors. A schematic representation of the highly conserved bHLH domain, which is generally involved in DNA binding.

The *fer* mutation is due to the presence of a large DNA insertion at the end of *LeFER* gene exon 1. The effects of the mutation at low and sufficient Fe supply were shown to be both on physiological and morphological level (Ling et al., 2002). *fer* mutants exhibited reduced FeIII-reductase capacity and *LeIRT1* expression level compared to wild type plants. Morphologically, *fer* mutant plants showed lower number of root hairs on the lateral root tips, and significantly reduced root weight due to inhibited lateral root growth. *LeFER* gene expression was detected in roots and root tips, and at a lower level in hypocotyls of seedlings, but not in cotyledons or leaves. No significant difference in the expression level was observed when plants were subjected to either low or sufficient Fe supply. Furthermore, an *in situ* hybridization analysis on root transverse sections revealed differential *LeFER* mRNA localization throughout the length of the root. In the dividing root zone where no vasculature is developed yet, *LeFER* was detected in the epidermis and outer cortical cell layers. In the elongation zone where vasculature starts to differentiate, *LeFER* was mainly observed in the epidermis cells. In the mature root-hair zone, *LeFER* transcripts were restricted to the vascular cylinder between the xylem and the phloem. This pattern was found similar at low and sufficient Fe supply. Due to the incapability of the *fer* mutant to switch on the Fe-deficiency response on either morphological, physiological, or gene expression level, it was concluded that the primary defect in the mutant is caused by a regulatory deficiency (Ling et al., 2002).

The expression of the tomato FeIII-chelate reductase gene *LeFRO1* (Li et al., 2004), and that of the transporter genes *LeIRT1* and *LeNRAMP1* (Bereczky et al., 2003) was shown to be downregulated in the roots of *fer* mutant plants, suggesting that *LeFER* acts upstream of the Fe-uptake machinery. Additionally, *LeNRAMP1* expression colocalized with that of *LeFER* in the vascular parenchyma. However, the *LeFER* gene was not

1. Introduction

sufficient for inducing *LeIRT1* and *LeNRAMP1* when ectopically expressed (Bereczky et al., 2003), suggesting additional level(s) of regulation acting upon LeFER function.

Furthermore, a double mutant of *fer* and *chloronerva* has been characterized (Ling et al., 1996). The severe phenotype, together with a significantly decreased expression of *LeIRT1* and *LeNRAMP1* in those mutant plants, suggest a synergistic effect of the lack of *LeFER* and *LeNAS* genes. Interestingly, expression levels of both *LeIRT1* and *LeNRAMP1* were elevated in the *chloronerva* mutant despite sufficient Fe supply and the presence of a functional *LeFER* gene (Bereczky et al., 2003), suggesting that NA is required for the proper regulation of the two genes.

In an attempt to identify membrane-localized proteins under the control of LeFER, Bienfait (1988) has performed a comparison of two-dimensional protein gel on membrane fractions of wild type and *fer* mutant plants. At least two membrane proteins that are produced under Fe-deficiency conditions in tomato roots were found to absent in the *fer* mutant. However, due to technical reasons, identification was not possible at the time. Since then, no further proteomic studies on the response in tomato roots to Fe deficiency have been performed.

Recently, the *LeFER*-like regulator of Fe uptake in *Arabidopsis* was cloned and is known respectively as **AtFIT1** (Fe-DEFICIENCY INDUCED TRANSCRIPTION FACTOR 1), **AtFRU** (FER-LIKE REGULATOR OF IRON UPTAKE), or **AtBHLH29** (Colangelo and Guerinot, 2004; Jakoby et al., 2004; Yuan et al., 2005). Throughout the following chapter the gene is named acording to the origin of the data discussed. Of the 162 predicted bHLH proteins in *Arabidopsis* (Heim et al., 2003; Toledo-Ortiz et al., 2003), *AtFIT1* is the closest homologue to the tomato *LeFER* gene (Colangelo and Guerinot, 2004), and it can functionally complement the tomato *fer* mutant (Yuan et al., 2005). *AtFRU* was shown to be necessary for upregulation of Fe mobilization genes, suggesting that Fe uptake is controlled by conserved regulatory genes in dicots (Jakoby et al., 2004).

AtFIT1 mRNA, similar to observations for *AtFRO2* and *AtIRT1*, was detected in the outer cell layers of the root and accumulated in response to Fe deficiency. *fit1* mutant plants are chlorotic and need Fe supplementation in order to survive. These plants also accumulated less Fe than wild type in roots and shoots. Microarray analysis revealed

1. Introduction

many genes under the control of *AtFIT1*, which are either novel or implicated in Fe homeostasis (Colangelo and Guerinot, 2004).

In a parallel study, Jakoby et al. (2004) analysed the function of *AtFRU*, and could show that the gene was mainly expressed in roots in a cell-specific pattern and induced by Fe deficiency. However, some of the obtained results regarding *AtFRO2* and *AtIRT1* expression levels differed from the ones reported by Colangelo and Guerinot (2004), probably due to differences in the growth conditions and mutant alleles used. Jakoby et al. (2004) showed that in *fru* knockout plants, *AtFRO2* and *AtIRT1* gene expression was downregulated, whereas in *AtFRU* overexpression lines it was induced upon low Fe supply in roots and/or in leaves. The gene expression results were paralleled by FeIII-reductase and chlorophyll measurements.

Both *LeFER* and *AtFRU* genes appear to play similar roles in their respective systems in controlling Fe-deficiency responses in the root (Colangelo and Guerinot, 2004; Bauer et al., 2004a; 2004b). Both, *LeFER/AtFRU/ATFIT1* are essential and act upstream in inducing the *AtFRO2/AtIRT1* system in roots. The *BHLH* genes are themselves up-regulated by low Fe supply although this up-regulation is not as strong as that of *AtIRT1*. Overexpression studies showed that LeFER and AtFRU can enhance Fe-uptake responses but only at low Fe supply suggesting additional posttranscriptional activation by low Fe or inactivation by high Fe (Bereczky et al., 2003; Jakoby et al., 2004).

The superfamily of bHLH transcription factors is conserved from yeast to mammals. bHLH proteins are the second largest transcription factor family in plants and govern a wide range of biological processes (Riechmann et al., 2000). The conserved bHLH domain consists of approx. 18 hydrophilic and basic amino acids comprising the basic region, which permits binding to DNA at the hexanucleotide E-box sequence 5'-CANNTG-3'. Two stretches of hydrophobic residues separated by a loop region form two amphipathic α-helices and allow these proteins to form homo- and/or heterodimers (Voronova and Baltimore, 1990; Toledo-Ortiz et al., 2003).

Expression of the *Arabidopsis* Fe-deficiency response genes *AtFRO2*, *AtIRT1*, *AtIRT2*, and *AtNRAMP1*, *AtNRAMP3*, *AtNRAMP4* is controlled by Fe status at the level of transcript accumulation. Their mRNAs accumulate in roots in response to Fe

deficiency and are rapidly switched off by Fe resupply (Eide et al., 1996; Curie et al., 2000; Connolly et al., 2002). The same holds true for the tomato genes *LeFRO1*, *LeIRT1*, and *LeNRAMP1* (Bereczky et al., 2003; Li et al., 2004).

1.6.1.2. Other Transcriptional Regulators in Plants

A putative bHLH transcription factor gene, named **OsIRO2**, has been identified by using a rice 22K oligo-DNA microarray as strongly expressed in both roots and shoots during Fe deficiency. Expression of the barley homologue of *OsIRO2*, *HvIRO2*, was also found induced by Fe deficiency, and an *in silico* search revealed that IRO2 is highly conserved among graminaceous plants. The binding sequence of OsIRO2 (5'-CACGTGG-3') was determined, and similar sequences were found in the promoter regions of several genes involved in Fe acquisition, such as *OsNAS1*, *OsNAS3*, *OsIRT1*, *OsFDH*, *OsAPT1*, and *IDS3*, suggesting that OsIRO2 is involved in the regulation of these genes under Fe-deficient conditions (Ogo et al., 2006).

The control of gene expression through transcription factors is exerted through *cis*-regulatory elements contained in the promoter regions of the respective genes. Studies on the genes involved in Fe-deficiency responses in various plants have identified Fe-responsive *cis*-elements, such as the 16bp-long **IDRS** (Iron-Dependent Regulatory Sequence), conserved among Arabidopsis and maize, and found in the promoters of ferritin genes. IDRS was shown to be responsible for the downregulation of ferritin under Fe deficiency (Petit et al., 2001).

Two *cis*-acting elements, **IDE1** and **IDE2** (Iron-Deficiency Responsive Element) were identified in the promoter of the barley *HvIDS2* (*Iron-Deficiency Specific clone 2*) gene (Kobayashi et al., 2003), which encodes a dioxygenase involved in the hydroxylation of the PS deoxymugineic acid (DMA) (Nakanishi et al., 2000). These two elements were found responsible for the induction of *HvIDS2* by Fe deficiency. IDE sequence homologues were also found in the promoter regions of other Fe-inducible genes, such as *HvNAAT*, *HvNAS1*, *HvIDS3*, *OsNAS1*, *OsNAS2*, *OsIRT1*, *AtIRT1*, and *AtFRO2*, suggesting the conservation of Fe-responsive *cis*-regulatory elements among various genes and species (Kobayashi et al., 2003).

1. Introduction

Using homologous sequences in the promoter regions of *HvIDS2* and *HvIDS3* as a bait, a Yeast One-Hybrid screen has yielded a novel DNA-binding gene, which encodes a putative basic leucine-zipper transcription factor. Its expression was found upregulated during the early stages of Fe deficiency, making it a good candidate for a regulator of Fe-deficiency responses in barley (Itai et al., 2004; Von Wiren, 2004).

1.6.2. Posttranscriptional Regulation

Many plant species possess strategies to endure abiotic stresses, and to respond to challenges from pathogens. Although these responses are frequently regulated at the transcriptional level, there is extraordinary diversity in the posttranscriptional mechanisms that promote developmental plasticity and adaptation. The function of many plant genes is known to be controlled posttranscriptionally (Bailey-Serres, 1999).

Posttranscriptional regulation can be exerted in several different ways, such as alternative splicing, mRNA turnover control, protein modifications, targeted protein degradation.

It is suggested that at least 5 % of all predicted genes in Arabidopsis are alternatively spliced (Kazan, 2003; www.plantgdb.org/ASIP). The great majority of such genes encode proteins with regulatory functions (http://www.tigr.org/tdb/e2k1/ath1/altsplicing/splicing _variations.shtml). In addition, the genes associated with various stress responses, especially with abiotic stress, seem to be particularly prone to alternative splicing (Kazan, 2003). One such example is presented by the regulation of the relative abundance of two splicing forms of the *AtSOS4* (*Salt Overly Sensitive 4*) gene by salt stress (Shi et al., 2002).

The rate of mRNA turnover, which is the half-life of normal (nonaberrant, nonviral) mRNAs, provides a major posttranscriptional step to regulate gene expression (Wilusz and Wilusz, 2004). The importance of mRNA turnover is revealed by the phenotypes of plants in which the expression of genes involved in controlling mRNA stability has been disrupted. For example, the Arabidopsis mutant for *Downstream 1*, which regulates the mRNA stability of *Cinnamoyl CoA reductase-like* (*CCR*) and *Senescence-associated gene 1*, have defects in their circadian rhythm (Lidder et al., 2005).

1. Introduction

Over the past few decades, numerous reversible and irreversible covalent modifications that alter protein activity, location, state, and/or turnover have been recognized as prominent players in the regulation of gene function. Examples include phosphorylation, methylation, acetylation, myristylation, ADP ribosylation, and glycosylation. Both biochemical data and the number of protein kinase/phosphatase genes present in plant genomes point to phosphorylation as a dominant modifier (Callis and Vierstra, 2000). Recently, however, polypeptide tags also have emerged to be important posttranslational regulators of protein function. Among them are ubiquitin (Ub), RUB-1 (related to Ub-1; also known as NEDD8), SUMO (small Ub-like modifier), ATG-8 (autophagy-8) and ATG-12, UFM-1 (Ub-fold modifier-1) and HUB-1 (homology to Ub-1) (Downes and Vierstra, 2005). The best known is Ub (ubiquitin) that serves as reusable tag for selective protein degradation by the 26 S proteasome and for endosomal trafficking. Genomic analyses indicate that Ub pathway alone comprises over 6% of the Arabidopsis proteome with thousands of proteins being targets (Downes and Vierstra, 2005). Consequently, this pathway influences much of plant biology (Hatakeyama and Nakayama, 2003). Preliminary studies for the rest of the above mentioned polypeptide tags indicate that these tags have much more limited sets of targets and provide more specialized functions, including transcriptional regulation, protein localization, autophagic turnover and antagonizing the effects of Ub. On the basis of their widespread distribution and pervasive functions, peptide tags can now be considered as prime players in plant cell regulation (Downes and Vierstra, 2005).

In the context of Fe-deficiency response regulation, several genes are known to be controlled posttranscriptionally. However, the detailed mechanisms of these regulatory processes still remain to be elucidated.

For two of the major genes involved in Fe uptake, *AtIRT1* and *AtFRO2*, an additional posttranscriptional level of control was observed (Connolly et al., 2002; Connolly et al., 2003). *35S:AtIRT1* transgenic plants were shown to accumulate higher levels of Cd and Zn compared to wild type, indicating a successful overexpression of the gene. However, although *AtIRT1* mRNA was expressed constitutively in these plants, AtIRT1 protein was present only in the roots when Fe is limiting, suggesting that the expression of *AtIRT1* is

controlled posttranscriptionally (Connolly et al., 2002). A regulation of *AtIRT1* expression by ubiquitination under sufficient Fe/Zn conditions has been hypothesized, due to the high degree of sequence similarity between AtIRT1 and the Zn-regulated yeast transporter ZRT1 (Zhao and Eide, 1996; Connolly et al., 2002). ZRT1 was shown to be posttranscriptionally regulated via Zn-mediated ubiquitination (Gitan et al., 1998; Gitan and Eide, 2000).

AtFRO2, together with *AtIRT1*, was found induced under Fe starvation and coordinately repressed following Fe resupply. *AtFRO2* mRNA was detected at high levels in the roots and shoots of *35S:AtFRO2* transgenic plants. However, FeIII-chelate reductase activity was only elevated in the overexpressing plants under conditions of Fe deficiency, indicating that AtFRO2 is subject to posttranscriptional regulation, as shown for AtIRT1 (Connolly et al., 2003; Vert et al., 2003).

1.6.3. Transcriptional and Posttranscriptional Regulation by Fe in Other Organisms

1.6.3.1. Fe Uptake Regulation in Bacteria

In bacteria, the expression of a large number of genes – more than 90 in some cases (Hantke, 2001) is directly controlled by the prevailing intracellular concentration of FeII via its complexing to a regulatory protein (the FUR protein or equivalent). In this way, the biochemistry of the bacterial cell can accommodate the challenges from the environment or the host (Ratledge and Dover, 2000).

The **FUR** (FERRIC UPTAKE REGULATOR) protein, present in gram-negative and certain gram-positive bacteria, and the **DtxR** (DIPHTHERIA TOXIN REPRESSOR) protein, in gram-negative bacteria, repress gene transcription when loaded with FeII (Hantke, 1981; Boyd et al., 1990; Schmitt and Holmes, 1991).

FUR regulates also other genes in addition to those involved in Fe acquisition. Fe availability regulates various toxins and other virulence determinants (Litwin and Calderwood, 1993), presumably because a lack of Fe signals the pathogen that it is likely to be inside its host organism.

1.6.3.2. Fe Uptake Regulation in Yeast

In yeast, homeostatic control of cellular Fe uptake is mediated by the key transcriptional activator **AFT1** (ACTIVATOR FERROUS TRANSPORT), which binds to a consensus sequence present in the promoters of its target genes (Yamaguchi-Iwai et al., 1995; 1996). Under Fe-deficiency conditions, AFT1 induces transcript accumulation of *FRE1*, *FRE2*, *FET3*, *FTR1* and other genes that are Fe-uptake components in yeast (Yamaguchi-Iwai et al., 1996; Eide, 1998). By contrast, in Fe-replete cells, AFT1 does not bind to its target *cis*-element. It was shown that the Fe-regulated DNA binding by AFT1 is not due to a change in the expression level of the protein or to alteration of its DNA binding activity (Yamaguchi-Iwai et al., 2002). Instead, AFT1 has different intracellular localization based on the Fe status of the cell. Under Fe-limited conditions it is located within the nucleus where it activates its target genes. Under Fe-sufficient conditions, AFT1 is in the cytoplasm and thus kept "inactive". Furthermore, it was suggested that the nuclear export of AFT1 is critical for ensuring Fe-responsive transcriptional activation of the AFT1 regulon and that the nuclear import/export systems are involved in Fe sensing by AFT1 in *S. cerevisiae* (Yamaguchi-Iwai et al., 2002).

Based on its amino acid sequence, AFT1 may directly bind an Fe atom and therefore acts as an Fe sensor in the cytoplasm, reaching the nucleus only when not bound to Fe as a result of low Fe status (Yamaguchi-Iwai et al., 2002). Alternatively, since AFT1 can be phosphorylated (Casas et al., 1997), the intracellular Fe status may modify the phosphorylation state of AFT1, thus controlling its localization in the cell.

In the fission yeast *Schizosaccharomyces pombe*, **FEP1** is required for downregulation of genes encoding components of the reductive Fe transport machinery. It exerts its repressor function by binding to a conserved regulatory element upstream of the genes encoding the cell surface FeIII reductase (*FRP1*), and the two-component Fe-transporting complex (*FIP1* and *FIO1*) (Pelletier et al., 2002). Additionally, FEP1 represses the expression of the Fe-siderophore transporter STR1 under Fe-sufficient conditions, and thus occupies a central role in coordinating transcriptional regulation of genes encoding components of the reductive and non-reductive Fe-transport systems in fission yeast (Pelletier et al., 2003).

1. Introduction

A recent study by Puig et al. (2005) has elucidated coordinated global metabolic reprogramming in response to Fe deficiency and identified a mechanism for achieving this by targeting specific mRNA molecules for degradation. In response to Fe deficiency, the *Saccharomyces cerevisiae* **Cth2** protein was shown to specifically downregulate mRNAs encoding proteins that participate in many Fe-dependent processes. mRNA turnover requires the binding of Cth2 to specific AU-rich elements in the 3' untranslated region of mRNAs targeted for degradation.

1.6.3.3. Fe Uptake Regulation in Mammals

In mammals, the signal and regulatory mechanisms that orchestrate the expression of the proteins involved in Fe uptake, storage, utilization, and export have been best studied on the posttranscriptional level of control.

IRE/IRP – In animals, expression of the different players in Fe homeostasis is regulated posttranscriptionally, via the IRE/IRP system (Klausner et al., 1993). **IRP1** and **IRP2** (IRON-RESPONSIVE PROTEIN) are Fe-sensing RNA-binding proteins that bind to the **IRE** (iron-responsive element) sequence present in the 5' or 3' untranslated regions (UTRs) of several genes involved in Fe homeostasis. IREs are conserved hairpin structures found in the UTRs of Fe-related mRNAs. IRP binding in the 5'-UTR of ferritin H and L chains and ferroportin mRNAs inhibits translation. In contrast, binding of IRPs to IREs in the 3'-UTR of the transferrin receptor 1 (TfR1) and NRAMP2 mRNAs stabilizes the transcripts (Hentze and Kühn, 1996; Rouault and Klausner, 1997; Schneider and Leibold, 2000; Hentze et al., 2004).

Although the genes encoding IRP1 and IRP2 are highly homologous (Rouault and Klausner, 1997), they sense cytosolic Fe levels by different mechanisms. IRP1 is a bifunctional protein. When cellular Fe is high, IRP1 binds a 4Fe-4S cluster and functions as a cytoplasmic aconitase, interconverting citrate and isocitrate, without an RNA-binding ability. Under these conditions, transferrin receptor (TfR) mRNA is degraded and ferritin mRNA is translated. When cellular Fe is low, loss of the 4Fe-4S cluster allows IRP1 apoprotein to bind IREs with high affinity, resulting in TfR mRNA transcript stabilization, and prevention of ferritin mRNA translation (Beinert et al., 1996). Unlike

IRP1, IRP2 undergoes Fe-dependent degradation in Fe-replete cells (Guo et al., 1995). It can bind heme, triggering oxygen-dependent oxidation, ubiquitination by the E3 ubiquitin-protein ligase HOIL1, and degradation by the proteasome (Kang et al., 2003; Yamanaka et al., 2003). Thus, neither IRP binds to IREs when cellular Fe is high.

The activities of the two IRPs are only partially redundant, and it was shown that they occupy different regulatory niches. In normal physiology, tissue oxygen tension determines the contribution of each IRP to the regulation of Fe homeostasis. At the ambient oxygen concentrations in tissues of healthy animals, the Fe-S cluster of IRP1 appears to be stable, and IRP1 is therefore poorly suited to function as an Fe sensor (Meyron-Holtz et al., 2004a). In contrast, IRP2 has a different mechanism of Fe sensing that relies on Fe-dependent degradation (Guo et al., 1995). Fe-dependent turnover is intact at physiologically relevant oxygen concentrations, which enables IRP2 to dominate normal regulation of Fe homeostasis in mammals (Meyron-Holtz et al., 2004b).

1.6.3.4. Possibilities for Regulation of Transcription Factors

Since transcription factors are the proteins responsible for regulating cellular processes, it is interesting and important to know in turn how their own expression and function are regulated. This regulation can occur through different mechanisms, such as transcriptional regulation by other transcription factors, posttranscriptional regulation through protein-protein interactions, protein modifications, protein stability control, etc.

A very well studied example of transcriptional regulation of transcription factors is presented by the genes involved in meristem maintenance and lateral organ specification. They were shown to be regulated in part by negative interactions between the Myb-domain transcription factor *ASYMMETRIC LEAVES1*, which is expressed in lateral organ primordia, and homeobox transcription factors which are expressed in the shoot apical meristem (KNOX genes). The KNOX gene *SHOOT MERISTEMLESS* (*STM*) negatively regulates *ASYMMETRIC LEAVES1* (*AS1*) which, in turn, negatively regulates other KNOX genes including *KNAT1* and *KNAT2* (Byrne et al., 2002; Iwakawa et al., 2002).

1. Introduction

Several examples of posttranscriptional modulation of transcription factor function through direct interactions between different transcription factors have been reported in Arabidopsis. In addition to increasing the regulatory repertoire, direct interactions between transcription factors are one of the mechanisms by which proteins with very similar DNA binding domains might achieve regulatory specificity (see, for example, Grotewold et al., 2000). Direct interactions can occur between members of the same protein family, to form dimeric complexes that bind to palindromic DNA sequences, or between transcription factors of different families. Examples of the latter include Arabidopsis, maize, and petunia proteins of the MYB and bHLH families (Hobo et al., 1999; Nakamura et al., 2001).

Posttranscriptional regulation on the level of protein stability has been shown for several transcription factors. Recent research in the field of auxin signaling, for example, has discovered a diverse array of posttranscriptional control mechanisms. In 2005, three groups reported independently that auxin homeostasis and related developmental processes in Arabidopsis depend on microRNA-mediated regulation of key components of auxin signaling. The effects of auxin on plant development are mediated by several transcription factor families, including the auxin response factors (ARFs) and NAC-domain transcription factors. First, ARGONAUTE1 (AGO1), a key player in microRNA pathways, was shown to regulate auxin-induced adventitious root formation associated with its effect on the expression of *AUXIN RESPONSE FACTOR17* (*ARF17*) and auxin-inducible *GH3* genes that are presumed targets of ARF17 (Sorin et al., 2005). Second, Mallory et al. (2005) show that plants expressing a form of *ARF17* that is resistant to transcript cleavage mediated by the microRNA miR160 produce high levels of *ARF17* mRNA and have altered accumulation of *GH3*-like mRNAs associated with numerous dramatic growth defects. Finally, it was shown that miR164-directed cleavage of *NAC1* mRNA affects auxin regulation of lateral root development, suggesting that microRNA-mediated regulation may function in maintaining auxin homeostasis (Guo et al., 2005).

Another interesting example of posttranscriptional control of transcription factors is also coming from research on auxin action, making auxin signaling research a good representative of the complexity of regulatory mechanisms occuring in plants. Cloning of the *TRANSPORT INHIBITOR RESPONSE 1* (*AtTIR1*) gene (Ruegger et al., 1998)

1. Introduction

revealed that it encodes an F-box protein, the specificity factor of the SCF (for Skp1p, Cdc53p/cullin, and F-box protein in yeast and mammals) class of ubiquitin E3 ligases (Deshaies, 1999). AtTIR1 was shown to interact with the Arabidopsis Skp1-like proteins, AtASK1 and ASK2, and the cullin AtCUL1 to form a functional SCF^{AtTIR1} degradation complex (Gray et al., 1999; Gray et al., 2001), which targets the Aux/IAA family of transcription factors (Kepinski and Leyser, 2002).

An interesting example of complex transcription factor regulation comes from research on oxygen sensing in mammals, which is also linked to cellular Fe levels, and shows the regulatory connection between signal perception and effects on a transcription factor function. The cellular hypoxic response includes the transcriptional activation of genes involved in angiogenesis, erythropoiesis and anaerobic metabolism. This response is mediated by the transcription factors HIF1α (HYPOXIA INDUCIBLE FACTOR) and HIF2α (Iliopoulos et al., 1996). Under normal oxygen tension, HIF is rapidly targeted for proteasomal degradation through an interaction with the von Hippel-Lindau (VHL) tumor suppressor. When oxygen levels become limiting, this interaction is disrupted and HIF accumulates in local regions of hypoxia (Cockman et al., 2000). Interestingly, the bHLH-PAS (basic helix–loop–helix Per/Sim/Arnt) transcription factor HIF1α is composed of two subunits, an oxygen-sensitive and a constitutively expressed one (Wang et al., 1995; Wang and Semenza, 1995). The oxygen-sensitive subunit becomes stabilized in response to hypoxia, Fe chelators, and divalent cations. Under normoxic conditions, hydroxylation of this subunit is essential for HIF proteolytic degradation. As oxygen levels decrease, hydroxylation of HIF also decreases and it becomes stabilized. Interestingly, the hydroxylase activity was found dependent on the cellular availability of both oxygen and FeII (Schofield and Ratcliffe, 2004).

2. Aim of the Project

Plants are the primary source of Fe for humans and understanding the mechanisms that underlie plant Fe homeostasis is of interest for addressing agricultural problems, and Fe malnutrition in humans. Great progress has been made in recent years towards describing the general strategies for Fe uptake in different plant species, and identifying and characterizing the genes responsible for these processes. Since these events need to be strictly regulated in space and time, an extensive effort is underway for identifying the regulators of Fe uptake. Genetic analyses in tomato led to the identification of *LeFER* (Ling et al., 2002) – the single known Fe uptake regulatory gene in plants.

The goal of our project was to investigate the regulation of LeFER and the mechanism of its action. This is of critical importance not only for basic science but also from a biotechnological point of view with respect to potential applications of the acquired knowledge for improving the bioavailablity of Fe in crops. To achieve this goal we have defined four specific aims.

First, the regulation of *LeFER* on transcriptional level should be addressed by using gene expression profiling on different plant genotypes (*fer* mutant, wild type, 35s1 overexpressing line) grown under varying Fe-supply conditions.

Second, the possibility of posttranscriptional control of LeFER should be investigated by using anti-LeFER antisera for protein level determination and immunolocalization on the same plant genotypes and growth conditions.

Third, the mode of action of LeFER protein might be dependent on direct Fe sensing and interaction(s) with other proteins. To address this, Fe binding assays and screening for LeFER interaction partners in a heterologous yeast system should be performed.

Fourth, understanding the function of LeFER at a broader molecular level should be achieved by investigating the changes in the tomato root proteome with respect to *LeFER* presence and Fe availability. This would reveal its role in the crosstalk of different metabolic and signaling pathways in the plant.

3. Materials and Methods

3.1. Materials

3.1.1. Plant Material

Tomato plant lines used were *fer* mutant (T3238*fer*), *chloronerva* mutant, and wild type cultivars Moneymaker and Bonner Beste. Transgenic lines 35s1 and 35s2 contained an intact *FER* cDNA starting at the first ATG (position 20; AF437878) and second ATG (position 41; AF437878) start codons, respectively, driven by the constitutive cauliflower mosaic virus 35S promoter in the *fer* mutant background, as described previously (Ling et al., 2002; Bereczky et al., 2003). 35s1 and 35s2 plants were complemented by *LeFER* overexpression and grew similar to wild type (Ling et al., 2002).

3.1.2. Bacterial Strains

Bacterial strains used for molecular cloning:

- *E. coli* DH5α; genotype: *recA1 endA1 gyrA96 thi-1 hsdR17* (*rk-, mk+*) *relA1 gyrA96 supE44* (*Φ 80 lacZ ΔM15*) *Δ* (*lacZYA-argF*) *U169* (Sambrook et al., 1989)

- *E. coli* InαF'; genotype: F' *endA1 recA1 hsdR17* (*rk-, mk+*) *supE44 thi-1 gyrA96 relA1 Φ80 lacZΔM15 Δ* (*lacZYA-argF*) *U169* (Invitrogen)

Bacterial strain used for recombinant protein expression:

- *E. coli* HMS 174; genotype: F' *recA hsdR* (*rk12-, mk12+*) Rif^r (Novagen)

3.1.3. Yeast Strains

Yeast strains used for Yeast One-Hybrid assays, and Yeast Two-Hybrid library construction and screening:

- AH109; genotype: *MATa trp1-901 leu2-3 112 ura3-52 his3-200 gal4Δ gal80Δ LYS2::GAL1$_{UAS}$-GAL1$_{TATA}$-HIS3 GAL2$_{UAS}$-GAL2$_{TATA}$-ADE2 URA3::MEL1$_{UAS}$-MEL1$_{TATA}$-lacZ MEL1* (James et al., 1996)

3. Materials and Methods

- Y187; genotype: *MATα ura3-52 his3-200 ade2-101 trp1-901 leu2-3 112 gal4Δ met⁻ gal80Δ URA3::GAL1$_{UAS}$-GAL1$_{TATA}$-lacZ MEL1* (Harper et al., 1993)

3.1.4. Plasmids

- pCR2.1: *E.coli* cloning vector; Kan^R, Amp^R (Invitrogen)
- pET-29a: *E.coli* recombinant protein expression vector; Kan^R (Novagen)
- pGBKT7 BD: yeast bait expression vector; Kan^R, *TRP1* (Clontech)
- pGADT7-Rec AD: yeast library expression vector; Amp^R, *LEU2* (Clontech)
- modified pFF19: plant protoplast transformation vector for expression of protein-GFP fusions; Amp^R (Hofius et al., 2004)

3.1.5. Chemicals, Enzymes and Kits

Chemicals for general use were mainly purchased from Roth (Germany). Enzymes, kits and special consumables were purchased from the following companies:

- Amersham (GE Healthcare, Germany): Megaprime DNA Labelling Kit, ECL^{TM} Detection Reagent Kit, Hybond-N$^+$ nylon membrane, [α32P] dCTP, chemicals used for two-dimensional electrophoresis, 2D-Quant Kit, IPG strips, NHS-Activated Agarose
- BioRad (Germany): Bradford buffer
- Clontech (USA): Yeast growth media, BD Matchmaker Library Construction & Screening Kit
- Corning (USA): 245x245 mm plates
- Dianova (USA): Rhodamine-Red Anti-Rabbit Antibody
- Duchefa (The Nederlands): Plant growth media
- Fermentas (Germany): Restriction endonucleases, DnaseI, Taq DNA polymerase, T4 DNA ligase, Shrimp Alkaline Phosphatase, Prestained Protein Marker, RevertAid First Strand cDNA Synthesis Kit
- Invitek (Germany): Invisorb Spin Plant RNA Mini Kit
- Invitrogen (The Nederlands): TA-Cloning Kit

3. Materials and Methods

- Kodak (USA): X-Omat AR film

- Macherey-Nagel (Germany): NCL nitrocellulose membrane

- Metabion (Germany): Oligonucleotides

- Millipore (USA): Ultrafree-MC Filter Units

- Molecular Probes (USA): DAPI

- Novagen (USA): S-Protein Agarose, S-Protein Conjugated Alkaline Phosphatase

- Pierce (USA): Goat Anti-Rabbit Horseradish Peroxidase Antibody, GelCode Blue Stain Reagent

- Promega (USA): Sequencing Grade Modified Trypsin V511

- Qiagen (Germany): QIAquick Gel Extraction Kit, Plasmid Purification Kit (mini and midi), Rneasy Plant Mini Kit

- Roche Diagnostics (Germany): NBT, BCIP

- Schleier & Schuell (Germany): Protran nitrocellulose membrane

- Sherwood Medical (USA): Paraplast Plus

- Sigma-Aldrich (USA): Ponceau S, Anti-Rabbit Alkaline Phosphatase-Conjugated Antibody

- Takara (Japan): ExTaq DNA polymerase

3.2. Methods

3.2.1. Plant Methods

3.2.1.1. Plant Growth

Tomato (*Lycopersicon esculentum*) seedlings were grown in a hydroponic system in Hoagland solution (1 mM $MgSO_4$, 5 mM KNO_3, 5 mM $CaNO_3$, 4.55 mM KH_2PO_4, 0.45 mM K_2HPO_4, 46 µM H_3BO_3, 0.3 µM $CuSO_4.5H_2O$, 4.5 µM $MnCl_2.4H_2O$, 0.1 µM $(NH_4)_6Mo_7O_{24}.4H_2O$, 4 µM $ZnSO_4.7H_2O$, pH 5.8) supplied with 10 µM FeNaEDTA, according to Stephan and Prochazka (1989). Twelve days after germination the plants were transferred into Hoagland solution with different Fe concentrations – 0.1 µM FeNaEDTA for limiting Fe supply conditions, 10 µM FeNaEDTA for sufficient Fe supply, and 100 µM FeNaEDTA for generous Fe supply, and grown for additional 8 days

3. Materials and Methods

before harvesting for further analyses (100µM FeNaEDTA is physiologically optimal and recommended for multiple plant growth media (see catalogue from Duchefa Biochemie, Haarlem, The Nederlands).

3.2.1.2. Reductase Assay

FeIII-chelate reductase activity assays were performed according to Stephan and Prochazka (1989) and Ling et al. (2002) on 4 to 5 plants per condition. Plant roots were placed into Hoagland solution with 40 µM FeNaEDTA and 170 µM sodium bathophenanthrolinedisulfonate (BPDS). Reduction rates were calculated from the absorption of FeII-BPDS at 540 nm in 1 h in the medium and per gram root material (molar extinction coefficient 22.5).

3.2.2. Yeast Methods

3.2.2.1. Small Scale Yeast Transformation

Small scale yeast transformation was performed according to Gietz et al. (1992) as follows: 2 ml seed culture of AH109 in YPAD medium was diluted in 50 ml to OD_{600} 0.5 and incubated at 30ºC for 4 h. Cells were collected at $OD_{600} > 1.5$, washed once with 25 ml dH_2O, and resuspended in 1 ml 0.1 M lithium acetate (LiAc). Subsequently, cells were pelleted and resuspended in 0.1 M LiAc to a final volume of 0.5 ml. The obtained cell suspension was divided into 0.05 ml samples, the cells were pelleted and mixed with a transformation mixture containing 33 % polyethyleneglycol (PEG) 3350, 0.1 M LiAc, 0.5 mg denatured herring testes carrier DNA, 2 µl purified plasmid of interest. Following incubation at 30ºC for 30 min and 42ºC for 30 min, cells were brought to 0.2 ml final volume, plated on small SD-Trp plates, and grown for 2 days at 30ºC.

3.2.2.2. Yeast One-Hybrid Assay

For the purpose of LeFER activation domain identification, ten GAL4 DNA-binding domain fusion constructs containing different parts of LeFER into pGBKT7 (Clontech), as described in Table 1, were created by cloning the *EcoRI* restriction fragments from the respective pET-29a constructs (for LeAll, LeN, and LeC, see section 3.2.4.1.) or by amplifying from pET-29a:LeFER (see section 3.2.4.1.) using the primers listed in Table

3. Materials and Methods

2. The verified constructs were transformed into the yeast (*Saccharomyces cerevisiae*) strain AH109 (Clontech) according to (Gietz et al., 1992) (see section 3.2.2.1.) and grown on synthetic dextrose (SD) medium containing amino acid supplements without tryptophane (SD-Trp). After two days of growth at 30°C, the obtained colonies were assayed for *lacZ* reporter gene activation according to the manufacturer's instructions. Yeast cells transformed with the empty pGBKT7 vector were assayed in parallel and used as a negative control.

Primer combinations	Code	Construct	Size
LeN-5' + LeC-3'	LeAll	LeFER coding	915 bp
LeN-5' + LeN-3'	LeN	LeNshort + basic	474 bp
LeC-5' + LeC-3'	LeC	LeC	327 bp
LeN-5' + LeNshort-3'pGB	Le7	LeNshort	348 bp
LeN-5' + LeHLH-3'pGB	Le8	LeNshort + basic + HLH	588 bp
Lebasic-5'pGB + LeN-3'	Le9	Lebasic	123 bp
LeHLH-5'pGB + LeHLH-3'pGB	Le10	LeHLH	117 bp
Lebasic-5'pGB + LeC-3'	Le11	Lebasic + HLH + C	567 bp
LeHLH-5'pGB + LeC-3'	Le12	LeHLH + C	444 bp
Lebasic-5'pGB + LeHLH-3'pGB	Le13	Lebasic + HLH	240 bp

Table 1: GAL4 DNA-binding domain fusion constructs containing ten different parts of *LeFER* coding sequence.

Primer name	Primer sequence
LeN-5'	5'-aatggagagtggtaatgcatcaatgg-3'
LeN-3'	5'-ttaggctttatccatctttgtgatattaggaac-3'
LeC-5'	5'-aatgaatttcacaacctattatccagcaat-3'
LeC-3'	5'-ttagaccaacggagatgtctcgaagt-3'
LeNshort-3'pGB	5'-ttttctgcagttagcttgttggagtcattttgg-3'
LeHLH-5'pGB	5'-ttttccatggagatgtccatcattggagatg-3'
LeHLH-3'pGB	5'-tttgctgcagttatttctttgcattttgaaata-3'
Lebasic-5'pGB	5'-ttttccatggagatgaaaggcacgaggac-3'

Table 2: Primers used for the construction of GAL4 DNA-binding domain fusion constructs containing ten different parts of *LeFER* coding sequence (see Table 1).

3.2.2.3. Yeast Two-Hybrid Library Construction and Screening

- **Yeast Two-Hybrid Library Construction**

Yeast Two-Hybrid library was constructed from roots of wild type tomato plants (cv. Moneymaker) grown at 0.1 µM FeNaEDTA using BD Matchmaker Library Construction

3. Materials and Methods

& Screening Kit (Clontech) according to the manufacturer's instructions. Some specific points of the protocol were performed as follows: RNA was extracted using RNeasy Plant Mini Kit (Qiagen). The first-strand cDNA synthesis was performed using an oligo (dT) primer. Double-stranded (ds) cDNA was amplified by Long Distance PCR at 30 cycles. Ds cDNA was purified over BD Chroma Spin Columns (Clontech). For the library construction, yeast strain AH109 was used as follows: 10 ml seed culture of AH109 in YPAD medium was diluted in 50 ml to OD_{600} 0.5 and incubated at 30ºC for 4 hours. Cells were collected at $OD_{600} > 1.5$, washed in 0.5 volume of dH_2O, and resuspended in 3 ml 0.1 M LiAc. After 15 min incubation at 30ºC, cells were pelleted and resuspended in transformation mixture containing 33 % PEG 3350, 0.1 M LiAc, 0.5 mg denatured herring testes carrier DNA, 20 µl purified ds cDNA, 6 µg pGADT7-Rec AD Cloning Vector (Clontech). Following incubation at 30ºC for 30 min and 42ºC for 30 min, cells were brought to 10 ml final volume and plated on large SD-Leu plates (245 x 245 mm, Corning, USA) (800 µl/plate). After 4 days at 30ºC, cells were collected in YPAD containing 25 % glycerol and 0.015 mg/ml Kanamycin, and stored at -80ºC.

- **Yeast Two-Hybrid Library Screening**

The obtained library was used for a Yeast Two-Hybrid assay in four experiments with different parts of LeFER used as bait – LeC, Le7, Le11, and Le12 (see above, Table 1). The assay was done by yeast mating between strain AH109 containing the library, and strain Y187 containing the bait, as follows: 100 OD-units of seed bait culture were collected in 1/100 volume YPAD and mixed with a thawed aliquot of library incubated in YPAD for 10 min at 30ºC. The mixture was plated on small YPAD plates (400 µl/plate) and incubated for 4.5 hours at 30ºC. Cells were collected with 6 ml YPAD/plate, resuspended in 25 ml dH_2O, and plated (1ml/plate) on large SD-His/Trp/Leu plates containing 4 mM 3-amino-1,2,4-triazole (3-AT) (low stringency screening). Plates were incubated at 30ºC and single colonies were collected from day 5 to 10, regrown on SD-His/Trp/Leu + 3-AT and tested for the presence of a positive binding partner of the bait by *lacZ* assay. Yeast media and *lacZ* assay were prepared as described in the Yeast Protocols Handbook (Clontech).

3. Materials and Methods

- **Yeast Two-Hybrid Library Screening Quality Control**

For each Yeast Two-Hybrid screening performed, the quality of the screen was estimated according to several criteria (Table 3). Mating efficiency was calculated based on plated dilution series (1:10, 1:100, 1:1000, 1:10 000) on SD-Trp (selects bait strain), SD-Leu (selects library strain), and SD-Trp/Leu (selects diploids) media. Plates with 30 to 300 colony forming units (cfu) were counted, and the number (#) of viable cfu/ml was calculated according to the formula: "cfu/(plated volume (ml) * dilution factor)". The number of viable cfu/ml for the two mating partners was compared to determine the "limiting" partner (the strain with lower viability). The mating efficiency (% diploid) was calculated according to: "(# of cfu/ml of diploids)/ (# of cfu/ml of limiting partner) * 100". This value has to be above 2 %. Finally, the number of clones screened was calculated: "(# of cfu/ml of diploids) * resuspension volume (ml)". The calculated values for each criterion for the four Yeast Two-Hybrid screens performed are presented in Table 3.

| Y2H Screen | # viable cfu/ml | | | limiting partner | | % diploid | # of clones screened |
	SD-Leu	SD-Trp	SD-Trp/Leu	bait	library		
LeN	$2*10^7$	$2*10^7$	$1*10^6$		X	6.4	$3.1*10^7$
LeC	$2*10^7$	$1*10^7$	$6*10^5$	X		4.3	$1.4*10^7$
Leb+HLH+C	$2*10^7$	$3.8*10^7$	$3.6*10^6$		X	18	$9*10^7$
LeHLH+C	$2*10^7$	$3*10^7$	$2.2*10^6$		X	11.6	$5.5*10^7$

Table 3: Quality control criteria for monitoring the efficiency of a Yeast Two-Hybrid screen. The values for four screens are presented.

3.2.3. DNA and RNA Techniques

3.2.3.1. Molecular Cloning

Molecular cloning techniques such as PCR, enzyme digestion, and DNA ligation were performed according to manufacturer's instructions and standard protocols (Sambrook et al., 1989).

3. Materials and Methods

3.2.3.2. Gene Expression Analysis

Total RNA was extracted using Invisorb Spin Plant RNA Mini Kit (Invitek) according to the manufacturer's instructions. 1 μg of Dnase I-treated RNA was used for cDNA synthesis using the RevertAid First Strand cDNA Synthesis Kit (MBI Fermentas). Semiquantitative reverse transcription (RT)-PCR was performed as described in Bereczky et al. (2003). The utilized primers surrounded an intron to distinguish between cDNA and genomic amplification products. The reactions were analysed by agarose gel electrophoresis and Southern blot hybridization according to standard procedures. The *LeFER* expression signals (5'- tttcggagcgcaaaaggagag-3' and 5'-cttgattgctggataataggttgtgaaat-3', amplified in 20 cycles) were normalized according to the constitutive control product of the elongation factor gene *LeEF-1a* (5'-actggtggttttgaagctggtatctcc-3' and 5'-cctcttgggctcgttaatctggtc-3', amplified in 15 cycles).

3.2.4. Protein Techniques

3.2.4.1. Recombinant Protein and Antibody Production and Purification

- **Construct Preparation**

The entire coding region of the *LeFER* cDNA (5'-aatggagagtggtaatgcatcaatgg-3' and 5'-ttagaccaacggagatgtctcgaagt-3'), the region between the first ATG and the helix-loop-helix domain (*N-LeFER*, 5'-aatggagagtggtaatgcatcaatgg-3' and 5'-ttaggctttatccatctttgtgatattaggaact-3'), and the region between the helix-loop-helix domain and the stop codon (*C-LeFER*, 5'-aatgaatttcacaacctattatccagcaat-3' and 5'-ttagaccaacggagatgtctcgaagt-3') were amplified by PCR and cloned into pCR2.1 plasmid via TA cloning (Invitrogen, Carlsbad, CA). After sequence verification, the fragments were subcloned into the expression vector pET-29a (Novagen, Madison, WI) by using the *EcoRI* restriction site.

- **Recombinant Protein Expression and Purification**

Protein expression was performed in the *E. coli* strain HMS174 with 0.5 mM isopropylthio-β-galactoside (IPTG) induction at OD_{600} of 0.6 for 3 hours at 30°C. The expressed proteins were purified using S-protein Agarose columns (Novagen) according to the manufacturer's instructions.

3. Materials and Methods

- **Antibody Production and Purification**

Both the purified LeFER and N-LeFER proteins were used to obtain rabbit polyclonal antisera by a service facility at the Institute of Plant Genetics and Crop Plant Research (IPK). NHS-Activated Agarose (Amersham) was covalently linked to purified LeFER or C-LeFER protein according to the manufacturer's instructions, and used to affinity-purify the anti-N-LeFER and anti-LeFER antisera, respectively. The purified antisera recognized full-length LeFER protein by Western blot analysis of *E. coli*-expressed LeFER protein as well as in wild type, 35s1, and 35s2 plant samples. No protein of the correct size was detected in *fer* mutant protein extracts. Throughout the following sections, the affinity-purified anti-N-LeFER and anti-LeFER antisera are named anti-N-FER antiserum and anti-FER antiserum, respectively.

3.2.4.2. Western Blot Analysis

- **Bacterial Protein Extracts**

Bacteria were grown as descibed in section 3.2.4.1. Cultures were harvested by centrifugation for 20 min at 5,000 x g. The supernatant was used as a crude bacterial protein extract for Western blot analysis after diluting it 1:1 with 2x Laemmli loading buffer (0.1 M Tris-HCl pH 6.8, 4 % SDS, 20 % Glycerol, 10 % β-ME, 0.005 % bromphenol blue) and subsequent denaturation at 95°C for5 min. The same preparation method was used for purified recombinant proteins (obtained as described in section 3.2.4.1.). Protein concentration of the bacterial extracts was measured by Bradford buffer (BioRad). Equal amounts of total protein extracts were loaded onto a 12% SDS-polyacrylamide gel for separation. Samples were transferred to Protran nitrocellulose membrane (Schleier & Schuell), stained with Ponceau S (Sigma-Aldrich), and photographed. Subsequently, the membranes were probed with S-Protein Conjugated Alkaline Phosphatase (Novagen) and the signals were visualized by a nitroblue tetrazolium chloride/5-bromo-4-chloro-3-indolyl-phosphate toluidine salt (NBT/BCIP) color reaction (violet staining) according to Roche Diagnostics (Mannheim). Alternatively, protein blots were probed with anti-N-FER antiserum or anti-FER antiserum as described below.

3. Materials and Methods

- **Plant Protein Extracts**

Total plant protein extracts were obtained as follows: Leaves and roots were harvested and weighed after grinding. The plant material was extracted in 2x Laemmli loading buffer and subsequently centrifuged for 5 min at 10,000 x g. The amount of 2x Laemmli loading buffer added was adjusted according to the weight of ground material. Crude nuclear protein fractions were isolated according to Escobar et al. (2001). Protein concentrations were measured using the 2D-Quant Kit (Amersham Biosciences). Equal amounts of the supernatants containing the total protein extracts (9µg) were denatured at 95°C for 5 min and loaded onto a 12% SDS-polyacrylamide gel for separation. Samples were transferred to Protran nitrocellulose membrane (Schleier & Schuell), stained with Ponceau S (Sigma-Aldrich), and photographed. Subsequently, the membranes were probed with anti-N-FER antiserum or anti-FER antiserum (1:2,000 or 1:1,000, according to the concentration of the eluate used) followed by goat anti-rabbit horseradish peroxidase secondary antibody (Pierce Chemical, 1:4,000). Western blots were developed using ECL chemiluminescence detection reagents (Amersham Biosciences) according to the manufacturer's instructions. The accuracy of loading was further controlled by Coomassie Blue staining of protein gels loaded with the same amounts of protein samples (9µg) as used for Western blots.

3.2.4.3. Immunolocalization on Single Nuclei

Single nuclei were obtained from paraformaldehyde-fixed root tips after cellulase/pectinase enzyme treatment and subsequent cell disruption (Houben et al., 1999). The isolated nuclei were probed with anti-N-FER antiserum (1:200) followed by rhodamine red-conjugated anti-rabbit secondary antibody (Dianova, 1:100) and counterstained with 4',6'-diamidino-2-phenylindole (DAPI) (Molecular Probes). The fluorescent signals were detected by a confocal laser scanning microscope (CLSM 510 Meta, Zeiss). For DAPI, the 364-nm line of an argon laser was used for excitation and the emission was measured at 450 to 490 nm. For rhodamine red fluorescence, the excitation used was 543 nm (helium-neon laser) with a band-pass filter at 560 to 600 nm. The number of rhodamine red fluorescent signals per nucleus were counted using the Zeiss LSM Image Examiner Software after generation of six-step diagrams where the intensity

3. Materials and Methods

of the signal was plotted over the area of the confocal image. Different levels of relative pixel intensities were presented as RGU (relative grayscale units): 1 to 50, 51 to 100, 101 to 150, and 151 to 200.

3.2.4.4. Immunolocalization on Transverse Root Sections

Tomato roots from plants grown under different Fe-supply conditions were formaldehyde-fixed, eosin-counterstained, and embedded in Paraplast Plus (Sherwood Medical). Immunolocalization was performed on 10-μm transverse sections using anti-N-FER antiserum (1:200) followed by anti-rabbit alkaline phosphatse-conjugated secondary antibody (Sigma, 1:200) according to Smith et al. (1992). The signals were visualized by NBT/BCIP color reaction (violet staining) (Roche Diagnostics, Mannheim) according to manufacturer's instructions. Images were recorded using an Axioplan 2 imaging microscope (Zeiss).

3.2.4.5. GFP Fusion Protein Localization in Arabidopsis Protoplasts

- **Construct Preparation**

Three different *LeFER* C-terminal GFP fusion constructs were generated by first amplifying cDNA fragments: *35S::LeFER-GFP*, the whole coding sequence of *LeFER* (5'-aatggagagtggtaatgcatcaatgg-3' and 5'-ttagaccaacggagatgtctcgaagt-3'); *35S::N-LeFER-GFP*, the N-terminal coding sequence in front of the helix-loop-helix domain (5'-aatggagagtggtaatgcatcaatgg-3' and 5'-ttaggctttatccatctttgtgatattaggaact-3'); *35S::C-LeFER-GFP*, the C-terminal coding sequence behind the helix-loop-helix domain (5'-aatgaatttcacaacctattatccagcaat-3' and 5'-ttagaccaacggagatgtctcgaagt-3'). PCR fragments contained a *KpnI* and *SalI* restriction site at the 5' and 3' termini, respectively, and were cloned behind the 35S promoter into a modified pFF19 vector that contained *mGFP5* (Hofius et al., 2004).

- **Protoplast Transformation**

The verified constructs were transformed into Arabidopsis protoplasts according to (Reidt et al., 2000) as follows: Suspension cultures of *A. thaliana* were used for protoplast isolation. Following cell wall digestion in a 1% cellulase R10 (Duchefa Biochemie) and 0.5% macerozym R10 (Duchefa Biochemie) solution, protoplasts were

centrifuged and washed two times in W5 medium (0.9% NaCl, 1.8% CaCl$_2$, 0.04% KCl, 0.1% Glucose, pH 5.6). Next, they were concentrated in Mg Mannitol (0.45 M Mannitol, 15 mM MgCl$_2$, 0.1% MES pH 5.6) to a density of approximately $3x10^6$ cells/ml. To transform the resulting protoplasts, solution containing plasmid DNA (5 μg of each plasmid) and carrier DNA (160 μg) was added to 330 μl Mg Mannitol containing $1x10^6$ protoplasts. Equal amount of PEG solution (40% PEG 6000, 0.1 M Ca(NO$_3$)$_2$, 0.4 M Mannitol, 0.1% MES, pH 6.5) was added to the mixture after 10 minutes incubation. After 20 min, the transformed protoplasts were diluted into 4 ml K3 medium and transferred to small Petri dishes. Following a 16 to 18 hours incubation, GFP fluorescent signals were detected using a laser scanning microscope (CLSM 510 Meta, Zeiss) by 488 nm argon laser excitation and a band-pass filter at 505 to 525 nm.

3.2.4.6. Recombinant Protein Fe Binding

The experiment was performed following a procedure described by Krueger et al. (2002). Affinity purified recombinant LeFER, N-LeFER, C-LeFER proteins (see above), AtITP (kindly provided by Prof. R. Hell; used as a positive control), and BSA (bovine serum albumine; used as a negative control) were dialysed against Binding buffer (0.05 M N-(2-hydroxyethyl)piperazine-2'-(2-ethanesulfonic acid) (HEPES) pH 7.0, 0.3 M NaCl, 100 % Glycerol), and spotted on a 40 µm nitrocellulose membrane (Schleier & Schuell) in equal molarity ($7.2*10^{-6}$ mol). The membrane was then incubated with radioactive solution - 0.55 µM ^{55}FeCl$_3$ in Metal Binding buffer (MBB) (25 mM Tris pH 6.8, 0.15 M NaCl). If needed, FeIII was reduced to FeII by addition of 55 µM Na ascorbate. After 2 hours, the membrane was washed three times for 30 min with MBB and exposed for 72 hours to a Phosphoimager screen (Fuji).

3.2.4.7. Two-Dimensional Gel Electrophoresis (2-DE)

- **Sample Preparation**

Sample preparation and 2-DE of tomato roots from different plants (*fer* mutant, wild type, 35s1) grown at different Fe concentrations (0.1, 10, 100 µM FeNaEDTA) have been performed as previously described (Amme et al., 2005; Schlesier and Mock, 2006). Briefly, the plant material was ground under liquid nitrogen to fine powder. One part (1 g

3. Materials and Methods

usually) of this material was precipitated by 10 parts of precipitation solution containing 10% w/v trichloroacetic acid (TCA) and 0.07% w/v β-mercaptoethanol (β-ME) in acetone for 45 min at -20ºC. After washing twice with acetone containing 0.07% w/v β-ME, the precipitate was dried in a vacuum centrifuge. Proteins were dissolved using 50 µl/mg of lysis buffer (8 M urea, 2% 3-[(3-cholamidopropyl)dimethylamonio]-1-propanesulfonate (CHAPS), 0.5% IPG buffer, 20 mM dithiothreitol (DTT)). The supernatant was clarified by centrifugation through 0.45 mm Ultrafree-MC filter units (Millipore). The protein concentration of the samples was measured with 2D-Quant Kit (Amersham Biosciences).

- **Sample Separation by 2-DE**

175 µg of protein were loaded by rehydration to 13 cm immobilized pH gradient (IPG) strips pH 3–10 and separated on IPGphor unit (Amersham Biosciences), using the following settings: 1 h gradient 250 V, 1 h gradient 500 V, 1 h gradient from 500 to 4000 V, and 5 h 4000 V with a total of about 24 kVh. After isoelectric focusing (IEF), strips were equilibrated for 15 min in equilibration buffer (50 mM Tris-HCl pH 8.8, 6 M urea, 30% v/v glycerol, 2% w/v sodium dodecyl sulfate (SDS), 20 mM DTT, 0.01% w/v bromphenol blue), and mounted on top of a SDS polyacrylamide gel with stacking gel in a Hoefer S600 apparatus (Amersham Biosciences). After washing three times with dH$_2$O, gels were stained with colloidal Coomassie Brilliant Blue (CBB) G-250 solution (GelCode Blue Stain Reagent, Pierce) for 1 h, washed with dH$_2$O for 5 min, and stored in dH$_2$O.

- **2-DE Gel Image Analysis**

The obtained CBB stained 2-DE gels were scanned on UMAX Power Look III scanner with Power Scan 3.0 software (Nonlinear Dynamics). Gel images were initially analyzed for differentially expressed protein spots with Progenesis software package Phoretix 2D Evolution v2005 (Nonlinear Dynamics). Following settings were used: Background Substraction enabled; Total Spot Volume normalization; Eq. Radius > 7, and Volume/Area > 1000 spot detection parameters. Protein spots with minimum 1.5 times difference in expression intensity in pairwise comparisons for each condition were selected, cut out from the respective 2-DE gel and subjected to identification by mass

3. Materials and Methods

spectrometry. Detailed expression profiling for each selected protein spot throughout all experimental conditions was performed using PDQuest Advanced 8.0 software (BioRad).

3.2.4.8. Identification of Proteins by Mass Spectrometry (MS)

Protein identification was performed by using Matrix-Assisted Laser Desorption Ionization Time-Of-Flight (MALDI-TOF) MS (Bruker Daltonics) and/or nanoscale Liquid Chromatography-Electrospray Ionization (LC-ESI) MS/MS (Waters) systems as described by Amme et al. (2005).

- **Protein Spot Digest**

After comparison of the obtained 2-DE gel images (see section 3.2.4.7.), 155 differentially expressed protein spots were chosen for analysis. Protein spot gel pieces of about 1.5 mm in diameter were manually cut out from the 2-DE gels, and washed for 30 min at room temperature under vigorous shaking with 400 ml buffer (10 mM ammonium bicarbonate/50% acetonitrile (ACN)). After removing the supernatant, the gel pieces were dried. For the digestion of proteins, 10 ml trypsin solution (Sequencing Grade Modified Trypsin V511, Promega, Madison; 10 ng/ml in 5 mM ammonium bicarbonate/5% ACN) were added to each sample. After incubation for 5 h at 37°C, the reaction was stopped by adding 2 ml 1% trifluoroacetic acid (TFA) (Schlesier and Mock, 2004).

- **Protein Identification by MALDI-TOF MS**

For MALDI-TOF MS, 1 ml of the protein spot digest was mixed with 2 ml of the matrix solution (5 mg α-cyano-4-hydroxycinnamic acid (CHCA) in 80% v/v ACN and 0.1% w/v TFA) and 1 ml of this mixture was deposited onto the MALDI target. The tryptic peptides were analyzed with a REFLEX III MALDI-TOF mass spectrometer (Bruker Daltonics, Leipzig, Germany). Spectra were calibrated using trypsin autolysis products (m/z 842.501 and 211.101) as internal standards under application of the Xtof software Version 5.1.5 (Bruker Daltonics).

- **Databse Searches for MALDI-TOF MS Data**

Protein identification was performed by searching for *Viridiplantae* in the nonredundant NCBI database and the SwissProt database using the MASCOT search engine (Matrix Science, London, UK) with the following parameters: monoisotopic mass

3. Materials and Methods

accuracy, 100 ppm; missed cleavages, 1; allowed variable modifications, oxidation (Met) and propionamide (Cys). Successful protein identification by MALDI-TOF MS was achieved for 66 (43 %) of the 155 analysed spots.

- **Protein Identification by LC-ESI MS/MS**

89 protein spots were subjected to LC-ESI MS/MS nanoscale analysis. 6 ml of the protein spot digest was used for the nanoscale reversed phase (RP) LC analyses, which was conducted on a modular CapLC LC system (Waters, Milford, MA, USA). The mobile phase flow from the C pump was used to preconcentrate and desalt the digest samples on a 5 mm x 300 mm Symmetry C18 precolumn (Waters) for 5 min at 20 ml/min with an aqueous 0.1% formic acid solution. The peptides were subsequently eluted onto a 150 mm x 75 mm analytical Atlantis C18 column (Waters) and separated with an increasing ACN gradient from 5% to 50% B in 30 min. Mobile phase A consisted of 0.1% formic acid in ACN/water (5:95, v/v) and mobile phase B of 0.1% formic acid in ACN/water (80:20, v/v). The nanoscale LC effluent from the analytical column was directed to the NanoLockSpray source of a Q-Tof Ultima API hybrid quadrupole/TOF mass spectrometer (Waters). The mass spectrometer was operated in a positive ion mode with a source temperature of 80°C and a cone gas flow of 25 l/h. A voltage of approximately 2 kV was applied to the nano flow probe tip. The mass spectra were acquired with the TOF mass analyzer in V-mode of operation and spectra were integrated over 1 sec intervals.

MS and MS/MS data were acquired in a continuum mode using MassLynx 4.0 software (Waters). The instrument was calibrated with a multi-point calibration using selected fragment ions of the CID of Glu-Fibrinopeptide B. Automatic data directed analysis was employed for MS/MS analysis on doubly and triply charged precursor ions. The product ion MS/MS spectra were collected from m/z 50 to m/z 2000. Lock mass correction of the precursor and the product ions was conducted with a mixture of Glu-Fibrinopeptide B and erythromycin in 0.1% formic acid in ACN/water (50:50, v/v), respectively, and introduced via the reference sprayer of the NanoLockSpray interface.

- **Databse Searches for LC-ESI MS/MS Data**

ProteinLynx GlobalSERVER v2.1 (Waters) software was used as a software platform for data processing, deconvolution, and *de novo* sequence annotation of the spectra, and

3. Materials and Methods

various database search types. The MS/MS spectra searches were conducted with a protein *Viridiplantae* index of the nonredundant NCBI database and an EST database comprising nucleotide sequences of *L. esculentum*, *S. tuberosum*, and *N. tabacum*. A 25 ppm precursor, a 0.05 Da product ion tolerance, one missed cleavage, and variable methionine oxidation were used as the search parameters. BLAST homology and similarity searches were conducted with a protein *Viridiplantae* index of the NCBI database and the nonredundant NCBI database as a whole. Successful protein identification by LC-ESI MS/MS was achieved for 73 (76 %) of the 89 analysed spots, which is 47 % of all 155 differentially expressed protein spots.

3.2.4.9. Statistical Analysis on Proteomics Data

Statistical analysis on the proteomics data set was performed as an external collaboration in the group of Pattern Recognition (Dr. Udo Seiffert) at the Leibniz Institute of Plant Genetics and Crop Plant Research (IPK), Gatersleben, Germany.

3.2.5. Sequence Analysis
3.2.5.1. Sequence Searches and Alignments

Sequence searches were performed using the Basic Local Alignment Search Tool (BLAST) (Altschul et al., 1997) available on the NCBI website (http://www.ncbi.nlm.nih.gov/BLAST/). Alignments were done with the DNASTAR software (Lasergene) using either the ClustalW algorithm or as one pair alignments by Martinez-NW method.

3.2.5.2. Sequence Data

Gene identities are available at the EMBL/GenBank data libraries under accession numbers AF437878 (*LeFER*) and XI4449 (*LeEF-1a*).

4. Results

4.1. Regulation of *LeFER* on Transcriptional and Posttranscriptional Level by Fe and NA Availability

4.1.1. *LeFER* Gene Expression in Response to Fe Availability

LeFER is the central regulator of Fe mobilization in response to Fe deficiency in tomato. Previous experiments have demonstrated that LeFER is active in plants exposed to Fe deficiency but not at high Fe supply (Ling et al., 2002). One possibility to control LeFER action would be a differential gene expression in response to Fe availability. *LeFER* was previously reported to be expressed at similar level upon low (0.1 µM FeNaEDTA) and sufficient (10 µM FeNaEDTA) Fe supply, suggesting that its mRNA abundance might not be regulated at the transcriptional level (Ling et al., 2002). However, the effect of a generous Fe supply, such as 100 µM, on *LeFER* gene expression was not tested.

We investigated tomato plants grown under three different Fe supply conditions – low (0.1 µM FeNaEDTA), sufficient (10 µM FeNaEDTA), and generous (100 µM FeNaEDTA) Fe supply. We observed that wild type plants grew well in the hydroponic condition when supplied with 10 or 100 µM FeNaEDTA in Hoagland medium, whereas at 0.1 µM FeNaEDTA, plants developed leaf chlorosis (Fig. 4A, compare also to *fer* mutant plants). Since 100 µM is the regular concentration of Fe in multiple plant growth media (Duchefa Biochemie), this concentration can be regarded as physiologically optimal.

As an indirect measure of Fe uptake efficiency and *LeFER* gene activity, a reductase assay was performed on *fer* mutant and wild type plants grown at the three different Fe supply conditions. At low Fe supply, the root FeIII-reductase activity in wild type plants was found the highest. The increase of Fe concentration up to sufficient or generous Fe supply led to approximately 2.5 and 4.5 times decrease in the activity values, respectively. *fer* mutant plants grown under Fe-deficient conditions exhibited only a weak background level of reductase activity irrespective of Fe supply conditions (Fig. 4B, only data for *fer* mutant plants grown at low Fe supply is shown).

4. Results
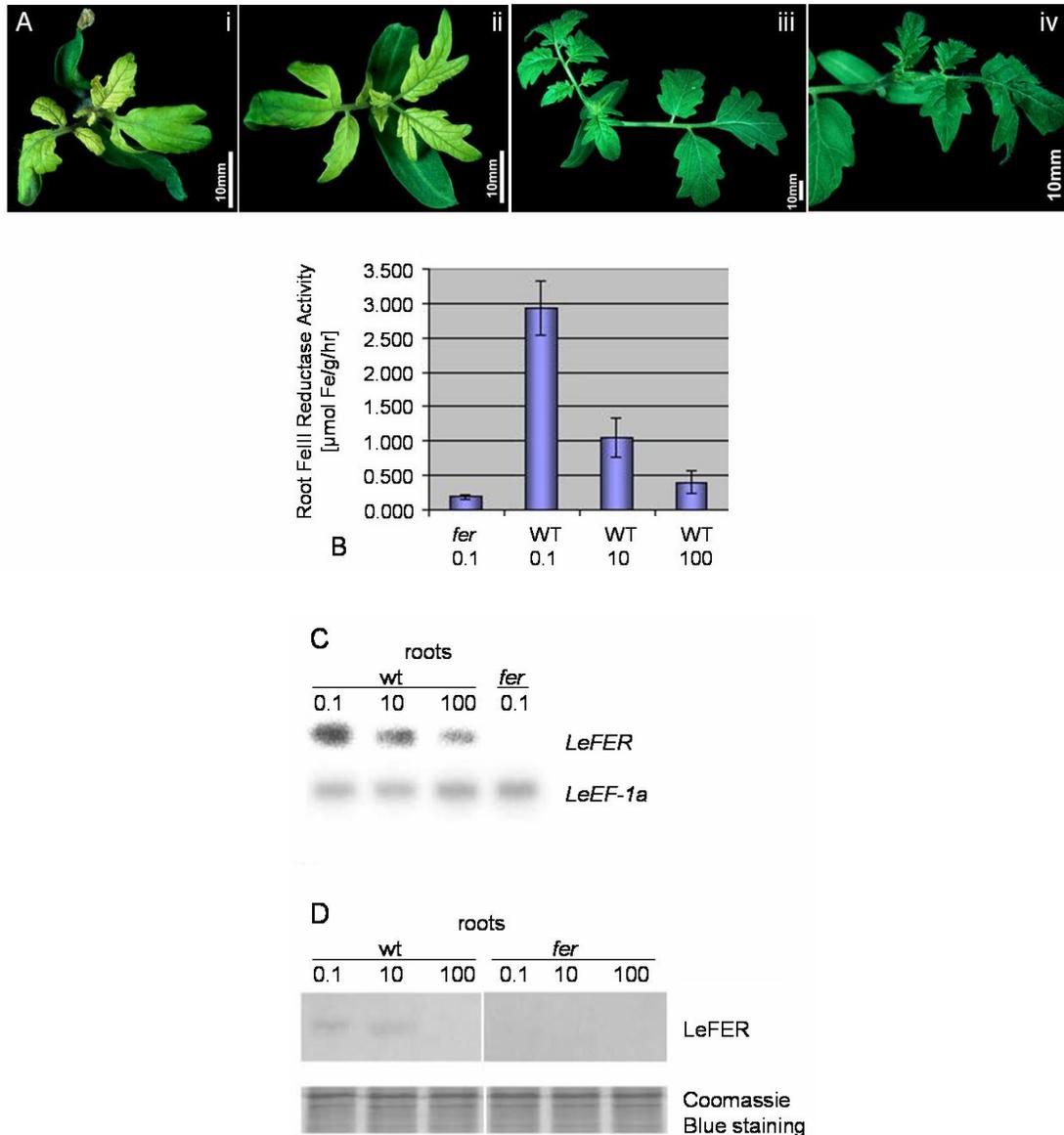
Figure 4: Morphological and physiological responses to Fe deficiency, and regulation of *LeFER* gene and LeFER protein expression by Fe availability in roots.

Wild type (wt) and *fer* mutant plants were grown in the presence of 0.1, 10, or 100 µM FeNaEDTA. (A) Comparison of Fe-deficiency leaf chlorosis between *fer* mutant (i) and wild type (ii-iv) plants grown at 0.1 (i, ii), 10 (iii), and 100 (iv) µM FeNaEDTA. (B) Root FeIII reductase activity assay of *fer* mutant and wild type (WT) plants grown under different Fe supply conditions. SD are indicated; n = 4-5 plants/condition. (C) Semiquantitative RT-PCR analysis of *LeFer* mRNA levels in tomato roots. *LeFER* expression levels were normalized according to the constitutively expressed *LeEF-1a* gene. *LeFER* signals were absent in *fer* mutant plants due to the presence of an insertion within the region to be amplified. (D)

4. Results

Western blot analysis on total root protein extracts; 9 µg protein were loaded in each lane. Coomassie Blue staining was used to demonstrate equal protein loading.

LeFER gene expression was determined by semiquantitative reverse transcription (RT)-PCR. The signals obtained were normalized according to the constitutively expressed *LeEF-1a* gene. We found highest *LeFER* expression in response to Fe deficiency. At sufficient Fe supply, *LeFER* expression was either decreased compared to low Fe supply, in two out of four experiments (Fig. 4C; see also Fig. 8B, wild-type lanes), or at a similar level, in two out of four experiments, as found previously by Ling et al. (2002). At generous Fe supply, *LeFER* transcript levels were consistently downregulated (Fig. 4C; see also Fig. 8B). No signal was obtained in *fer* mutant plants, regardless of Fe supply, due to the presence of a large insertion of approximately 4kb in between the binding sites for primers used in the RT-PCR experiments (Fig. 4C; Ling et al., 2002). Taken together, *LeFER* mRNA levels responded to different Fe availability conditions with a marked downregulation at generous Fe supply. Interestingly, the difference in reductase activity levels of wild type plants grown at different Fe supply conditions were following the same tendency as observed for difference in the expression levels of *LeFER* in these plants.

4.1.2. LeFER Protein Expression in Response to Fe Supply

To check whether LeFER protein levels parallel *LeFER* mRNA expression, we developed an affinity-purified polyclonal anti-FER antiserum from rabbit directed against the N-terminal LeFER peptide, excluding the helix-loop-helix domain (N-FER), termed anti-N-FER antiserum. In Western blot analysis the antiserum recognized recombinant N-FER and whole intact LeFER proteins when expressed in *E. coli* (data not shown). The anti-N-FER antiserum was subsequently used in Western blot analysis on total root and leaf plant protein extracts. In wild type root protein extracts, a specific band of approximately 35 kD was immunologically detectable (Fig. 4D). This band was absent in *fer* mutant root extracts regardless of Fe supply (Fig. 4D). It was also absent in wild type leaf protein extracts, but detectable in leaf protein extracts of transgenic plants that ectopically expressed the *LeFER* gene in leaves (see Fig. 5C). Since the detected band

4. Results

was with the predicted size of the LeFER protein, and it was absent in *fer* mutant plants, these results indicate that the anti-N-FER antiserum recognized specifically LeFER protein. We investigated LeFER protein abundance in tomato plants grown at low (0.1 µM), sufficient (10 µM), and generous (100 µM) Fe supply. In wild type plants, LeFER protein levels were either similar (in two out of three experiments) or slightly lower (in one out of three experiments) when plants were grown at sufficient compared to deficient Fe supply (Fig. 4D; see also Figs. 5A and 8C). At generous Fe supply, the amount of LeFER protein was consistently undetectable in wild type (Fig. 4D; see also Figs. 5A and 8C). Thus, LeFER protein expression showed a marked downregulation at generous Fe supply and was induced by Fe deficiency.
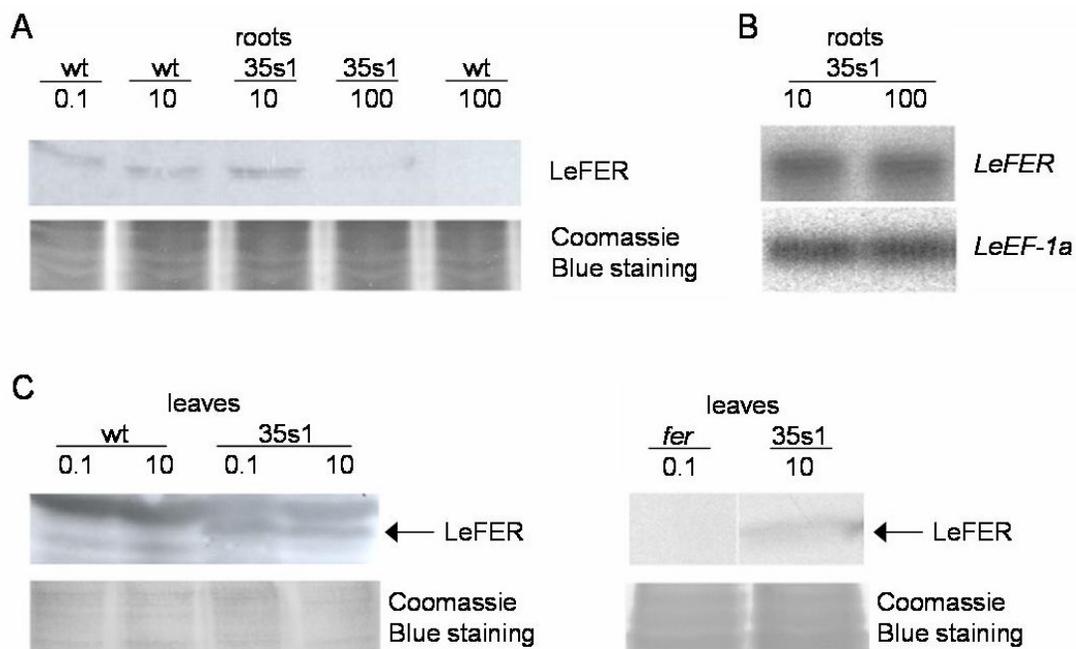
Figure 5: *LeFER* gene and LeFER protein expression in transgenic plants constitutively expresing *LeFER*.

(A) Western blot analysis using anti-N-FER antiserum on total protein extracts from roots of wild type (wt) and 35s1 transgenic plants overexpressing *LeFER*, grown at 0.1, 10, or 100 µM FeNaEDTA. (B) Semiquantitative RT-PCR analysis of *LeFer* mRNA levels in tomato roots of 35s1 plants grown at sufficient and generous Fe supply. *LeFER* expression levels were normalized according to the constitutively expressed *LeEF-1a* gene. (C) Western blot analysis using anti-N-FER antiserum (left), and

anti-FER antiserum (right), on total protein extracts from leaves of *fer* mutant, wild type, and 35s1 transgenic plants grown at 0.1 or 10 µMFeNaEDTA. LeFER protein is indicated by an arrow; 9 µg protein were loaded in each lane in A and C. Coomassie Blue staining was used to demonstrate equal protein loading.

4.1.3. *LeFER* Gene and LeFER Protein Expression in Transgenic Plants Constitutively Expressing LeFER

Previously, the functional complementation of transgenic *fer* mutant plants by overexpression of an intact *LeFER* cDNA behind the cauliflower mosaic virus 35S promoter was shown (lines C1-2 = 35s1 and C2-8 = 35s2; Ling et al., 2002; Bereczky et al., 2003). 35s1 plants contained a full-length *LeFER* cDNA, whereas that of the 35s2 plants was 21 bp shorter and started with the second ATG start codon, both in the *fer* mutant background (see section 3.1.1.). 35s1 plants were slightly better complemented than 35s2 plants (Ling et al., 2002). Bereczky et al. (2003) have observed that although *LeFER* was expressed constitutively at low and sufficient Fe supply in these transgenic plants, molecular Fe mobilization responses were stronger at low than at sufficient Fe supply, and detectable in roots but not in leaves. These previous results, suggested that *LeFER* gene action might be regulated at the posttranscriptional level, such as via protein stability or protein activation. Here, we investigated this possibility in more detail.

First, we analyzed whether *LeFER* mRNA and LeFER protein were expressed in transgenic 35s1 plants grown upon sufficient and generous Fe supply. We found that *LeFER* mRNA was produced in 35s1 plant roots regardless of Fe supply, as expected from a constitutive *LeFER* gene expression under the 35S promoter (Fig. 5B). However, the LeFER protein level was clearly downregulated at generous versus sufficient Fe supply in roots (Fig. 5A).

In leaves of transgenic *LeFER* overexpression plants, LeFER protein was stably expressed (Fig. 5C). Since the anti-N-FER antiserum recognized multiple protein bands in leaf protein extracts, we generated as a control an anti-FER antiserum that was directed against full-length LeFER protein and affinity purified against C-terminal LeFER peptides (C-FER). The anti-FER antiserum recognized a single protein band in leaf extracts of 35s1 plants but not of *fer* mutant plants that corresponded to a 35-kD LeFER protein (Fig. 5C, right). Taken together, *LeFER* mRNA and LeFER protein levels were

separately regulated in the transgenic 35s *LeFER* overexpression plants, indicating control of LeFER protein abundance at the posttranscriptional level.

4.1.4. LeFER Protein Expression in Single Root Nuclei

To further analyze LeFER protein expression, we employed immunolocalization of LeFER in single root tip nuclei (Houben et al., 1999). Briefly, isolated root tip nuclei were immunolabeled with anti-N-FER antiserum and rhodamine red-labeled secondary antibody. Nuclear genomic DNA was counterstained with 4',6-diamino-phenylindole (DAPI). The advantage of this method was that immunolocalization signals could be quantified. The intensities of fluorescent signals were examined by laser scanning microscope image software so that fluorescent signal peaks could be counted per nucleus and statistically analyzed (see section 3.2.4.3.). In *fer* mutant plants grown at 0.1, 10, and 100 µM FeNaEDTA, fluorescence levels of 1.27, 1.15, and 1.3 signal peaks/nucleus were observed, respectively (Fig. 6A, D, G, and J). In wild type plants, low-intensity signal peaks (between 51 and 100 relative greyscale units; RGU) were observed (Fig. 6B, E, H, and J). The signals were spread throughout the nucleus without an obvious pattern (Fig. 6B). On average, in nuclei of Fe-starved wild-type cells, 10.0 signal peaks were found, in nuclei of Fe-sufficient cells, 4.5 signal peaks were found, and in nuclei of generous Fe-treated plants, 1.3 signal peaks were found (Fig. 6J). In the 35s1 and 35s2 plants, the numbers of fluorescent signal peaks were about 100 to 400 times higher compared to wild type and of higher intensity (Fig. 6C, F, I, and K). Signal intensity and number of signals decreased in the nuclei of the transgenic plants when they were exposed to sufficient and generous Fe supply (Fig. 6K). For the 35s1 line, signal intensity and number were higher than in the 35s2 line (Fig. 6K). Additionally, the higher abundance of LeFER in the nuclei of 35s1 and 35s2 roots led to a rearrangement in the subnuclear signal localization. Compared to the diffused signals observed for wild-type nuclei, the transgenic lines exhibited a stronger concentration of the fluorescence signal in the nucleolus (Fig. 6C). In summary, the intensity of LeFER protein staining in single root tip nuclei suggested a Fe-dependent LeFER expression in the root tips.

4. Results
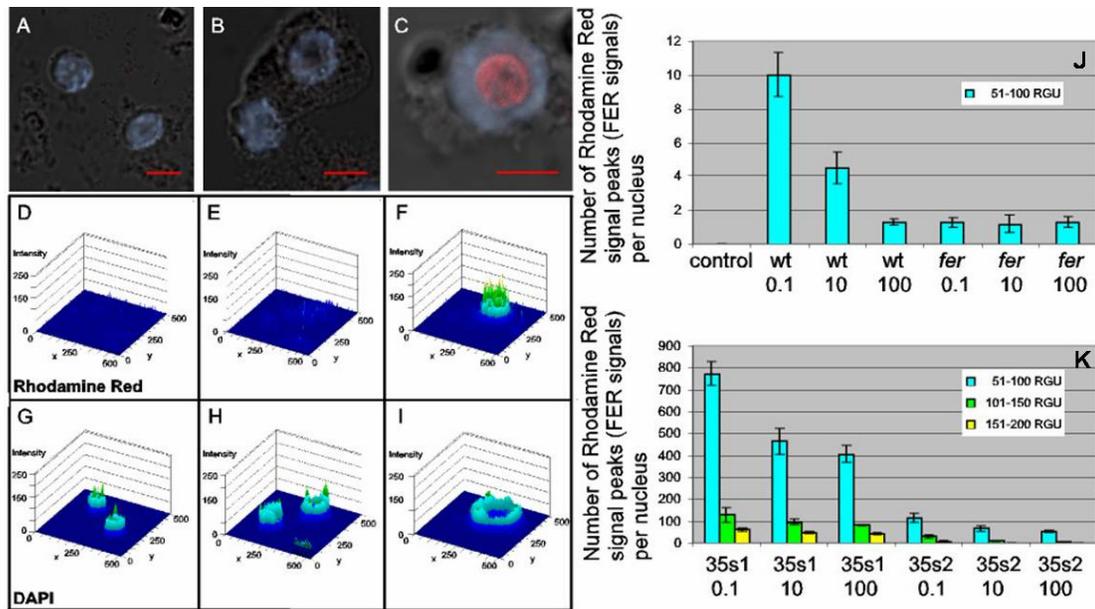
Figure 6: LeFER protein expression in single root nuclei.

Immunolocalization of LeFER on single root tip nuclei detected by anti-N-FER antiserum, followed by rhodamine red-coupled anti-rabbit IgG and counterstained with DAPI. (A to C) Superimposed confocal images of rhodamine red, DAPI, and differential interference contrast (DIC). (D to I) Diagrams, created by the laser scanning microscope 5 image software, presenting the respective rhodamine red (D–F) and DAPI (G–I) fluorescent signal peaks. The images represent the intensities of the fluorescent signals plotted on the same surface as the respective superimposed confocal image in A to C. Different levels of fluorescent signal intensities are represented by different colors: blue, 1 to 50 Relative Grey Scale Units (RGU); blue-green, 51 to 100 RGU; green, 101 to 150 RGU; and yellow, 151 to 200 RGU. The images represent examples for the *fer* mutant (A, D, and G), wild type (B, E, and H), and 35s1 plants (C, F, and I), grown at 0.1 µM FeNaEDTA. (J) Mean number of fluorescent rhodamine red signal peaks (LeFER signals) per nucleus for the negative control (secondary antibody omitted), *fer* mutant, and wild type plants, grown under all Fe supply conditions tested (µM FeNaEDTA). Only signal peaks with intensities between 51 to 100 RGU were counted. Higher signal intensities were not detected for these samples. SD are indicated; n = 10 nuclei. (K) Mean number of fluorescent rhodamine red signal peaks per nucleus for 35s1 and 35s2 plants, grown under different Fe supply conditions (µM FeNaEDTA). Three levels of fluorescent signal intensities were counted, between 51 and 200 RGU. SD are indicated; n = 10 nuclei.

4. Results

4.1.5. LeFER Protein Localization in Root Transverse Sections

To check whether LeFER protein might show differential cellular localization in response to Fe supply, we performed immunolocalization of LeFER in transverse root tip sections (Fig. 7). Wild-type, *fer* mutant, and transgenic 35s1 plants were grown at deficient, sufficient, and generous Fe supply conditions. *fer* mutant plants displayed no specific LeFER signals, showing again the specificity of the anti-N-FER antiserum (Fig. 7A, D, and G). In additional negative controls for secondary antibody specificity, no signals were detected throughout the root sections (data not shown). At generous Fe, no signals were detected both in wild type and in 35s1 plants (data not shown). LeFER protein expression signals were only detected in wild type and 35s1 plants grown at sufficient and low Fe supply. In these cases, the expression patterns were similar (Fig. 7 shows data for sufficient Fe supply). In wild type plants, LeFER protein was localized in cells of the root tip except those of the root cap (Fig. 7B). In the root elongation zone, a specific pattern of LeFER expression was observed, represented by two rings with higher signal concentration (Fig. 7E). The two rings of LeFER expression signals comprised the cell layer of the epidermis and a cell layer surrounding the vascular cylinder, perhaps the differentiating endodermis. Diffused signals could also be seen in the cortex cells. In the mature root hair zone, the signals were concentrated in the parenchyma cells inside the vascular cylinder (Fig. 7H). The 35s1 roots showed the same pattern of LeFER staining with more intense signals than the wild-type roots. Despite constitutive expression of *LeFER* mRNA in the 35s1 plants (Fig. 5B; for constitutive expression of the 35S promoter in transgenic tomato roots, see also Moghaieb et al., 2004), the LeFER protein pattern was the same in the 35s1 plants as in wild type (compare Fig. 7C, F, and I with Fig. 7B, E, and H). These results suggest that LeFER protein was expressed in distinct cell types at low and sufficient Fe supply, independent of *LeFER* mRNA expression. The cellular LeFER protein expression might be regulated by posttranscriptional in addition to transcriptional control.

4. Results
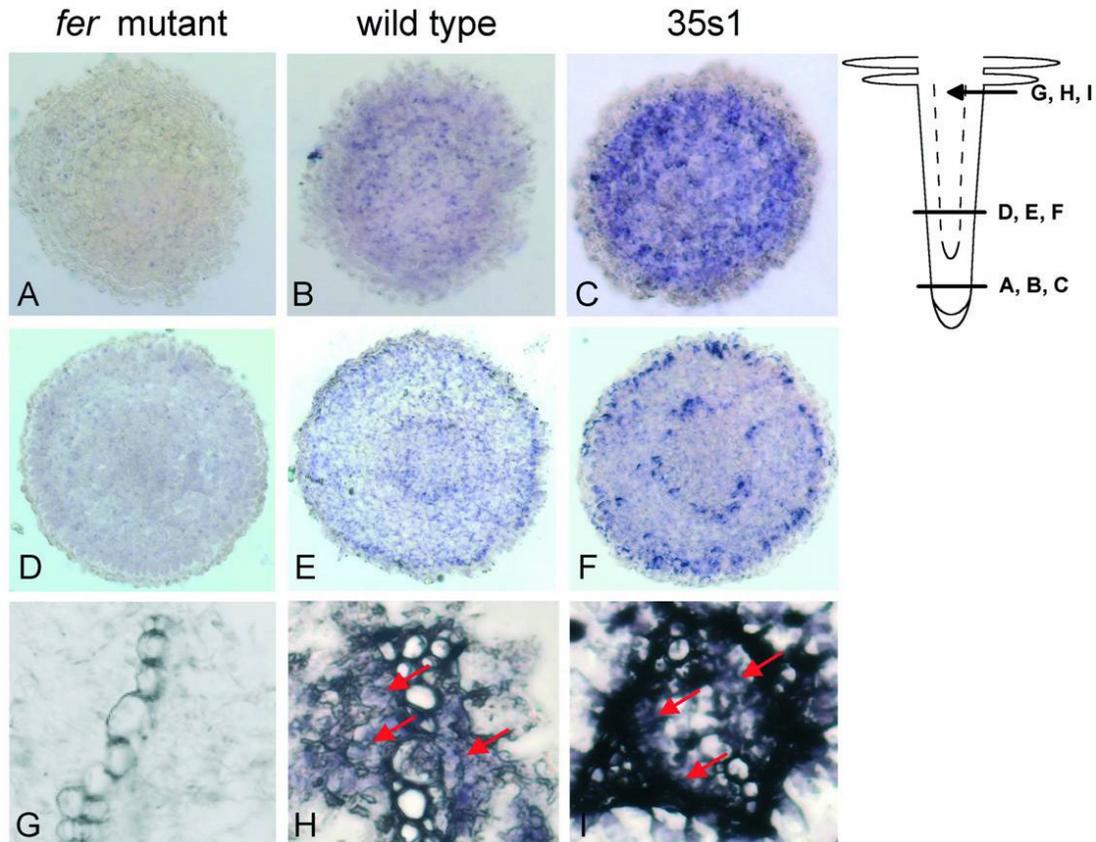
Figure 7: LeFER protein localization in root transverse sections.

LeFER immunolocalization using anti-N-FER antiserum on 10-µm paraffin-embedded tomato root cross-sections of *fer* mutant (A, D, and G), wild type (B, E, and H), and 35s1 (C, F, and I) plants. (A to C) Transverse sections from the meristematic root zone. (D to F) Transverse sections from the elongation root zone. (G to I) Magnified views of the central cylinder from transverse sections in the root hair zone, as indicated on the root scheme. The presence of LeFER protein was revealed by violet staining from indirect immunolabeling with a secondary antibody coupled to alkaline phosphatase.

4.1.6. Regulation of LeFER Protein Expression in *chloronerva* – dependence on NA Availability

To gain further insight into Fe-mediated downregulation of LeFER, we examined whether *LeFER* mRNA and LeFER protein expression were influenced by the availability of internal Fe (supplied by NA) or external Fe (supplied by the medium). For these experiments, we utilized the *chloronerva* mutant as a tool. *chloronerva* plants lack the metal and Fe chelator nicotianamine (NA), produced normally by an intact *LeNAS*

4. Results
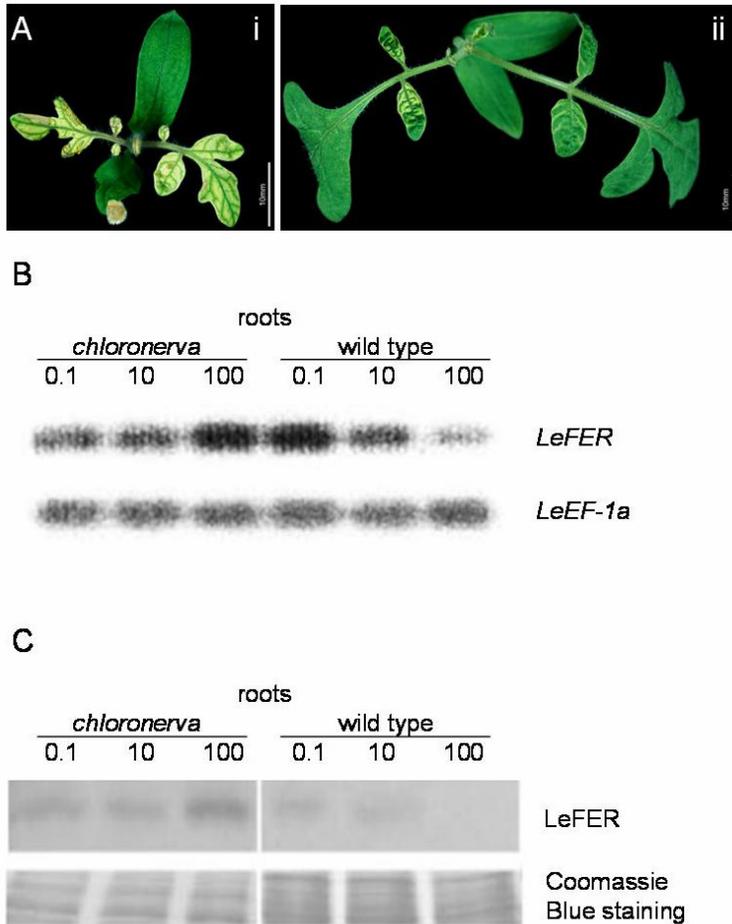
Figure 8: Regulation of *LeFER* gene and LeFER protein expression in *chloronerva* mutant plants.

(A) Generous (ii, 100 µM FeNaEDTA), compared to low (i, 0.1 µM FeNaEDTA) Fe supply partially rescues the *chloronerva* mutant phenotype. (B) Semiquantitative RT-PCR analysis of *LeFer* mRNA levels in roots from *chloronerva* and wild type plants grown under deficient (0.1 µM), sufficient (10 µM), and generous (100 µM) Fe supply. *LeFer* transcript abundance is normalized according to the constitutively expressed *LeEF-1a* gene. (C) Western blot analysis using anti-N-FER antiserum on total root extracts from *chloronerva* and wild type plants grown under 0.1, 10, or 100 µM FeNaEDTA; 9 µg protein were loaded in each lane. Coomassie Blue staining was used to demonstrate equal protein loading.

gene product (= nicotianamine synthase; Ling et al., 1999). NA is required for intracellular and intercellular transport of Fe to target components or compartments. Lack of NA (lack of internal Fe) causes local Fe deficiencies. Despite sufficient Fe supply,

4. Results

chloronerva plants mobilize and take up more Fe into the root than wild type (for review, see Scholz et al., 1992). Although extra Fe is transported to the shoots, it cannot be delivered to targets in all leaf cells, resulting in interveinal leaf chlorosis. It was previously found that the *LeFER* gene was expressed in *chloronerva* mutant roots (Bereczky et al., 2003). Here, we analyzed Fe dependence of *LeFER* gene and LeFER protein expression in *chloronerva* plants. We observed that at 100 µM Fe supply, *chloronerva* mutant leaves turned green and short-root phenotypes were rescued compared to low Fe supply (Fig. 8A). These findings indicate that *chloronerva* mutants were capable of responding to Fe. The wild type cultivar Bonner Beste (the background of the *chloronerva* mutant) showed decreased *LeFER* mRNA and LeFER protein expression at generous Fe supply (100 µM), similar to the wild type cultivar Moneymaker (Fig. 8B, C, compare with Fig. 4C, D). In *chloronerva* mutant plants, however, *LeFER* mRNA and LeFER protein expression levels were both enhanced compared to wild type, which was particularly evident at generous Fe supply (Fig. 8B, C). Therefore, external Fe supply was not sufficient to downregulate LeFER.

4.1.7. Subcellular Localization of LeFER Protein

The single-nuclei immunoassays indicated localization of the bHLH domain protein LeFER in nuclei. We analyzed whether LeFER protein might show differential localization within the cell in response to Fe supply. Therefore, we investigated subcellular localization of LeFER. Crude nuclear and remaining cellular protein fractions were prepared from root protein extracts of wild type and 35s1 plants. In Western blot analysis, LeFER protein was mainly detected in the nuclear, but not in the remaining, cellular fractions of the analyzed lines grown at deficient and sufficient Fe supply (Fig. 9A). Therefore, intracellular localization of LeFER was presumably not dependent on Fe concentration.

4. Results
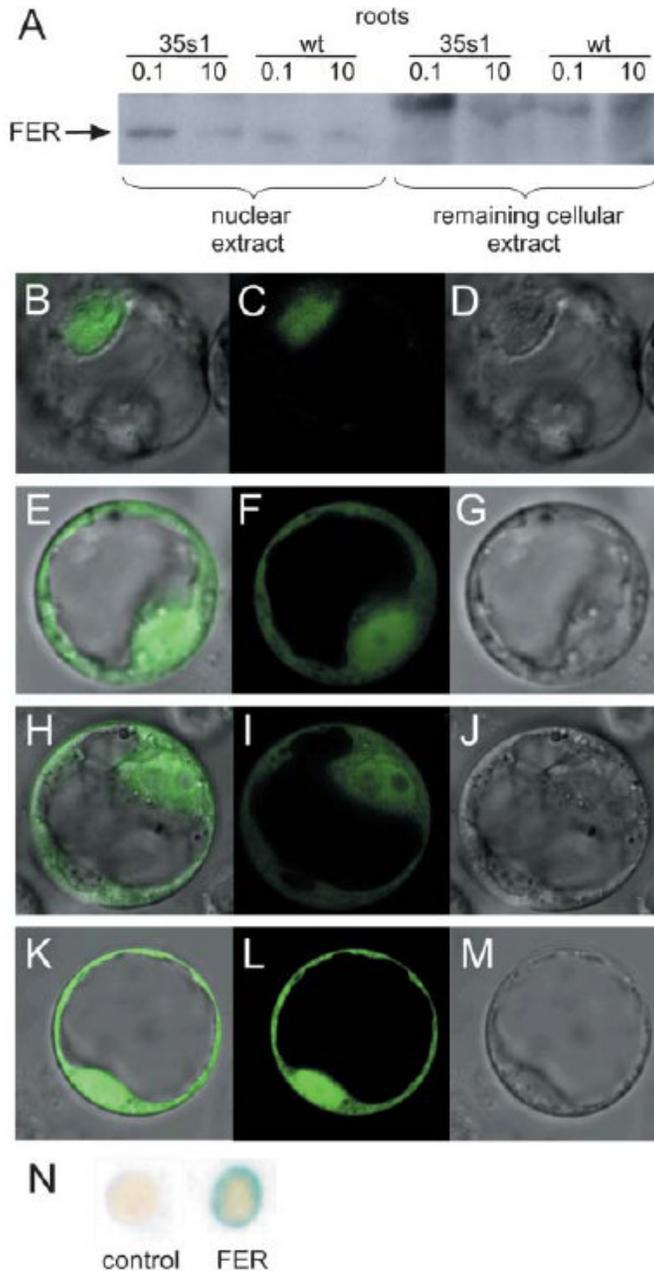
Figure 9: LeFER protein subcellular localization and transcriptional activation.

(A) Western-blot analysis using anti-N-FER antiserum on cytosolic and remaining cellular protein fractions from roots of wild type and 35s1 plants grown at 0.1 or 10 µM FeNaEDTA. The presence of LeFER protein is indicated by an arrow. (B to M) Confocal images of Arabidopsis protoplasts transiently transformed with C-terminal GFP fusion constructs showing GFP fusion protein localization. (B to D) Full-length LeFER::GFP. (E to G) N-LeFER::GFP. (H to J) C-LeFER::GFP. (K to M) Free GFP. (B, E, H, and K) Superimposed GFP and DIC images. (C, F, I, and L) GFP fluorescence. (D, G, J, and M) DIC images.

4. Results

(N) Yeast One-Hybrid assay showing transcription activation capacity of LeFER. Transcription activation is visualized by a positive *LacZ* assay (blue color of the colonies). Empty vector was used as a negative control.

To confirm the nuclear localization of LeFER, we employed a green fluorescent protein (GFP) tagging technique. Arabidopsis protoplasts were transiently transformed with a construct containing *35S::LeFER-GFP*. The LeFER::GFP fusion protein was localized in the nucleus (Fig. 9B–D). Only very few and light signals were located outside the nucleus. In contrast, free GFP was located in the cytoplasm and the nucleus (Fig. 9K–M). For the purpose of determining the location of the putative nuclear localization signal in the LeFER protein, two truncated N- and C-terminal LeFER::GFP fusion constructs were tested. Neither of the two protein parts contained the helix-loop-helix domain (N- and C-terminal parts) and was able to trigger GFP localization strictly to the nucleus, as was the case for full-length LeFER::GFP (Fig. 9E–J). Presumably, the presence of a sequence contained in the helix-loop-helix domain was necessary for the proper nuclear localization of the LeFER protein.

4.2. Transcriptional Activation of LeFER

bHLH domain proteins are usually nuclear transcription factors. Since LeFER was localized to the nucleus, we hypothesized it might act there as a transcription factor. To investigate the potential of LeFER to activate transcription, we performed a Yeast One-Hybrid assay. Full-length LeFER was fused to the GAL4 DNA-binding domain and transferred into yeast cells containing the GAL4-responsive upstream activating sequence fused to a minimal promoter and the *lacZ* reporter gene. Full-length LeFER was able to promote reporter gene activity, indicating that LeFER alone was able to activate transcription in this assay (Fig. 9N). Therefore, LeFER is presumably able to affect nuclear transcription in plants.

Furthermore, we created nine LeFER deletion constructs with different combinations of the N- and C-terminal, basic, and helix-loop-helix (HLH) domains for mapping the activation domain of LeFER (Table 1, Fig. 10). Similarly, they were fused to the GAL4 DNA-binding domain and screened in a Yeast One-Hybrid assay for *lacZ* reporter gene activation. From all nine constructs, only two were able to activate transcription in this

4. Results

system – LeN+b, containing the N-terminal part of LeFER and the basic part of the bHLH domain, and LeN+bHLH, containing the N-terminal part of LeFER and the whole bHLH domain (Fig. 10). Neither the N-terminal part of LeFER (LeN), nor the basic (Lebasic), helix-loop-heix (LeHLH) part, or whole bHLH domain (Leb+HLH) could activate transcription alone (Fig. 10), suggesting that the LeFER activation domain is shared between the N-terminal and the basic parts of the protein.
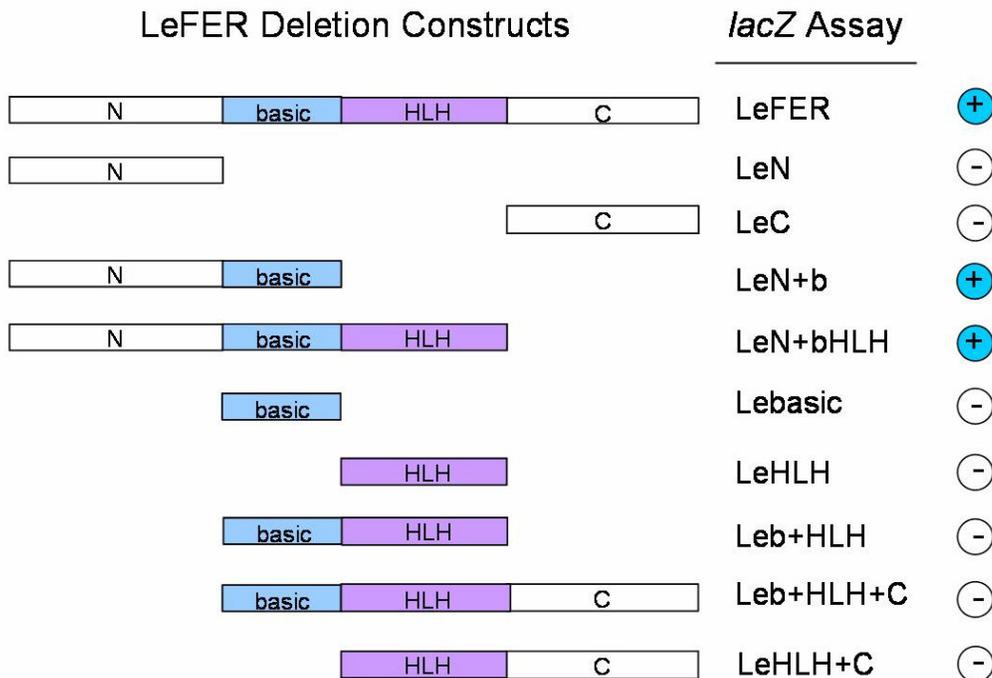
Figure 10: LeFER activation domain mapping.

LeFER deletion constructs were tested in a Yeast One-Hybrid assay for *lacZ* reporter gene activation ability. The constructs contained single or combination of more than one different parts of the whole LeFER protein, used here as a positive control. LeN, N-terminal part of LeFER; LeC, C-terminal part of LeFER; Lebasic, basic part of the LeFER bHLH domain; LeHLH, helix-loop-helix part of the LeFER bHLH domain. For each construct, transcription activation ability was tested and presented either by a positive (blue circles with plus), or negative (white circles with minus) *lacZ* assay result.

4. Results

4.3. LeFER Fe-Binding Assay

Another possibility for Fe-mediated downregulation of LeFER could be presented by a direct binding of Fe to LeFER. Therefore, we examined whether affinity purified recombinant LeFER protein could bind radioactive ^{55}FeIII or ^{55}FeII in a dot blot assay. The binding ability of the whole LeFER protein was compared to that of N- or C-terminal parts of the protein, excluding the helix-loop-helix domain (N-LeFER and C-LeFER, respectively). Arabidopsis Iron Transport Protein (AtITP) (kindly provided by Prof. R. Hell) was used as a positive control, and bovine serum albumin (BSA) – as a negative control. The whole LeFER protein showed Fe binding to both FeIII and FeII, although weaker than that of AtITP (Fig. 11). N-LeFER and C-LeFER had Fe binding levels similar to that of LeFER (Fig. 11). BSA showed no Fe-binding ability. The result suggests that LeFER can bind both FeIII and FeII in the described *in vitro* binding assay.
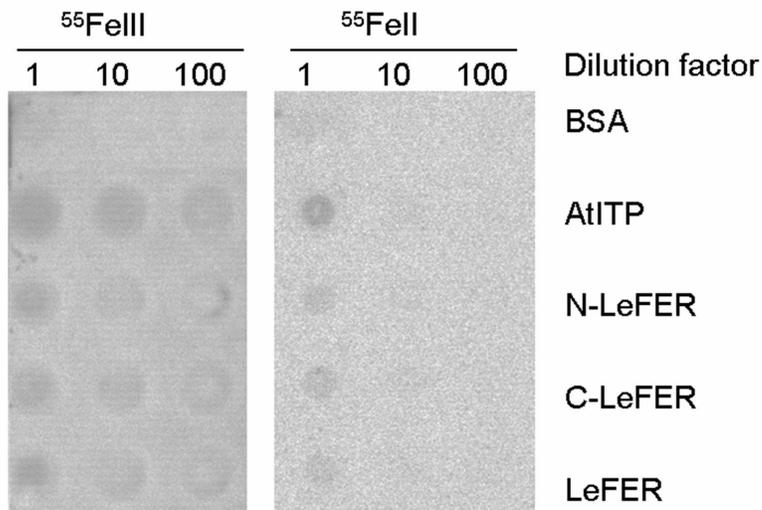
Figure 11: LeFER Fe binding assay.

Affinity purified recombinant LeFER, N-LeFER, and C-LeFER proteins were tested for Fe-binding ability in an *in vitro* dot blot assay with radioactive ^{55}FeIII or ^{55}FeII. AtITP (kindly provided by Prof. R. Hell) was used as a positive control; BSA was used as a negative control. All proteins were spotted in equal molarity ($7.2*10^{-6}$ mol), and in three different dilutions (dilution factor 1, 10, or 100).

4. Results

4.4. Screening for Putative LeFER Interaction Partners by Yeast Two-Hybrid Assay

We have shown that *LeFER* is regulated by Fe availability and may act as a transcription factor in Fe-deficiency induced responses of tomato roots. Homo- and/or heterodimerization have been reported for a number of bHLH transcription factors. We have performed a Yeast Two-Hybrid screening for putative LeFER interaction partners, using a cDNA library from Fe-deficient wild type tomato roots (see section 3.2.2.3.). Since the LeFER protein shows transcriptional self-activation in yeast (see above), we have performed independent screens with four LeFER deletion constructs – LeN, LeC, Leb+HLH+C, and LeHLH+C, which do not activate transcription on their own (Fig. 10). Yeast strain Y187 containing one of the deletion constructs (bait) was mated with strain AH109 containing the cDNA library. Diploids were selected on low stringency medium (SD-His/Trp/Leu + 4 mM 3-AT), which only allows growth of cells expressing bait (-Trp selection) and library cDNA fragments (-Leu selection) which interact (-His selection). Single colonies growing on the triple selection medium were additionally tested for *lacZ* reporter gene activation to confirm presence of interaction. Library cDNA fragments from *lacZ* positive colonies were amplified, sequenced, and database BLAST searches were performed. Sequences from positive clones were identified either as Expressed Sequence Tags (ESTs; partial, single-pass sequences from either end of a cDNA clone), such as AI, BI, BG Gene Bank identifiers, or as Tentative Consensus sequences (TCs; created by assembling ESTs in virtual transcripts).

When using the N-terminal part of LeFER (LeN) or the bHLH+C-terminal part of LeFER (Leb+HLH+C) bait constructs, no *lacZ* positive colonies or PCR products corresponding to putative interaction partners could be obtained (Table 4). However, both the HLH+C-terminal part of LeFER (LeHLH+C) and the C-terminal part of LeFER (LeC) bait constructs yielded several putative binding partners – 2 and 14, respectively (Table 4). PCR fragments amplified from different *lacZ* positive colonies, but with the same size and sequences corresponding to the same tomato identity, were considered as one PCR clone.

4. Results

	LeN	LeC	Leb+HLH+C	LeHLH+C
No of triple selection positive colonies	428	725	153	154
No of *LacZ* positive colonies	60	491	0	4
No of sequenced PCR products	7	133	-	4
No of failed sequences	0	18	-	0
No of false positives	7	13	-	0
No of putative interaction partners	0	14	0	2
No of genes represented in multiple clones	-	3	-	1
No of genes represented in single clones	-	11	-	1

Table 4: Summarized results from four independent Yeast Two-Hybrid screens with a cDNA library from Fe-deficient wild type tomato roots, and different LeFER deletion constructs used as a bait. For each experiment, the number (No) of selected diploid colonies, PCR products and identified genes is presented.

Only two putative interaction partners of LeFER could be identified from a Yeast Two-Hybrid screen using LeHLH+C as a bait (Table 5). TC15501 encodes a homologue of a ferredoxin nitrite reductase, whereas AI775423 has unknown function.

Tomato ID	Name	No of Fragments	No of Clones
TC155013	homologue to UP|Q76G13 (Q76G13) Nitrite reductase, partial (71%)	3	2
AI775423	tomato|AI775423	1	1

Table 5: Results from an Yeast Two-Hybrid screen of wild type Fe-deficient tomato roots cDNA library with the HLH+C-terminal part of LeFER (LeHLH+C) used as a bait. Tomato identifiers (IDs), sequence homology, and number (No) of PCR fragments and clones for each independent sequence obtained from *lacZ* positive colonies are presented.

A Yeast Two-Hybrid screen with LeC as a bait yielded 14 putative LeFER interaction partners (Table 6). Three of the sequences – corresponding to geranylgeranylated protein (NTGP5), protein phosphatase 2C (PP2C), and ferredoxin nitrite reductase, were identified in more than one PCR clones (Table 4, 6), which may reflect their higher degree of representation in the library, with NTGP5 identified in 46 % of all PCR fragments. From the three ESTs identified, only BI935216 showed similarity to a polyubiquitin mRNA from *Antirrhinum major* (snapdragon); for the other two ESTs (AI775423 and BG631146) no putative function could be assigned. Two of the identified sequences (TC154302 and BI925177) were considered as false positives due to their negative orientation in the vector pGADT7-Rec containing the cDNA library fragments.

4. Results

Tomato ID	Name	No of Fragments	No of Clones	Functional Cat.
TC155870	similar to UP|Q9ZRD0 (Q9ZRD0) NTGP5, complete (Geranylgeranylated protein)	61	9	1
TC155802	UP|Q6QLU0 (Q6QLU0) Protein phosphatase 2C, complete	24	8	1
TC155013	homologue to UP|Q76G13 (Q76G13) Nitrite reductase, partial (71%)	7	4	2
TC155690	similar to TIGR_Ath1|At5g65640.1 bHLH family protein , partial (48%)	1	1	3
TC153558	UP|Q39257 (Q39257) Ubiquitin, complete	1	1	4
TC155639	similar to UP|Q8VX74 (Q8VX74) Glycine-rich RNA-binding protein, partial (93%)	1	1	3
TC154715	similar to UP|O04287 (O04287) Immunophilin, complete	1	1	4
TC163025	similar to UP|Q84U56 (Q84U56) TMV induced protein 1-2, partial (96%)	1	1	5
TC168593	homologue to UP|Q6T7E8 (Q6T7E8) Adenylosuccinate synthase , partial (27%)	1	1	2
TC163084	homologue to UP|Q9FZ14 (Q9FZ14) Tuber-specific and sucrose-responsive element binding factor	1	1	3
AJ784514	gi|62719020|emb|AJ880385.1| Nt partial mRNA for putative stress related chitinase	1	1	5
BI935216	similar to A. major polyubiquitin mRNA, partial	1	1	4
AI775423	similar to potato|TC130616, EST from abiotic cDNA	1	1	6
BG631146	tomato|BG631146	1	1	6
TC154302	homologue to UP|Q947H2 (Q947H2) Ribosomal protein, complete, false positive	4	3	-
BI925177	homologue to SP|Q10597|ATPG_ ATP synthase gamma chain, false positive	9	7	-

Table 6: Results from an Yeast Two-Hybrid screen of wild type Fe-deficient tomato roots cDNA library with the C-terminal part of LeFER (LeC) used as a bait. Tomato identifiers (IDs), sequence homology, number (No) of PCR fragments and clones, and assigned functional category for each independent sequence obtained from *lacZ* positive colonies are presented. Functional categories are encoded by numbers: 1, signaling; 2, metabolism; 3, regulation; 4, protein degradation and maintenance; 5, biotic stress; 6, unknown.

The 14 identified putative LeFER interaction partners could be grouped in six functional categories (Fig. 12), where categories "regulation" and "protein degradation and maintenance", contained the highest number of identified proteins (each with three members). Each of the rest of the categories: "signal transduction", "metabolism", "biotic stress", and "unknown", contained two identified proteins.
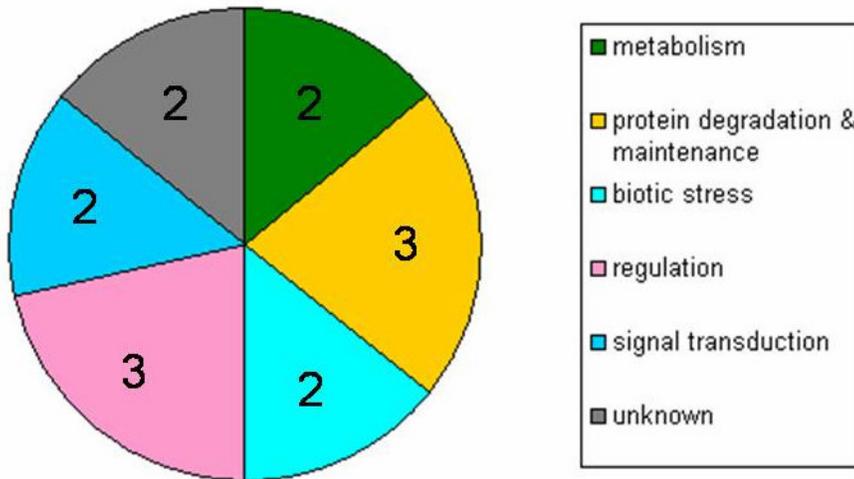
Figure 12: Functional assignment of putative LeFER interaction partners, identified through a Yeast Two-Hybrid screen using LeC as a bait.

Fourteen putative LeFER interaction partners are grouped in 6 functional categories (see Table 6). The number of proteins falling into each category is represented in the respective pie chart piece.

Interestingly, when comparing the two screens – with LeHLH+C and LeC baits, it becomes evident that although LeHLH+C yielded only 2 putative LeFER interaction partners, both of these proteins were also identified in the LeC screen. This result supports the reliability of the obtained data and hints towards a possible domain discrimination for the binding of the putative LeFER partners. Taken together, the screening in the heterologous yeast system has provided several candidate proteins as possible LeFER interaction partners. Most of them were identified when using the C-terminal part of LeFER as a bait, which is consistent with the general observation that C-terminal parts of bHLH proteins are responsible for protein-protein oligomerization (Murre et al., 1994).

4. Results

4.5. Screening for Fe- and LeFER-Regulated Proteins by Two-Dimensional Electrophoresis (2-DE)

So far, little is known about the signaling and metabolic networks underlying the complex processes in plants which lead to a response to Fe deficiency. We do not know which proteins, other than Fe-mobilization components, are acting in the LeFER pathway. With the aim to identify new proteins involved in the LeFER-regulated Fe-deficiency response, we have analyzed the root proteome from plants with different *LeFER* genotypes and exposed to varying Fe-supply conditions.

4.5.1. Design of the Proteomics Experiment

For proteomics studies, we employed two-dimensional gel electrophoresis (2-DE) coupled with protein identification by mass spectrometry. We screened for three groups of differentially expressed proteins, namely for proteins whose expression was dependent on Fe supply, for proteins whose expression was dependent on LeFER activity, and for proteins whose expression was dependent on both, Fe supply and LeFER activity. We have used for our experiments three different plant genotypes (*fer* mutant, wild type, and 35s1 transgenic plants) that we grew each for eight days under three different Fe-supply conditions (0.1, 10, and 100 µM FeNaEDTA). *fer* mutants can be considered Fe-deficient due to genetic factors (genetically induced Fe deficiency), whereas wild type and 35s1 plants were only Fe-deficient when exposed to low Fe supply (physiologically induced Fe deficiency). For these reasons we have examined the root proteome changes after a period of eight days of Fe deficiency. Prolonged changes to Fe deficiency will be manifested in the root proteome allowing for better comparison between genetically and physiologically-induced Fe deficiency. Roots from the nine samples were collected. Three independent biological repetitions (harvests) were examined, whereby each biological repetition included three technical repetitions. The structure of the experiment is presented in Figure 13.

4. Results
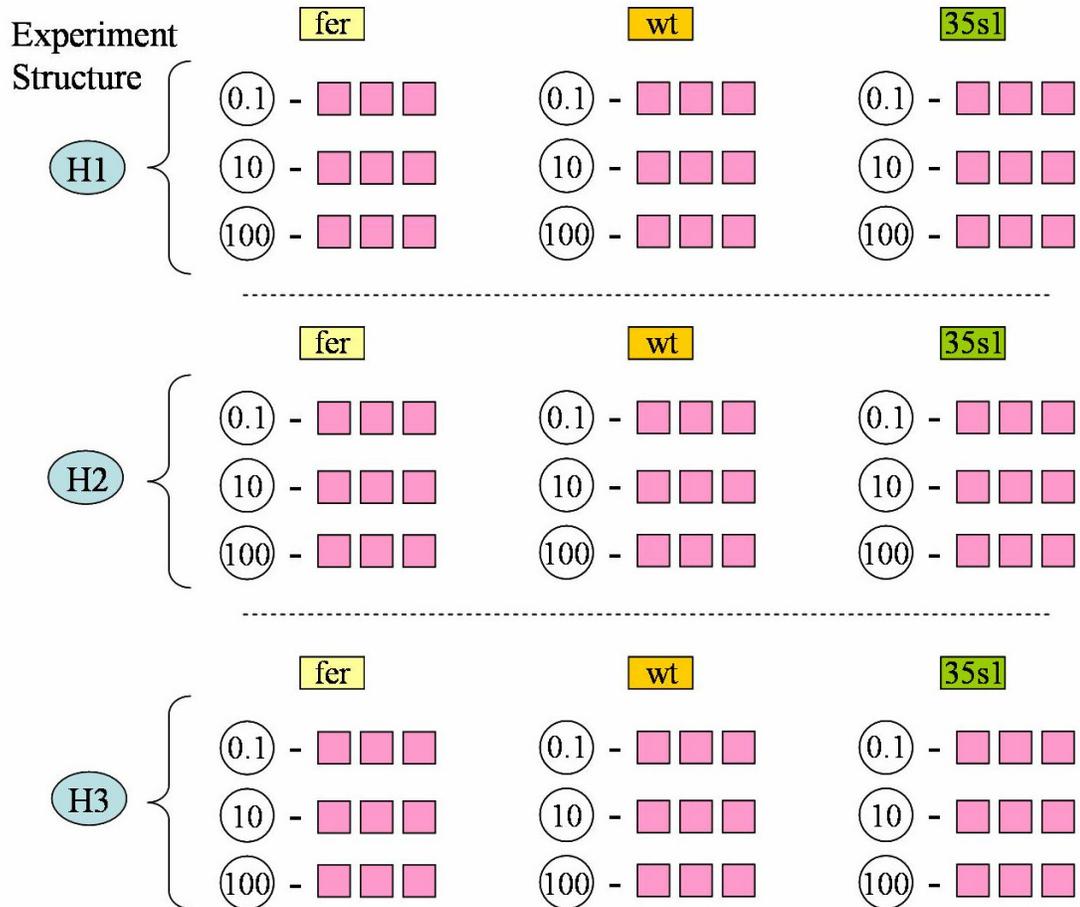
Figure 13: Structure of the proteomics experiment performed on tomato roots.

Protein samples for 2-DE were extracted from tomato roots from three different plant genotypes (*fer* mutant, wild type (wt), and 35s1 transgenic plants) grown under three different Fe-supply conditions (0.1, 10, and 100 µM FeNaEDTA). Three different biological repetitions (harvests, H1-3) were examined. For each harvest three technical repetitions were performed (represented as pink squares on the scheme). In total, 81 good quality 2-DE gels were obtained and processed.

We used a protocol for protein extraction from the collected tomato root samples for obtaining cytosolic and organelle (nuclei, mitochondria, plastids, etc.) proteins (see section 3.2.4.7.). 175 µg of total protein extract from each sample were subjected to isoelectric focusing on 13 cm immobilized pH gradient (IPG) strips in the linear pH range of 3 to 10, and consequently separated according to their molecular weight on 12.5 % SDS polyacrylamide gels. The obtained 2-DE gels (Fig. 14) were quantitatively stained

4. Results
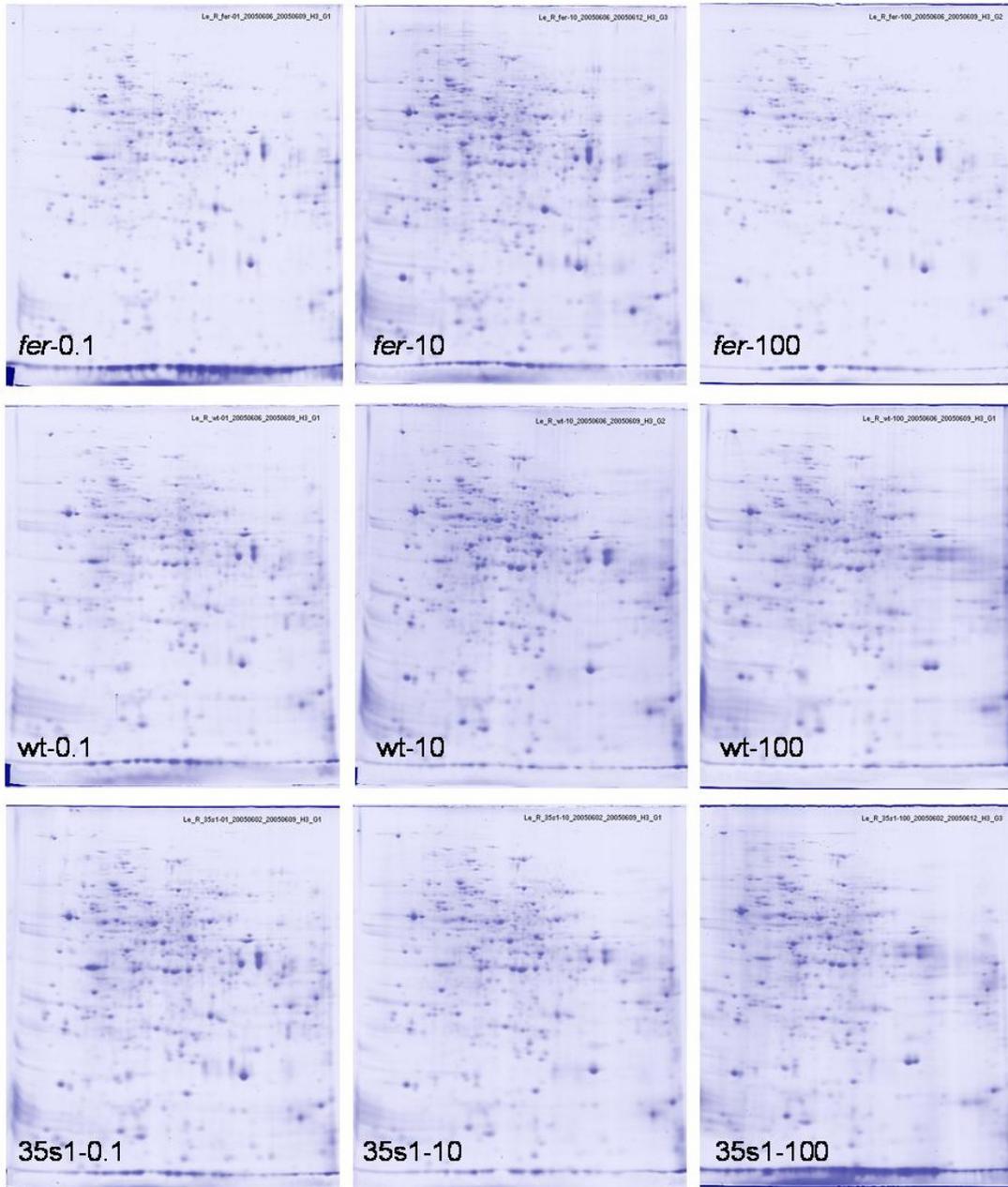
Figure 14: Representative 2-DE gels for each condition used in the tomato root proteomics approach.

Representative Coomassie Brilliant Blue stained 2-DE gels for *fer* mutant, wild type (wt) and transgenic 35s1 plants grown under low (0.1 µM), sufficient (10 µM), and generous (100 µM FeNaEDTA) Fe supply.

4. Results

with colloidal Coomasie Brilliant Blue reagent, imaged and compared in order to identify differentially expressed protein spots. The initial image comparisons were completed using the Phoretix 2D Evolution software, where images could be compared only pairwise, with a set threshold of 1.5 times expression change. However, due to the high number of 2-DE images we later used the more powerful software. PDQuest Advanced (Biorad). PDQuest allowed optimized spot detection and spot matching, and the possibility to compare multiple gels/ replicate groups simultaneously.

In our experimental conditions, we could detect 800-1000 protein spots per protein gel. Interestingly, the highest number of spots was always detectable in the *fer* mutant condition, and even more if *fer* mutants were grown under Fe deficiency (Fig. 15). On the other hand, in wild type and 35s1 samples, equal numbers of about 800 spots were detectable regardless of Fe supply. This observation can be due to an increased protein synthesis or increase in the number of stable degradation products under Fe-deficient conditions and in *fer* mutants.
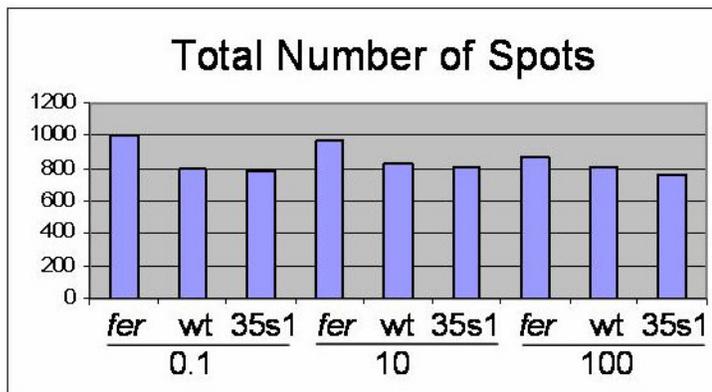
Figure 15: Total number of protein spots detectable by 2-DE analysis.

Nine experimental conditions were examined – *fer* mutant, wild type, and transgenic 35s1 plants grown at low (0.1 µM), sufficient (10 µM) and generous (100 µM FeNaEDTA) Fe supply.

4. Results

4.5.2. Protein Spot Identification

A total of 155 differentially expressed protein spots (Fig. 16) were selected for identification by mass spectrometry. These differentially expressed spots were either induced or repressed in any sample versus another sample. All other detectable spots showed constitutive expression in all genotypes and Fe-supply conditions, and were not considered for analysis. As described in Materials and Methods, we have used two techniques for identification of protein spots. First, all spots were subjected to MALDI-TOF-MS analysis. The determined peptide masses were used to screen the following plant databases: the whole nonredundant NCBI database, the *Viridiplantae* index of the nonredundant NCBI database, the whole SwissProt database, the *Viridiplantae* index of the SwissProt database, and an EST database comprising nucleotide sequences from *L. esculentum*, *S. tuberosum*, and *N. tabacum*. For 66 spots it was possible to obtain a high probability score for a protein identity. However, in 89 cases it was not possible to determine the protein spot identiy. In these cases, we employed nanoLC-ESI-MS/MS to obtain peptide sequences. These sequences were then used to screen the databases again. This way, it was possible to identify further 73 protein spots. Finally, only in the case of 16 out of the 155 spots we could not achieve protein identification. 8 of the protein spots had no known function. In 7 protein spots, 2 different proteins were identified. A list of all investigated protein spots (ordered by SSP number) with their respective putative identity, Gene Bank accession number(s) and assigned functional category is presented in Appendix A.

Several of the selected protein spots displayed obvious changes in their expression pattern throughout the investigated growth conditions. Two such representative spots are shown in Figure 17.
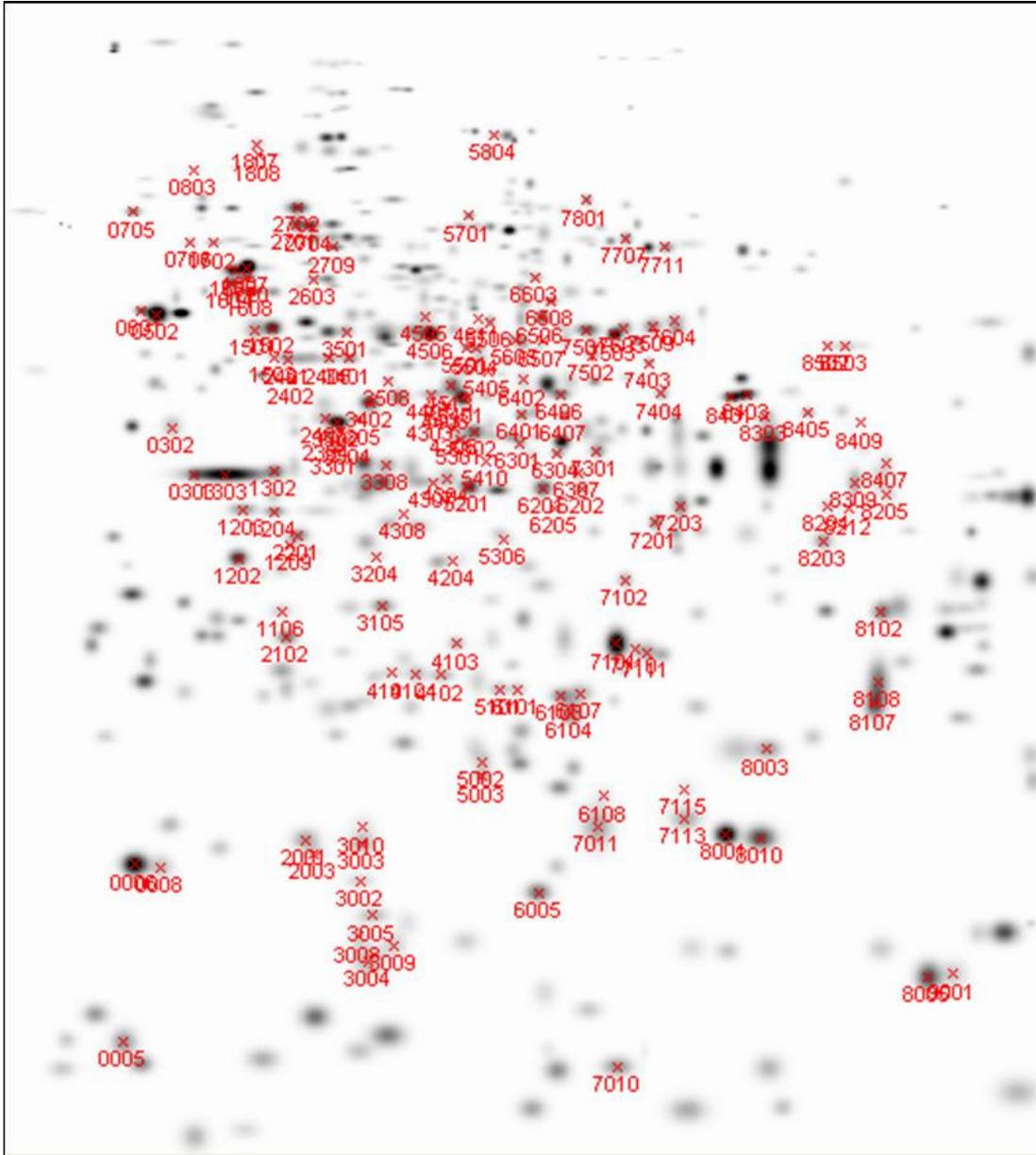
Figure 16: A virtual master 2-DE gel containing all 155 differentially expressed protein spots, which were identified from the tomato root proteomic analysis.

Differentially expressed protein spots are marked with their SSP numbers, obtained after analysis with the PDQuest Advanced software, according to their position on the master gel.

4. Results
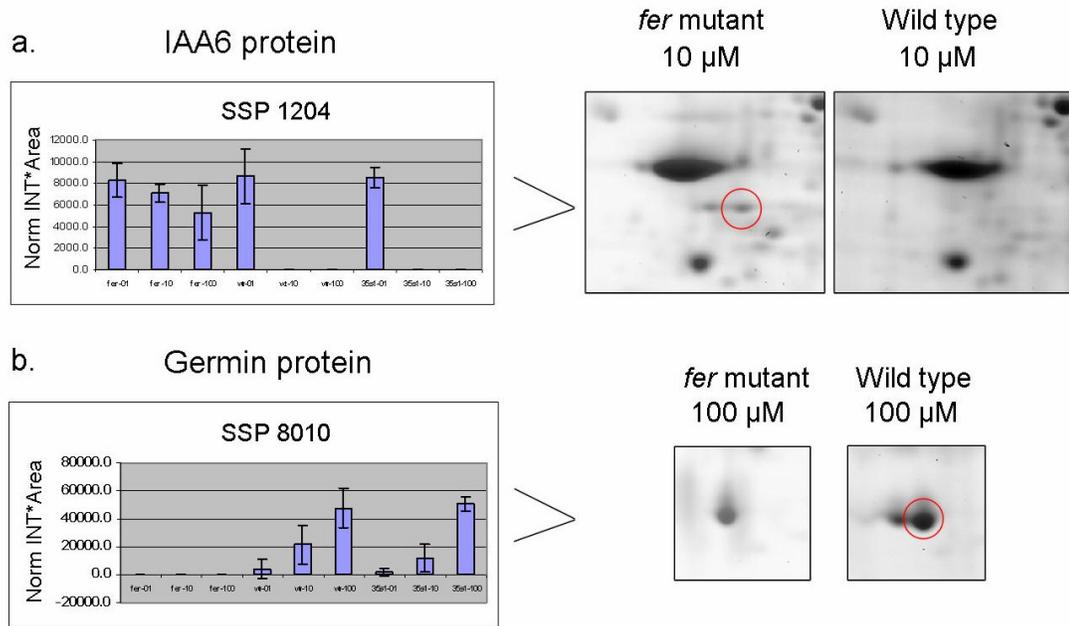
Figure 17: Representative differentially expressed protein spots.

Representatives of differentially expressed protein spots: (a.) with strongly induced expression by Fe deficiency in wild type (wt) and 35s1 plants, but only slight response to Fe supply in *fer* mutant plants, exemplified by IAA6 protein (SSP 1204), and (b.) with strongly induced expression by high Fe supply in wild type and 35s1 plants, but no expression in *fer* mutant plants, exemplified by germin protein (SSP 8010). Graphs represent protein expression levels based on normalized intensity for area (Norm INT*Area) for each investigated growth condition. n = 3 for 3 biological replicates (harvests). Bars indicate SD. Red circles indicate the respective protein spots on magnified views of representative Coomassie Brilliant Blue stained 2-DE gels.

Analysis of protein spot identities showed that the spots belong to proteins with different types of functions (Fig. 18). Almost one-third of all differentially expressed proteins have metabolic functions in energy, carbohydrate, nitrogen, amino acid, or other metabolic pathways. 19 % of the proteins are involved in the response to oxidative, abiotic, biotic or more general stress. The third largest group of differentially expressed proteins (15.4 %) function in protein degradation pathways or in maintaining protein folding and stability. The other proteins are involved in regulation (4.9 %), signal transduction (3.7 %), protein synthesis (1.9 %), hormone response (1.2 %), etc. 14.8 % of the proteins have unknown function.

4. Results
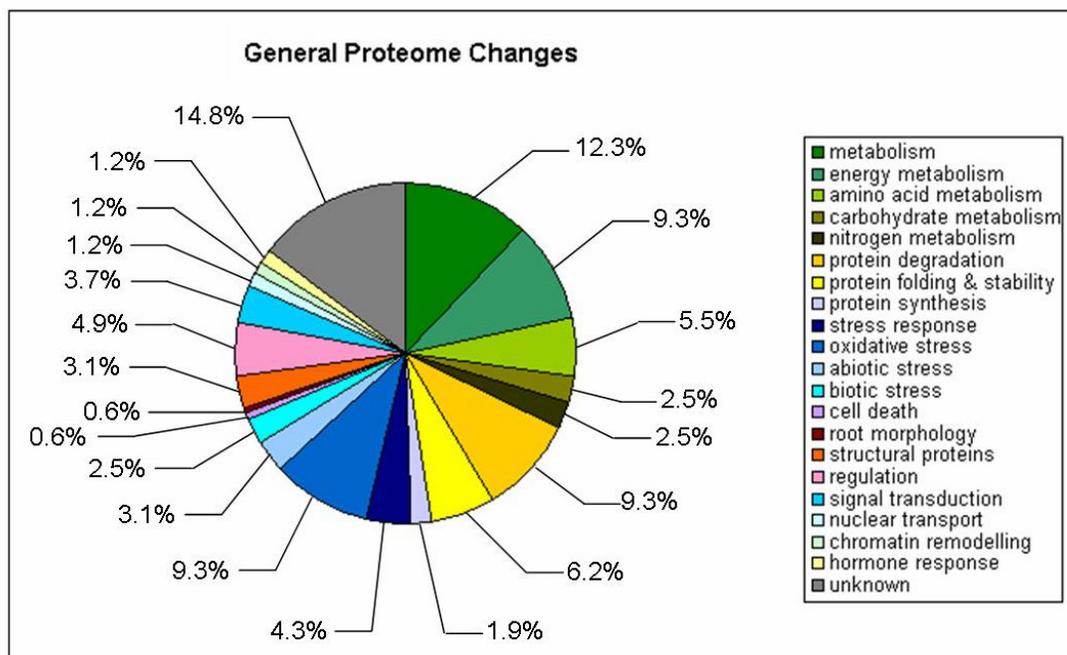
Figure 18: Representation of protein functions belonging to the analyzed protein spots that were differentially regulated by Fe supply conditions and LeFER activity.

Differentially expressed protein spots were organized in 12 functional categories based on their putative identity. In total, 155 protein spots were analyzed, whereby identities were obtained for 139 spots (here taken as 100 %). The number of protein spots falling into each functional category are expressed in percent from the total 139 identified protein spots. See also Appendix A for detailed information.

4.5.3. Statistical Analysis of Expression Data

In order to perform a detailed analysis on the expression pattern of each identified differentially expressed protein spot, the whole data set was subjected to a statistical quality control. First, the consistency of the technical repetitions was confirmed by using both correlation and Euclidean differences (Fig. 19), which made it possible to combine them together into one data matrix. Subsequently, based on the reshaped data set, the consistency of the biological repetitions was examined. As to be expected, these show higher variability, however, without corrupting the consistency of the data. Thus, the data was considered of good quality and suitable for further analysis.

Then, we investigated further the data with the aim to obtain distinctive clustering of protein identities based on their expression patterns.
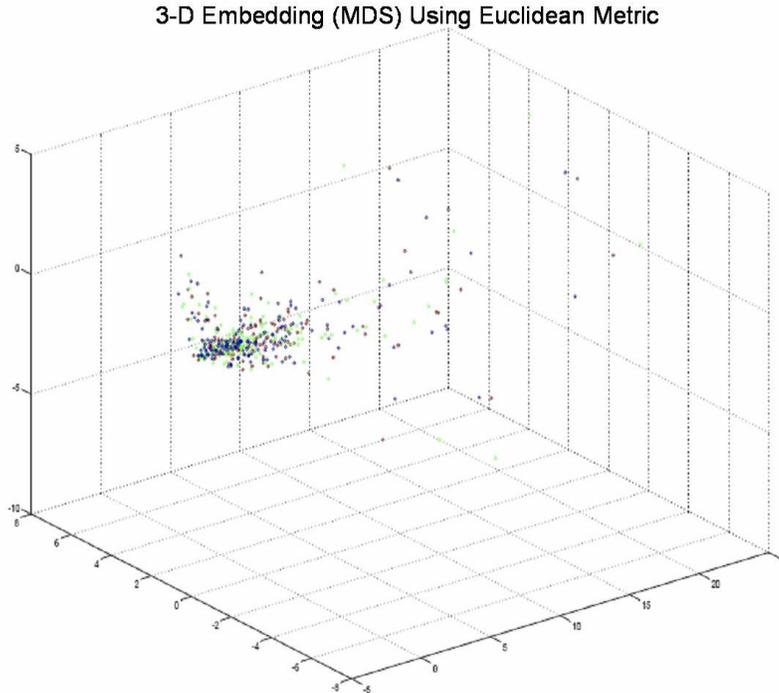
Figure 19: Three-dimensional structure of the tomato roots proteomics data set illustrated by an Euclidean-based embedding technique.

Technical repetitions are presented as data points in three different colours. Data point triplets belonging to the same experiment (harvest) are formed. Outliers, which are not contained in the main data cloud, can be seen on the right hand side of the plot (performed by Dr. Udo Seiffert).

4.5.4. Clustering of Expression Data Using Venn Diagrams

First, we chose to cluster protein spots that were induced in the same Fe-supply condition and in the same line versus any other conditions which could differ between these spots. Venn circle diagrams based on three experimental situations were created to illustrate the relations between different sets (clusters) of protein expression data. Different Venn diagrams were generated for different Fe-supply conditions. For example, protein spots which were found highly expressed in *fer* mutants upon Fe deficiency, but not highly expressed in wild type or 35s1 upon Fe deficiency, were found in the unique section of the *fer* circle. However, protein spots which were highly expressed upon Fe

4. Results

deficiency in *fer* mutants, in wild type and in 35s1 plants, but for example expressed at lower level in other conditions, were placed into the intersection of the three circles. This type of clustering revealed the number of proteins, which were co-induced by the given Fe-supply condition in the specified genotypes (Fig. 20). A list of all protein spots belonging to each of the different expression categories represented with Venn diagrams is provided in Appendix B.

From the Venn diagrams we could deduce the following: The highest number of induced proteins was observed in plants grown under Fe-deficient (0.1 µM, Fig. 20a), compared to sufficient (10 µM, Fig. 20b) and generous (100 µM FeNaEDTA, Fig. 20c) Fe supply conditions – 108 versus 63 and 59 proteins, respectively (all induced proteins irrespective of genotype found at low Fe in all three circles versus all induced proteins found at 10 and 100 µM Fe in all three circles). At the same time, the percentage of *fer* mutant specific spots (found in the *fer*-specific sections) was the lowest at 0.1 µM Fe (14 spots, 13 % of 108 spots), compared to 27 % (17 out of 63 spots) and 25 % (15 out of 59 spots) for 10 and 100 µM Fe, respectively. The number of proteins which were co-induced in an Fe-supply condition in all three genotypes (found in the intersections of all three circles) was two to three times higher upon Fe deficiency than upon Fe supply.

These data indicate that first of all, most of the differentially expressed spots were induced upon an Fe-deficiency condition rather than induced upon an Fe-supply condition. This suggests that proteins are perhaps more likely induced by Fe deficiency rather than suppressed, and that lack of LeFER also results in induction of spots rather than repression. Moreover, the numerous spots induced under Fe deficiency even in the absence of LeFER suggest that the plant can switch on a more general Fe-deficiency response, which does not directly rely on LeFER action.

4. Results
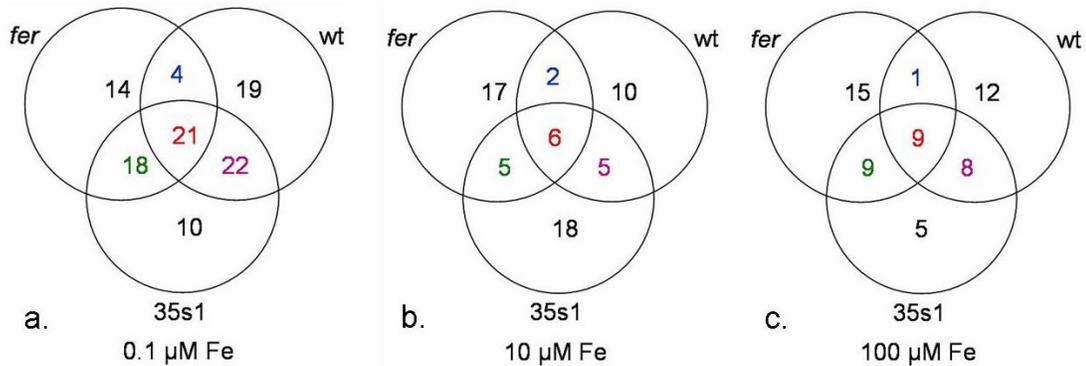
Figure 20: Venn diagrams, representing relations between three sets (clusters) of tomato root protein expression data.

Venn diagrams, illustrating the number of proteins induced in the specified genotype (*fer* mutant, wild type, or 35s1 transgenic plants) grown under the specified Fe concentration (a. - 0.1;b. - 10; or c. - 100 µM FeNaEDTA) versus any of the other Fe-supply conditions. The number of induced proteins which are shared between the different genotypes are found in the intersections and indicated in colour: blue, between *fer* mutant and wild type; green, between *fer* mutant and 35s1 plants; violet, between wild type and 35s1 plants; red, common for all three plant genotypes investigated.

Second, Venn diagrams were also arranged in a complimentary way by analyzing in one diagram two situations (two genotypes, *fer* and wild type, one Fe-supply condition, 0.1 µM Fe) (Fig. 21). This Venn representation describes the dependence of protein expression on LeFER. Proteins can either be induced or repressed, dependent on LeFER or independent (Appendix C; Fig. 21), respectively. Of special interest were proteins belonging to the group "LeFER induced, -Fe induced" (Fig. 21), since these would be proteins induced by LeFER under Fe deficiency, similarly to the FeIII reductase LeFRO1 and the FeII transporter LeIRT1. This expression group contains 9 protein spots, which correspond to 8 different protein identities (Table 7). Spots 8107 and 8108 were both identified as germin-like protein and represent either two different isoforms or modified protein species. The other proteins in the group belong to diverse functional categories such as metabolism, protein degradation, folding and stability, stress response, and structural proteins, indicating the broad spectrum of physiological and morphological processes influenced by the lack of Fe in the plant environment.

4. Results
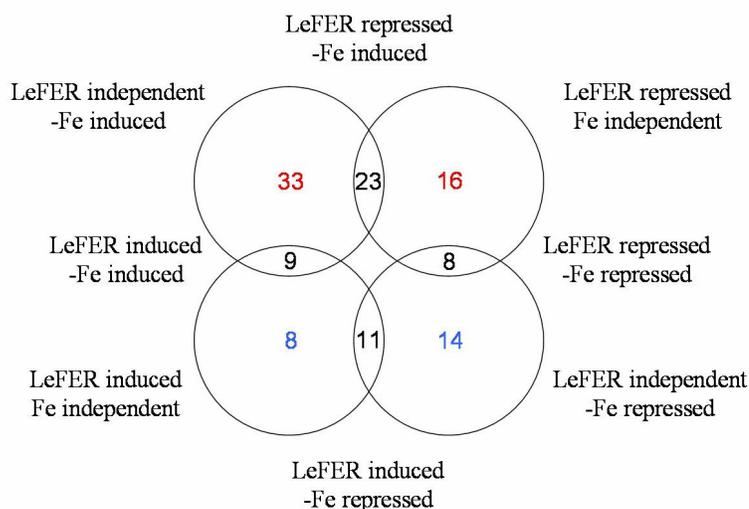
Figure 21: Venn diagrams, representing relations between four different sets (clusters) of tomato roots protein expression data based on LeFER and low Fe supply dependence.

Venn diagrams, illustrating the number of proteins distributed among four expression categories and their intersections. The red numbers indicate induction, the blue numbers repression. Two categories describe proteins with generally (throughout all Fe supply conditions tested) induced or repressed expression in *fer* mutant plants (upper right and lower left circles, respectively). Two other categories describe proteins with induced or repressed expression under Fe deficiency in wild type plants (upper left and lower right circles, respectively). The proteins belonging to each group presented on the diagram are listed in Appendix C.

SSP	Putative Identity	GI	Functional Cat.
0601	similar to 26S proteasome regulatory subunit S5A	TC149782	protein degradation
1503	alpha-tubulin	gi|17402471	structural protein
2702	glucose-regulated protein 78	gi|170386	protein folding & stability
4506	enolase	gi|19281	energy metabolism
5201	cytosolic malate dehydrogenase	TC142327	metabolism
6202	glyceraldehyde 3-phosphate dehydrogenase	gi|2078298	metabolism
6507	DnaJ like protein	gi|6782421	protein folding & stability
8107	germin like protein	TC138076	stress response
8108	germin like protein	TC138076	stress response

Table 7: A list of proteins belonging to the expression group "LeFER induced, -Fe induced" from the Venn diagram clustering shown on Figure 21. SSP number, putative identity, gene identifier (GI), and respective functional category for each protein spot are presented.

4. Results

4.5.5. Clustering of Expression Data Using Expression Patterns

Based on the two Venn diagram representations we obtained an overview about the number of protein changes. However, the Venn diagrams do not allow conclusions about the expression patterns of individual proteins, e.g. whether Fe-deficiency-induced proteins are also induced in *fer* mutants at high Fe or not.

To achieve a more distinctive clustering of proteins based on specific expression patterns, we defined 16 different patterns that included expression profiles throughout all Fe-supply conditions and *LeFER* genotype for each protein spot (Fig. 22). These 16 individual patterns were subgrouped into six categories based on common expression change tendencies (Fig. 22 I. – VI.). A list of all proteins belonging to the respective expression pattern cluster is presented in Appendix D.

Category I contains 14 proteins with LeFER-independent regulation, either induced by Fe deficiency (Fig. 22 Ia., 0.1 µM Fe) or induced by generous Fe supply (Fig. 22 Ib., 100 µM FeNaEDTA) Most of these proteins function in protein degradation, and protein folding and stability.

Categories II to VI contain LeFER-dependent proteins.

Category II contains one stress response protein in two isoforms (or modification states) that was induced by Fe deficiency only if LeFER is present (Fig. 22 II). In the absence of LeFER, this protein was not expressed.

Category III is defined by LeFER-dependent expression, especially at high Fe. This category consists of proteins with reduced (Fig. 22 IIIa. and b.) or zero (Fig. 22 IIIc.) expression in the *fer* mutant (Fig. 22 IIIa.) and high expression at high Fe in wild type (Fig. 22 IIIb. and c.). 50 % of these proteins have metabolism functions, 25 % are involved in different stress responses, 25 % belong to the protein folding and stability, root morphology, and regulation functional categories.

Category IV includes proteins that are expressed at low level at -Fe in the absence of LeFER whereas in the presence of LeFER the expression is constitutively high (Fig. 22 IV). Category IV proteins function in protein degradation, oxidative stress, and as structural proteins. Perhaps these proteins might be downregulated in *fer* mutant plants because they could be toxic at very low Fe, as would be the case in *fer* mutants grown

4. Results

under low Fe supply, or these proteins may have high requirements for Fe which cannot be met in Fe-deficient *fer* mutant plants.

Category V is the largest category (39 protein spots), defining proteins which are highly expressed in the absence of LeFER at low and/or high Fe supply. It contains three subcategories according to the responses of the proteins to Fe supply in the *fer* mutant. The first subcategory (Fig. 22 Va. to Ve.) defines proteins which do not respond to Fe supply in *fer* mutant plants. In wild type and 35s1 plants, their expression is either induced under Fe deficiency (Fig. 22 Va. to Vc.), repressed under Fe deficiency (Fig. 22 Vd.), or unchanged (Fig. 22 Ve.). The second subcategory (Fig. 22 Vf. and g.) describes proteins with induced expression under Fe deficiency in the *fer* mutant, and generally reduced (Fig. 22 Vf.) or zero (Fig. 22 Vg.) expression under all Fe-supply conditions in wild type and 35s1 plants. The third subcategory, Vh., is characterized by an induction at low Fe in both wild type and 35s1 plants but repression by low Fe in the *fer* mutant (Fig. 22 Vh.). Such proteins would need LeFER for their proper induction in response to different Fe supply conditions. In general, one-third of the proteins in category V have metabolic functions, 28 % are stress related, 23 % have unknown function. The remaining proteins are involved in protein degradation, regulation, signal transduction, and hormone response.

Category VI describes deregulated Fe-dependent expression in LeFER overexpressing plants, and contains a single protein involved in protein degradation (Fig. 22 VI). Its expression according to Fe supply is inverted in 35s1 compared to *fer* mutant and wild type plants. Interestingly, for this protein the lack of LeFER does not influence its expression, whereas the overexpression of LeFER does.
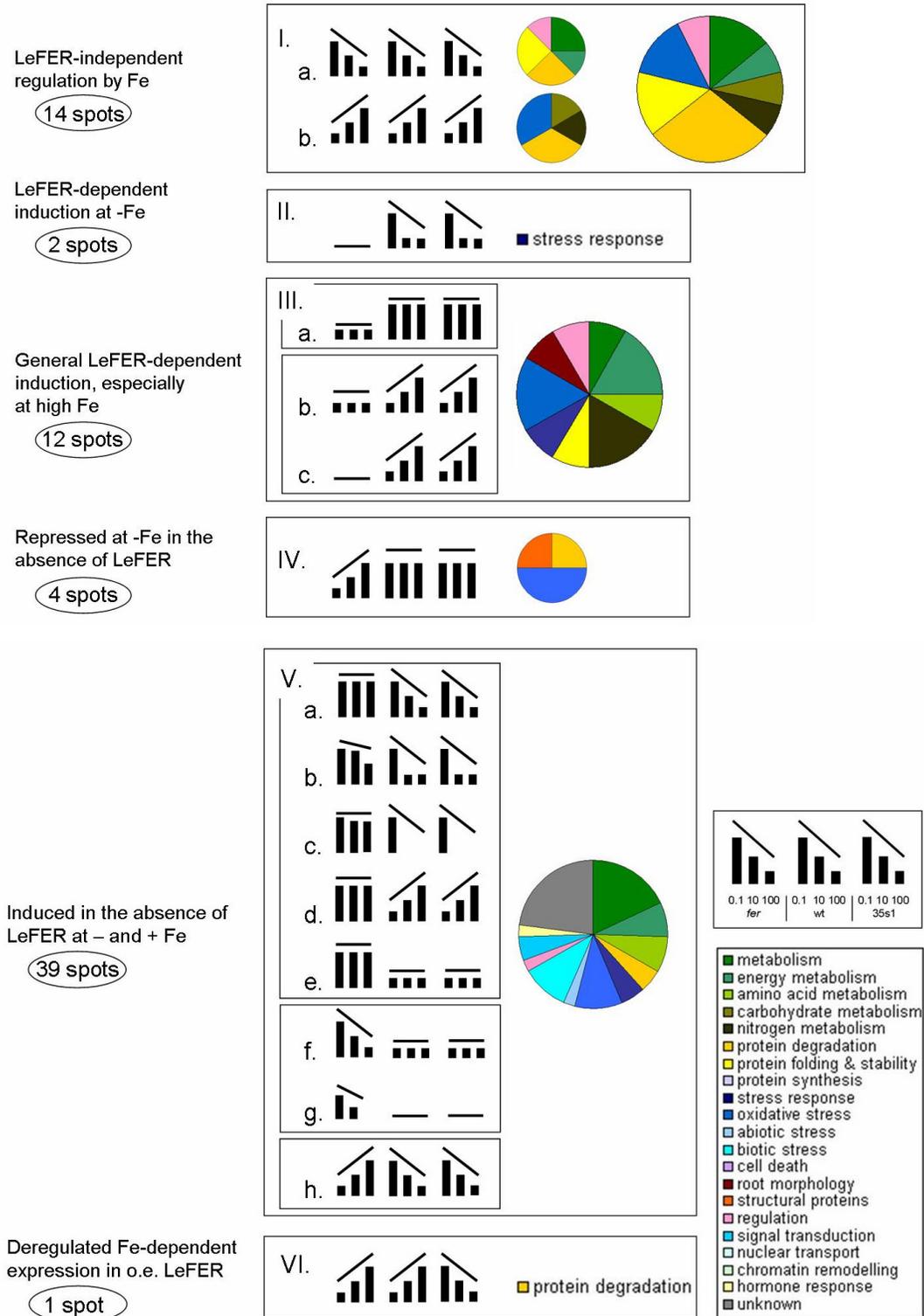
Figure 22: Expression pattern clustering of differentially expressed protein spots identified by the tomato roots proteomics approach (Legend continues on the next page).

4. Results

Differentially expressed protein spots were grouped in 16 distinctive expression patterns (clusters), organised in 6 categories (I. – VI.) with subcategories (Ia., b.; IIIa., b.-c.; Va.-e., f.-g., h.). I., "LeFER-independent regulation by Fe"; II., "LeFER-dependent induction at –Fe"; III., "General LeFER-dependent induction, especially at high Fe"; IV., "Repressed at –Fe in the absence of LeFER"; V., "Induced in the absence of LeFER at – and + Fe"; VI., "Deregulated Fe-dependent expression in o.e. LeFER". The number of protein spots belonging to each category is indicated. Protein expression patterns show the expression change in each plant genotype (*fer* mutant, wild type, 35s1 transgenic plants) throughout the three Fe-supply conditions tested (0.1, 10, and 100 µM FeNaEDTA), with expression change tendencies indicated. For each category, the distribution of the respective proteins in functional categories (in colour code) is presented. A list of all protein spots belonging to a specific category or expression pattern is provided in Appendix D.

4.5.6. Functional Analysis of Expression Data

The obtained clustering, described above, shows how diverse the expression profiles can be in response to LeFER presence and Fe supply. We used this clustering information to address the question how many and which functional categories of proteins are dependent only on Fe supply or only on LeFER. 72 differentially expressed protein spots were used for this functional analysis.

To start, we compared the functions of proteins that were characterized by expression strictly dependent only on Fe supply irrespective of LeFER activity (14 spots, Fig. 22 Ia. and b.; Fig. 23 a.) with the functions that proteins had that were not dependent on Fe and/or were dependent on LeFER (58 spots, Fig. 22 II. – VI.; Fig. 23 b.). Interestingly, we found that among the 14 LeFER-independent spots there were no proteins involved in amino acid metabolism, general stress response, abiotic and biotic stresses, root morphology, structural proteins, signal transduction, hormone response, and proteins with unknown function. But these 14 proteins included several that were involved in carbohydrate metabolism. The functional categories nitrogen metabolism, protein degradation, protein folding and stability, and regulation were also over-represented among the strictly Fe-dependent protein spots. On the other hand, among the 58 LeFER and/or Fe-dependent spots there were no proteins with carbohydrate functions. Protein functions metabolism, energy metabolism, and oxidative stress were similarly represented.

4. Results

Therefore, the protein group dependent only on Fe supply showed generally low functional diversity but elevated representation of specific functional categories like carbohydrate metabolism.

Next, we compared the functions of proteins that were dependent only on LeFER but not on Fe supply (26 spots) (Fig. 22 IIIa., IV., V.e.-g.; Fig. 23 c.) with the functions of proteins that were not dependent on LeFER and/or dependent on Fe supply (46 spots) (Fig. 22 I., II., IIIb. and c., Va.-d. and h., VI.; Fig. 23 d.). This time, we observed that the functional categories amino acid metabolism, abiotic and biotic stresses, and structural proteins, were specifically represented only among the 26 proteins that were LeFER-dependent. On the other hand, in this group, proteins from the categories carbohydrate metabolism, protein folding and stability, general stress response, root morphology, and hormone response, were not present. Reduced representation was noted for the categories energy metabolism, protein degradation, and oxidative stress. Proteins with unknown function were represented to a higher degree. The functional categories metabolism, nitrogen metabolism, regulation, and signal transduction, were regulated to a similar extent among the two groups of proteins.

In conclusion, this analysis shows that strictly Fe- and strictly LeFER-dependent spots were not only characterized by different expression patterns but also by different functions. Our analysis also showed that a majority of proteins have an expression pattern that was dependent on both LeFER and Fe supply.

We further refined the above functional analysis in order to distinguish spots with higher expression and lower expression inside the above specified strictly Fe- or strictly LeFER-dependent groups. For that purpose, the clustering of spots in the pie charts described in Figure 23, was used to produce a segregated version (Fig. 24). For segregation, we took apart the proteins with expression at low Fe supply (Fig. 24 a.) from the proteins with expression at high Fe supply (Fig. 24 c.) in the group of proteins with strictly Fe-dependent expression. Similarly, in the group of strictly LeFER-dependent expression, we took apart the proteins with high expression in the presence of LeFER (Fig. 24 e.) and low expression in the presence of LeFER (Fig. 24 g.).
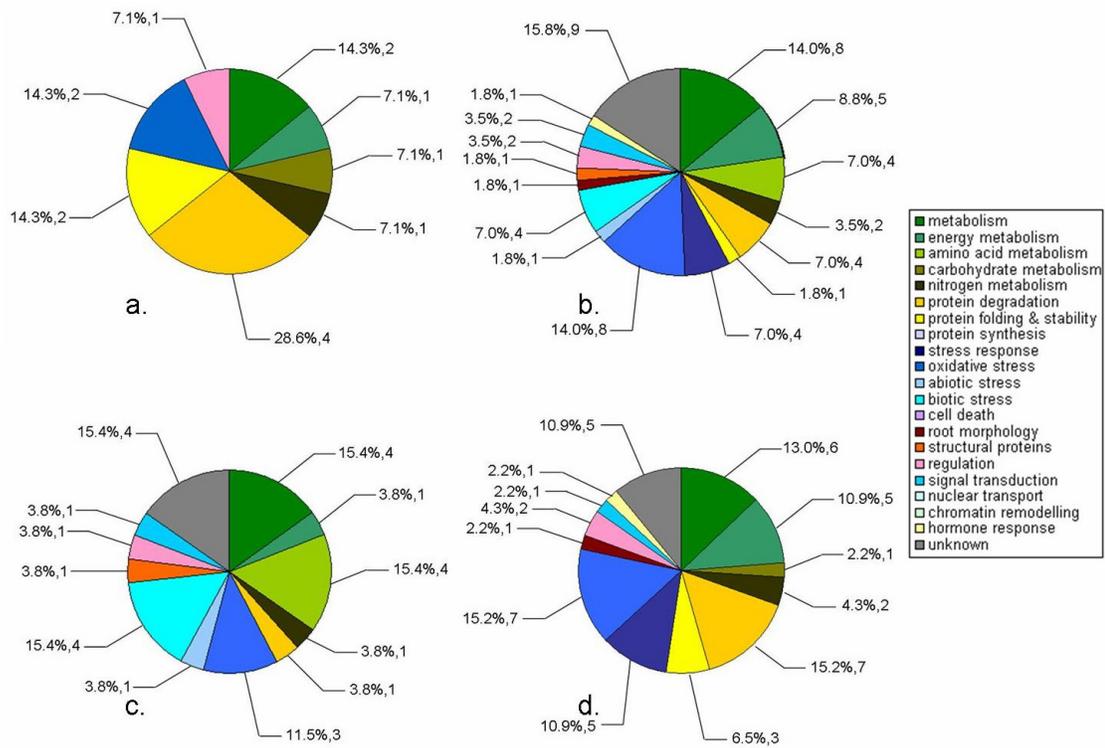
Figure 23: Pie charts representing differentially expressed protein spots grouped in functional categories according to the dependence of their expression on Fe supply and LeFER presence.

Colour coded pie charts represent: (a.) protein spots which expression depends only on Fe supply, versus (b.) the rest of the protein spots, with expression dependent on both LeFER presence and Fe supply; (c.) protein spots which expression depends only on LeFER presence in wild type plants, versus (d.) the rest of the protein spots, with expression dependent on both LeFER presence and Fe supply. The percentage and number of protein spots belonging to each functional category are presented.
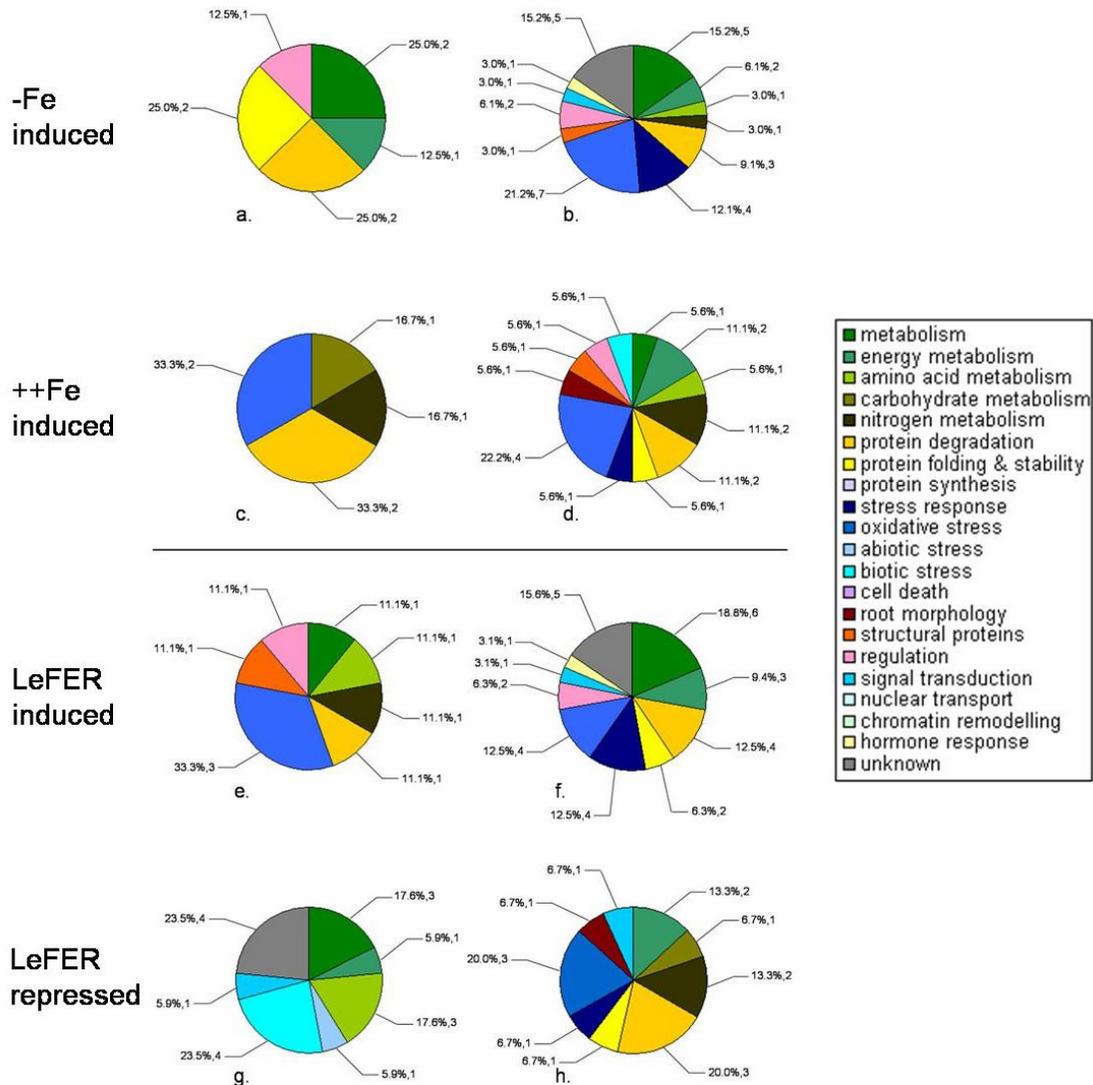
Figure 24: Pie charts representing differentially expressed protein spots grouped in functional categories according to the dependence of their expression on low or high Fe supply (a.-d.), and induction or repression by LeFER (e.-h.).

Colour coded pie charts representing additional segregation of functional categories extracted from Figure 23. **-Fe expressed**: (a.) protein spots with expression depending only on Fe supply which are induced by Fe deficiency, versus (b.) the rest of the protein spots, with expression dependent on both LeFER presence and Fe supply; **++Fe expressed**: (c.) protein spots with expression depending only on Fe supply which are induced by generous Fe availability, versus (d.) the rest of the protein spots, with expression dependent on both LeFER presence and Fe supply; **LeFER expressed**: (e.) protein spots with expression depending only on LeFER presence in wild type plants, which are induced by LeFER, versus (f.) the rest of the protein spots, with expression dependent on both LeFER presence and Fe supply; **LeFER**

4. Results

downrelated: (g.) protein spots with expression depending only on LeFER presence in wild type plants, which are repressed by LeFER, versus (h.) the rest of the protein spots, with expression dependent on both LeFER presence and Fe supply. The percentage and number of protein spots belonging to each functional category are presented.

With the help of this clustering, interesting correlations could be observed. Low and high Fe supply showed induction of distinct functional categories of strictly Fe-dependent proteins. The expression of proteins involved in metabolism, energy metabolism, protein folding and stability, and regulation was enhanced at low Fe. In contrast, high Fe resulted in higher expression of proteins with carbohydrate metabolism (which is specific for the group of strictly Fe-dependent proteins), nitrogen metabolism, and oxidative stress functions. The only shared functional category was protein degradation, with higher representation in the group of high Fe expressed protein spots.

In a similar fashion, proteins strictly regulated by the presence of LeFER fell into distinct functional categories depending on whether they were up- or down-regulated. The presence of LeFER resulted in upregulation of proteins with functions in nitrogen metabolism, protein degradation, oxidative stress, structural proteins, and regulation. On the other hand, the presence of LeFER resulted in downregulation of proteins involved in energy metabolism, abiotic and biotic stresses, signal transduction, and unknown proteins. Two functional categories were shared – metabolism and amino acid metabolism, both of them with higher representation in the group of proteins downregulated by LeFER.

Taken together, the clustering revealed striking discrimination in the regulation of distinct functional groups of proteins in response to Fe supply and LeFER activity.

5. Discussion

Here, we analyzed the upstream regulation of the *LeFER* gene and LeFER protein essential for the onset of Fe mobilization responses at low Fe supply. LeFER protein action is controlled through transcriptional regulation at the mRNA level and posttranscriptional regulation at the protein level, depending on the Fe nutritional status. The action of LeFER is suppressed by high Fe, whereas at low Fe LeFER exerts positive control over Fe mobilization responses. These findings are in agreement with the evolutionary tendency for negative control of key regulators in cellular processes.

We mapped the transcription activation domain in the LeFER protein, and identified putative interaction partners of the transcription factor in heterologous yeast system screens. A tomato roots proteomics approach identified a diverse set of proteins expressed under the control of LeFER and/or Fe supply. Their analysis revealed further functions of LeFER in plant defense and the maintenance of a fine-tuned balance between different stress responses according to the immediate plant needs.

5.1. Transcriptional and Posttranscriptional Control of LeFER

The bHLH domain protein LeFER is a nuclear protein in plant cells that has transcription factor activity in yeast cells and, presumably, also in plants. As a regulator for Fe uptake, LeFER is supposed to sense the Fe nutritional status upstream of its action. We found regulation of LeFER at different levels. First, the *LeFER* gene was regulated at the transcriptional level by Fe, whereby gene expression decreased with Fe supply. This effect was very consistent when comparing generous Fe supply (a physiologically optimal condition) with low or sufficient Fe supply conditions. However, Fe regulation was not consistent when comparing low and sufficient Fe supply. Occasionally, *LeFER* mRNA levels were higher at low Fe supply versus sufficient Fe supply, and, at other times, the levels were similar as was previously described by Ling et al. (2002). Up-regulation of *LeFER* mRNA at low and sufficient Fe supply compared to generous Fe supply suggests that additional upstream Fe-regulated transcription factors may control *LeFER* gene expression.

5. Discussion

Second, LeFER protein was controlled at the posttranscriptional or protein stability level. In wild type, *chloronerva*, and *fer* mutant plants, the amount of *LeFER* transcripts correlated well with the amount of LeFER protein. An exception to this was observed in transgenic lines expressing a functional LeFER protein using the constitutive 35S promoter in the *fer* mutant background instead of the natural *LeFER* promoter. The 35S promoter was not regulated by Fe and resulted in constitutive *LeFER* mRNA expression levels. Despite this, LeFER protein was downregulated at generous Fe supply in these transgenic lines. Since the transgenic *LeFER* cDNA constructs were devoid of the natural 5' and 3' untranslated region of the *LeFER* gene, downregulation of LeFER protein was presumably not the effect of low mRNA stability due to the untranslated regions. Most likely, LeFER was affected at the level of protein stability at generous Fe supply. Downregulation of LeFER protein was evident in Western blot experiments as well as in single root nuclei immunolocalization studies.

We also observed a discrepancy between previously studied mRNA in situ expression (Ling et al., 2002) and protein in situ expression investigated here. In the undifferentiated root cells of the root tip, *LeFER* mRNA in situ signals were detected in all cells in transverse sections, while protein signals were present in all cells except those of the root cap. In the elongating root zone, mRNA signals were mainly present in the epidermis and, to a lesser degree, in cortical cells. However, protein signals were mainly present in the epidermis and in an inner ring of cells, perhaps the differentiating endodermis, surrounding the vascular cylinder, as well as to a lower extent in cortical cells. In the root hair zone, expression of mRNA and protein signals were both confined to parenchymatic cells in the vascular cylinder. Since the same protein expression pattern was observed between plants expressing *LeFER* behind its natural promoter and behind the constitutive 35S promoter, we suggest that LeFER protein was differentially stable in different root tissues. The root cells that express LeFER protein seem relevant for regulation of Fe uptake at the root tip, such as the epidermis, the developing endodermis, and the vascular parenchyma.

Third, LeFER protein was controlled at the level of protein action. Ectopic expression of the LeFER gene in roots grown upon sufficient Fe supply or in leaves did not result in elevated expression of *LeFER* gene-dependent *LeIRT1* or *LeNRAMP1* genes as shown by

5. Discussion

Bereczky et al. (2003). Here, we showed that, in these cases, LeFER protein was produced. Despite that, LeFER was not sufficient for inducing the downstream responses. For its action as a transcription factor, LeFER might require an additional protein-binding partner or, alternatively, LeFER might be activated or inactivated by posttranslational modifications.

Control of LeFER at different levels may allow a rapid and fine-tuned adaptation to changing Fe requirements. Levels of active LeFER protein appear to be controlled more tightly than the levels of *LeFER* mRNA. Available *LeFER* mRNA may represent a reserve for new protein production even under conditions of generous Fe supply, where LeFER protein is rapidly degraded or not produced. At sufficient Fe supply, control of LeFER protein action seemed more important than control through protein production or stability. Interestingly, protein stability control was also discussed for AtIRT1 and AtFRO2, two essential components for Fe mobilization in Arabidopsis (Connolly et al., 2002, 2003), and might be a general feature involved in plant Fe regulation.

5.2. Fe-Availability Signals Regulating LeFER

It was previously hypothesized that nicotianamine (NA) may act as a sensor for Fe availability in the network of events controlled by *LeFER* (Bereczky et al., 2003). Increased *LeFER* mRNA and LeFER protein expression were detected at generous Fe supply in the *chloronerva* mutant. Despite the high Fe concentration in the environment, LeFER protein was stable in *chloronerva*. Phenotypic analysis showed that *chloronerva* mutant plants responded to Fe and were able to overaccumulate Fe and other metals in the roots and in the leaf veins (for review, see Scholz et al., 1992). Generous Fe supply partially rescued the plants, although the interveinal areas of the leaves remained chlorotic and clearly Fe deficient. Despite Fe uptake into *chloronerva* roots, *LeFER* mRNA and LeFER protein levels were elevated, and LeFER protein was active in inducing Fe mobilization genes (see also Bereczky et al., 2003). Thus, since LeFER is not switched off by the high Fe concentrations in the root, it is not likely controlled by a signaling cascade directly emitted from successful Fe transport signals in the root. Most probably LeFER responds to Fe-deficiency signals coming from the chlorotic parts of the shoot.

5. Discussion

We suggest the following model of *LeFER* regulation by NA and Fe availability (Fig. 25). In wild type plants (Fig. 25 A), low Fe supply triggers Fe deficiency in the shoot, which is a signal for upregulation of *LeFER* expression. LeFER, then, switches on the subsequent Fe-deficiency response of the plant – upregulation of the FeIII-chelate reductase (LeFRO1) and the FeII transporter (LeIRT1), leading to elevated Fe uptake into the root. When the plant is provided with generous Fe supply, optimal levels of NA-Fe complexes are available for transport to the shoot. As a result, sufficient Fe in the shoot signals downregulation of both *LeFER* mRNA and protein levels in order to avoid excess Fe accumulation. In this way, the availability of NA-Fe complexes allows the system to distinguish between the different Fe concentrations available to the plant and to adjust the *LeFER* expression levels accordingly. In the *chloronerva* mutant (Fig. 25 B), however, NA is not produced and as a consequence not enough Fe is delivered to the shoot. Fe-deficiency signal is generated into the shoot that triggers both *LeFER* mRNA and protein accumulation. Even when generous Fe is supplied to the plant, the system is misregulated and, as a result, excess Fe and other metals are overaccumulated in the root.

Interestingly, *in vitro* studies demonstrated an Fe-binding ability of the recombinant LeFER protein for both FeII and FeIII ions. It was not possible to determine whether the N- or the C-terminal part of the protein was responsible for the binding, since both parts were able to bind Fe to a similar extent. It is tempting to speculate that Fe (either as FeII or FeIII), possibly delivered as a NA-complex, may serve as an activity modifier of LeFER protein, although further experiments in planta would be necessary in order to prove such hypothesis.

5. Discussion
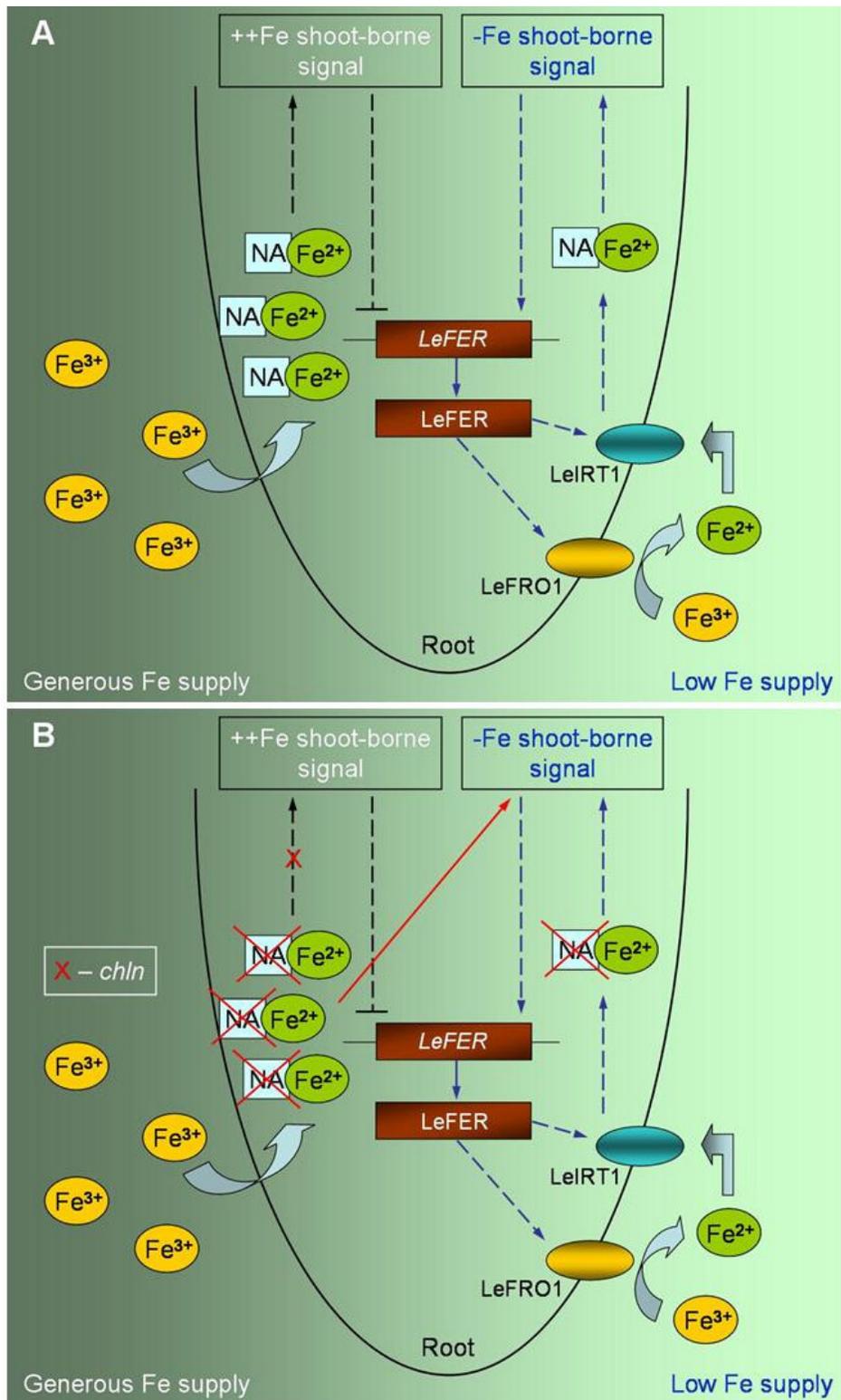
Figure 25: Model of *LeFER* regulation by NA and Fe availability signals (Legend continues on the next page).

5. Discussion

(A) Low Fe supply triggers Fe-deficiency responses in roots of wild type plants (blue arrows) by upregulation of *LeFER* mRNA and protein levels, which leads to upregulation of the FeIII-chelate reductase LeFRO1 and the FeII transporter LeIRT1, thus rendering more Fe available for the plant. Generous Fe supply provides sufficient Fe delivered to the shoot through NA-Fe complexes. This generates a signal leading to downregulation of both *LeFER* mRNA and protein levels, and, as a result, the Fe-deficiency response in the root is blocked (black arrows) in order to avoid excess Fe accumulation. (B) In the *chloronerva* (*chln*) mutant, which lacks NA (red crosses), even generous Fe supply fails to provide sufficient Fe to the whole shoot due to an interrupted Fe translocation. An Fe-deficiency signal is generated in the shoot (red arrow), which keeps LeFER active and the Fe-deficiency response of the root switched on irrespective of external Fe supply, demonstrating the crutial role of NA availability for proper *LeFER* function.

5.3. Protein Networks Involved in the Regulation of Fe- and/or LeFER-Dependent Tomato Root Homeostasis

The search for proteins and protein networks involved in the regulation of processes dependent on Fe and/or LeFER, was attempted in 2 complementary ways. On one hand, we have aimed at identifying proteins which directly interact with LeFER and may or may not depend on Fe availability. On the other hand, a comprehensive proteomics screen for differentially expressed proteins allowed us to pinpoint key changes in the tomato root proteome, and additionally to uncover crosstalks between major metabolic pathways in the cell, in response to changing Fe supply or LeFER presence/activity.

5.3.1. Interaction Partners of LeFER

We demonstrated that LeFER can activate transcription in a heterologous yeast system due to the presence of an activation domain in the protein. By using LeFER deletion constructs, the activation domain was mapped as being shared between the N-terminal part of the protein and the basic part of the bHLH domain. Neither of these two parts could trigger transcriptional activation on its own. The amino acid sequence of the LeFER activation domain region shows no obvious similarity to previously identified transcription factor activation domains which are mainly acidic, as it was shown for example for the herpes simplex virus virion protein VP16 (Triezenberg et al., 1988; Stringer et al., 1990). Most probably LeFER possesses a novel type of transcriptional

5. Discussion

activation domain. Still, the activation ability of LeFER deletion constructs should be additionally verified in planta.

For its action as a transcription factor, LeFER might require an additional protein-binding partner. bHLH domain proteins bind DNA as homo- or heterodimers. The activation domain mapping experiments allowed the use of non-activating LeFER deletion constructs in yeast two-hybrid assays with the purpose of identifying putative direct binding partners of LeFER. The expression of such proteins would not be necessarily dependent on the Fe supply, as LeFER binding partners could either serve for modulating the activity of the protein in response to Fe, or contribute to the cell-specific expression/activity of LeFER in the root.

The use of four different LeFER deletion constructs in Yeast Two-Hybrid assays led to the interesting observation that the domain structure of LeFER based on amino acid sequence apparently reflects functional speciation. The N-terminal part of the protein (LeN), under our screening conditions, did not "fish out" any direct binding partners. On the contrary, the C-terminal part of the protein (LeC) readily interacted with a number of putative protein partners. Regarding the bHLH domain of LeFER, when the whole domain was fused to the C-terminus of the protein (Leb+HLH+C), no binding partners could be identified. Removing the basic part of the bHLH domain from this construct (LeHLH+C) yielded binding partners, although fewer than with LeC – 2 versus 14, respectively. Interestingly, these 2 hits were also identified from the LeC screen, showing the reproducibility of the interactions. Thus, the N-terminal part of the protein, together with the basic part of the bHLH domain, could be responsible for transcriptional activation. The bHLH domain is supposed to act in the process of DNA binding, and the C-terminal part of the protein could be specifically mediating the interaction of LeFER with other proteins. The latter is consistent with the general observation that C-terminal parts of bHLH proteins are responsible for protein-protein oligomerization (Murre et al., 1994).

The identified putative LeFER binding partners fall into 3 categories – nuclear, cytosolic and organelle proteins. An interaction of LeFER with the first group of proteins is consistent with its nuclear localization and transcription factor activity. Of specific interest is the identified bHLH family protein. Interestingly, the interaction occurs also

5. Discussion

through the C-terminal part of this protein, consistent with the above mentioned observation. Additionally, the respective tomato gene shows highest sequence similarity to the Arabidopsis gene At5g65640, which belongs to the same group III of bHLH transcription factors (based on sequence similarity and domain structure) (Heim et al., 2003) as the Arabidopsis homologue of LeFER – AtFRU (At2g28160). According to the Arabidopsis microarray database Genevestigator (https://www.genevestigator.ethz.ch/at/), there is a certain level of tissue and stress response coexpression of the two Arabidopsis genes, which makes At5g65640, and its tomato homologue, good candidates for AtFRU and LeFER binding partners, respectively.

Other putative interaction partners with nuclear localization are the glycine-rich RNA-binding protein, tuber-specific and sucrose-responsive element binding factor, and protein phosphatase 2C. The latter is also of high interest since our data suggests that LeFER, additionally to being transcriptionally and posttranscriptionally regulated by Fe availablity, is also affected on the level of its activity, and phosphorylation would be a possible means for exerting such control on LeFER. Glycine-rich RNA-binding proteins (GRP) have been identified in a number of plants and animals. Most of them have on their N-terminus RNA recognition motif (RRM), which is RNA binding domain, and on their C-terminus glycine-rich domain. It has been suggested that some of them may be involved in stress response, as their mRNA accumulation level was modified following exposure to cold, wounding, acute hypersensitive response, ABA treatment, salicylic acid treatment, or water stress. For example, GRP homologues in Arabidopsis (AtGRP7 and AtGRP8) are regulated by low temperature as well as circadian clock (Heintzen et al., 1997). But the molecular function of GRP remains unknown. The tuber-specific and sucrose-responsive element binding factor (a Myb-related transcription factor) may be involved in sugar signaling and gene expression in relation to carbohydrate metabolism under abiotic stresses. Many environmental stresses like drought, cold and salinity lead to major alternations in carbohydrate metabolism and the sugar signaling pathways interact with stress pathways to modulate metabolism (Price et al., 2004).

A more complex explanation is needed for understanding the identified interactions of LeFER with cytosolic and organelle proteins. First of all, LeFER is synthesized in the cytosol and it may be possible that it is involved in protein-protein interactions before

5. Discussion

being translocated into the nucleus, especially if it has a relatively rapid turnover rate. Second, our data show that LeFER is predominantly localized in the nucleus but we cannot exclude that some portion of the protein remains in the cytoplasm always or only under certain conditions. Interestingly, excluding the enzymes adenylosuccinate synthase (AMP biosynthesis; first committed step) and chitinase (biotic stress response), the rest of the identified cytosolic interaction partners of LeFER – geranylgeranylated protein, ubiquitin, and immunophilin, are involved in posttranslational protein modifications. Ubiquitin acts through its post-translational attachment (ubiquitinylation) to other proteins, where these modifications alter the function, location or trafficking of the protein, or targets it for destruction by the 26S proteasome (Burger and Seth, 2004). Regulatory proteins such as transcription factors and histones are frequent targets of ubquitination (de Napoles et al., 2004). However, it should be noted that ubiquitination normally occurs when the target protein interacts with a specific E3 ligase and then becomes covalently linked to one or more ubiquitin residues (Hatakeyama et al., 2001). In our case, we observe a putative direct interaction with ubiquitin which may reflect a proposed function of ubiquitin as molecular chaperone (Passmore and Barford, 2004) and lead to another type of posttranslational modification – conformational change. Similarly, immunophilin, also known as rotamase or peptidyl-prolyl cis-trans isomerase (PPIase), is involved in proper protein folding and conformational changes (EC 5.2.1.8). The observed interaction with a geranylgeranylated protein may reflect either a transfer of the geranylgeranylted residue to LeFER, thus modifying it, or it may be part of a signaling cascade, since geranylgeranylated proteins have been shown to act as signal transductors (Figueroa et al., 2001; van de Donk et al., 2005). Geranylgeranylated proteins have also been shown to interact with certain proteins and regulate their localization between a membrane and the cytoplasmic pool (Magee and Seabra, 2003).

Clearly, the indication for LeFER modification of any nature is an exciting possibility which has to be pursued in more detail in the future.

LeFER was also shown to interact with nuclear-encoded organelle protein, such as ferredoxin-nitrite reductase (EC 1.7.7.1), in two of our heterologous yeast screens (with both LeC and LeHLH+C used as a bait). Such interaction, as already mentioned above, may occur in the cytoplasm. Nitrite reductase has a single (4Fe-4S) cluster and a

5. Discussion

siroheme, also containing one Fe atom in its structure, as prosthetic groups, thus rendering the molecule highly susceptible to Fe shortage in the cell. Thus, it is tempting to speculate that the loss of the cofactors of nitrite reductase under conditions of Fe deficiency may change the function of the molecule from enzymatic conversion of nitrite to ammonia (using reduced ferredoxin as an electron donor), to a signaling compound, and that change, through interaction of LeFER, could trigger upregulation of Fe-deficiency response in the cell. Such scenario would resemble the well described dual function of the animal aconitase in response to low Fe supply (Klausner et al., 1993). However, more detailed investigations would be necessary in order to check that hypothesis.

In addition, it is important to mention that three of the putative LeFER interaction partners identified in our Yeast Two-Hybrid screens – chitinase, immunophilin, and nitrite reductase, were also detected as differentially expressed proteins in the tomato roots proteomics approach (see below). This shows the good complementarity of the two techniques in discovering proteins involved in the complex networks of Fe-availability dependent and LeFER-controlled events.

5.3.2. LeFER- and Fe-Regulated Protein Networks

Proteomic analysis is recently becoming a powerful tool for the functional characterization of proteins in plants. To date, most broad-scale analysis is performed by transcriptomics, due to its easier handling compared to proteomics. However, many types of information cannot be obtained from the study of genes alone. For example, proteins, not genes, are responsible for the phenotypes of cells. It is impossible to elucidate biological mechanisms, such as the effects of the environment for example, solely by studying the genome. And only through the study of proteins we can characterize posttranscriptional effects and protein modifications.

Due to the availability of vast nucleotide sequence information and based on the progress achieved in sensitive and rapid protein identification by mass spectrometry, proteome approaches open up new perspectives to analyze the complex functions of model plants and crop species at different levels. Along with general limitations of the currently available technologies, however, plant proteome approaches face specific

5. Discussion

challenges. Sample preparation is often more difficult due to the rigidity of plant cell walls or can be compromised by the accumulation of large quantities of secondary compounds in the central vacuole, which upon tissue disruption can lead to protein precipitation (Canovas et al., 2004).

Due to the availability of complete genomic sequence information and of large mutant collections, a number of recent proteome studies have focused on Arabidopsis as a model plant. Still, with the completion of the rice genome and the progress of EST sequencing projects for many other plant species, we are observing an increased use of crop and other model plants.

Here, we have investigated the tomato roots proteome and its response to different Fe supply and LeFER plant genotypes. In particular, we performed protein expression proteomics, which is defined as the quantitative study of protein expression between samples that differ by some variable. In this approach, protein expression of the entire proteome (or of subproteomes) between samples can be compared, and novel proteins involved in the biological process in question can be identified (Graves and Haystead, 2002).

In our study, the proteomes of 9 different samples were compared – *fer* mutant, wild type, and 35s1 *LeFER* overexpressing plants, grown at low (0.1 µM Fe), sufficient (10 µM Fe), and generous (100 µM FeNaEDTA) Fe supply. As a result, 155 differentially expressed protein spots were detected and subjected to protein identification. 139 of them could be identified by MALDI-TOF MS and/or ESI-nanoLC-MS/MS mass spectrometry, that is an almost 90 % success rate. Most of the proteins were identified by LC-MS/MS; MALDI-TOF identification was difficult to obtain for proteins with relatively high or low molecular weights. Database searches, in most cases, yielded identities from tomato or other solanaceous species, such as tobacco and potato, and more rarely from Arabidopsis. This may be due to the fact that tomato is a member of the asterid clade, whereas Arabidopsis belongs to the rosid clade (Savolainen et al., 2000). Approximately 75-125 million evolutionary years separate the two clades.

Comparing the total number of protein spots per 2D-gel for each experimental condition, we observed that *fer* mutant plant gels had more protein spots than those for wild type and 35s1 plants. In addition, for *fer* mutant, this number was decreasing

5. Discussion

gradually from low to generous Fe supply (*fer* 0.1 > *fer* 10 > *fer* 100), whereas for wild type (and 35s1 plants) it did not change (wt 0.1 ~ wt 10 ~ wt 100) (see Fig. 15). Thus, the highest number of protein spots was detected in *fer* mutant plants grown under Fe deficiency, and the lowest – in 35s1 plants grown under generous Fe supply. This may be due to several reasons – an increased number of newly synthesised proteins in response to the severe Fe deficiency, presence of stable degradation products, and/or stabilization of proteins as a result of decreased turnover rate probably due to absence of LeFER activity, in the *fer* mutant plants.

When comparing the number of protein spots among the 72 differentially expressed ones with clear expression patterns (see Fig. 22), which were induced under the respective experimental condition, the following tendency of decreasing spot number was observed: *fer* 0.1 (44 spots) (see Fig. 22 Ia., Va. – g.) > wt 0.1 (40 spots) (see Fig. 22 Ia.; II; IIIa.; IV; Va. – c., h.) > *fer* 100 (37 spots) (see Fig. 22 Ib.; IV; Va., c. – e., h.; VI) > wt 100 (24 spots) (see Fig. 22 Ib.; IIIa. – c.; IV; Vd.; VI). This suggests that the majority of proteins are induced by LeFER at low Fe supply, and much fewer spots are induced at generous Fe supply, leading to the conclusion that LeFER is not as active at generous as at deficient Fe availability, thus confirming our expectations and previous results.

Clustering of the differentially expressed proteins was attempted in several ways.

The distinction between proteins with Fe-regulated LeFER-independent, LeFER-regulated Fe-independent, and Fe-regulated LeFER-dependent expression, revealed that LeFER is involved in the majority of Fe-regulated changes of the proteome, since most of the proteins were dependent on both Fe supply and LeFER presence (32 spots), whereas fewer proteins depended only on LeFER or Fe (26 and 14, respectively) (see Fig. 23). The group of 14 protein spots with Fe-regulated LeFER-independent expression showed the lowest functional diversity, indicating that only very specific metabolic pathways are generally regulated by Fe supply, whereas LeFER regulates/influences a much broader spectrum of pathways.

Proteins with strictly Fe-dependent expression presumably do not act in the pathway of LeFER. If these proteins acted upstream of LeFER we would expect an effect on LeFER and the LeFER-dependent proteins by consequence. If these proteins acted downstream of LeFER we would expect that they would also be influenced by the *LeFER*

5. Discussion

genotype. It is very puzzling the genetically-induced Fe deficiency does not result in differential regulation of these strictly LeFER-dependent proteins. One possible explanation is that the plant acts very early to genetically-induced Fe deficiency via a separate mechanism from the later LeFER-dependent physiologically-induced Fe-deficiency response. From previous studies we know that the *fer* phenotype gets manifested only in the post-cotyledon seedling stage suggesting that LeFER is not essential for early germination and seedling growth. Yet the plants may sense the *fer* defect at this early time point, and adjust accordingly in a manner that renders altered expression of these strictly Fe supply-dependent proteins unnecessary at a later time point.

On the other hand, the presence of strictly LeFER-dependent proteins suggests that LeFER has additional regulatory functions which were previously not known. From the finding that LeFER repressed proteins involved in abiotic and biotic stress irrespective of Fe supply we deduce that this could be a preventive function. Interestingly, *fer* mutant leaves show typical necrosis in addition to chlorosis. Necrosis is never observed in normally Fe-deficient plants.

Based on our observations from the conducted proteomics study, we suggest a model for the network of metabolic pathways regulated by Fe supply and LeFER presence/activity (Fig. 26). Lack of Fe, in LeFER-dependent manner, influences the majority of uncovered metabolic pathways in our study. For example, it affects the expression of proteins involved in general, nitrogen, and energy metabolism, perhaps in an attempt to counteract the increased energy demands of the cells, since the lack of Fe, an important cofactor of many enzymes involved in energy production, depletes the cells of vital reducing agents. Proteins involved in degradation, and proper protein folding and stability, are also regulated by the Fe-deficiency stress through the action of LeFER. The expression of oxidative stress-related proteins is controlled, suggesting the importance of protecting the cells from reactive oxygen species. The activated LeFER protein triggers the expression of signal transduction and regulation proteins, thus probably affecting a wide range of processes and coordinating the flow of the above mentioned metabolic pathways. Interestingly, the regulation of a number of proteins which were annotated as involved in general stress response, root morphology, and hormone response, was not

5. Discussion

possible, in our study, without the coordinated action of Fe supply signals and LeFER, suggesting the need of tight control over these interconnected plant processes.

However, our data shows that the response of the plant on protein level to Fe deficiency in the environment depends mainly but not only on LeFER action. Fe deficiency, independently of LeFER, is sufficient to downregulate enzymes involved in carbohydrate metabolism, which was shown to be highly susceptible to different abiotic stresses (Gupta and Kaur, 2005).

On the other hand, there is a number of pathways regulated only by LeFER presence/activity without direct dependence on Fe supply (in wild type conditions). This category is of particular interest, since it reveals that LeFER does not only serve to induce Fe mobilization responses to Fe deficiency in the root, but it has also additional functions. It influences the expression of certain proteins from functional categories, with shared regulation also by Fe availability with or without LeFER dependence, such as different metabolism branches, protein degradation, oxidative stress, and regulation. However, there are certain categories of proteins which are specifically influenced by LeFER. Structural proteins are upregulated, probably supporting root growth in search of Fe-rich soil patches; different amino acid metabolism proteins are either up- or downregulated; whereas abiotic and biotic stress responses are downregulated. On one hand, the latter is somewhat surprising, since Fe-deficient plants are known to have elevated susceptibility to diseases and one would expect them to counteract this by upregulating defensive biotic stress-related enzymes, such as chitinase, for example. On the other hand, the changes in the proteome suggest that Fe-deficient plants have higher energy demands due to impaired function of the energy producing metabolic pathways. Therefore, it is probably of higher priority for the plant to tightly control all stress-related responses and allow the induction of only those processes which would specifically counteract the Fe-deficiency problem, saving much needed energy and avoiding a hypersensitive response.

Thus, our study revealed an important additional function of LeFER – in protecting the plant and allowing a fine-tuned balance between the different stress responses in accordance with the immediate demands of the organism. An independent confirmation of this is the fact that *fer* mutant, unlike Fe-deficient wild type plants, develops necrotic spots on the leaves, probably due to the lack of protective LeFER activity.

5. Discussion
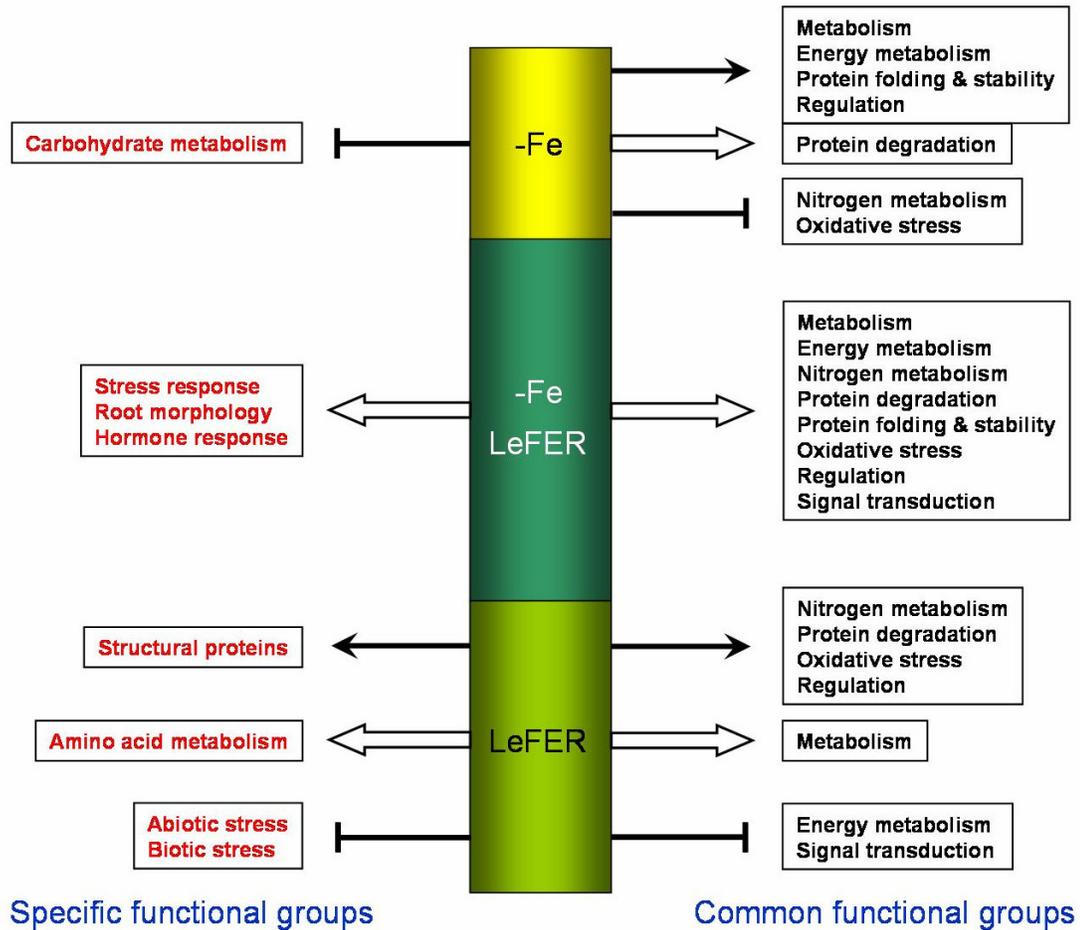
Figure 26: Model of Fe-deficiency and LeFER-action controlled metabolic pathways.

The majority of tomato roots proteome changes are dependent on the concerted action of Fe-supply signals and LeFER presence/activity (**-Fe, LeFER** section of the scheme). A smaller number of metabolic pathways is controlled in a LeFER-regulated Fe-independent manner (in wild type conditions) (**LeFER** section of the scheme). An even smaller diversity of controlled functional groups of proteins is observed in the Fe-regulated LeFER independent group (**-Fe** section of the scheme). The 3 different regulatory sections are scaled to represent the respective amount of regulated proteins. Specific and common functional groups are shown for each regulatory section on the left and right side of the scheme, respectively. Upregulation is indicated by black arrows; downregulation – by black stunted lines; up- and downregulation at the same time – by white arrows. See text for details.

5. Discussion

It is interesting to compare our protein expression data with transcriptomic studies revealing changes on the level of gene expression in response to Fe deficiency, which would allow conclusions about the correlation between the two levels of regulation.

Microarray data for Fe-deficiency responses in tomato was presented by Wang et al. (2002). A high-density array containing 1,280 mineral nutrition-related genes was screened with cDNA probes from mRNA isolated from roots of tomato plants exposed to -Pi, -K, or -Fe hydroponic medium for 0, 1, 3, 6, 12, 24, or 48h. Genes previously not associated with P, K, and Fe nutrition were identified, such as the leucine-zipper transcription factor *Nitf* (*nutrient-induced transcription factor*), MAP kinase, MAP kinase kinase (*MEK1*), and 14-3-3 proteins. These genes had the strongest and most rapid increase in expression in response to changes in plant status for all three mineral nutrients. Unfortunately, it is difficult to compare this data with the results of our proteomics study. The authors have aimed at identifying early changes in transcription in response to the three mineral deficiencies. In our case, the proteome of tomato roots was studied after a prolonged exposure to Fe deficiency in order to identify changes in the protein complement that are specifically caused by the lack of Fe. As it becomes evident from the study of Wang et al., after short exposure to a mineral deficiency the response in the cell is general, not necessarily specific for the exact type of stress that the plant is experiencing.

Two different transcriptomic studies have been performed in Arabidopsis. Colangelo and Guerinot (2004) have reported a microarray analysis of wild type and *fit1-1* mutant plants (lacking a functional *AtFIT1* gene, the Arabidopsis homologue of *LeFER*) grown under Fe-sufficient (50 µM FeIII-EDTA) and Fe-deficient conditions (0 µM Fe + 300 µM ferrozine) for 3 days. In their study, only genes which are upregulated by Fe deficiency in wild type plants and deregulated in Fe-deficient *fit1-1* mutant plants have been analysed. 72 such genes were further divided in three categories according to the expression in the mutant – (a.) with a complete loss of Fe regulation (59 genes), (b.) with a partial Fe regulation (8 genes), and (c.) upregulated at sufficient Fe supply (5 genes). In our case, a more complex array of expression patterns was investigated. Among them, 23 proteins had deregulation at low Fe supply in *fer*, and upregulation by low Fe in wild type plants. 16 of those proteins had expression patterns corresponding to group (a.), 7

5. Discussion

proteins – to group (b.), and no proteins were detected that correspond to group (c.) of the above described study. On the level of gene/protein identity, only few correlations were observed – 4 identities, which generally followed the same corresponding expression patterns – zinc finger (C3HC4-type RING finger) family protein; β-glucosidase; translation initiation factor (5A, in our study, represented in two protein spots); and subtilisin-like Ser protease (represented by two different proteins in three protein spots, in our study). In conclusion, the study of Colangelo and Guerinot is difficult to use for direct comparison with our data because different plants and experimental growth conditions were employed. The authors also observed that certain genes are regulated only by Fe supply without AtFIT1-regulation dependence, however, they did not suggest any additional functions of AtFIT1 except its role in upregulating Fe-deficiency response in Arabidopsis roots.

A second study, by Thimm et al. (2001), used a 6000 cDNA chip and studied expression in Arabidopsis plants of a different ecotype (Landsberg *erecta*) that were grown hydroponically. Here, a set of genes induced under Fe deficiency were identified. Similarly to Collangelo and Guerinot, several genes encoding cytochrome P450-like proteins and zinc finger proteins were reported to accumulate in response to Fe deficiency. Generally, however, the results of these 2 array studies showed little similarity.

In our proteomics study and the study of Thimm et al., changes in the expression of 20 common enzymes, mainly involved in glycolysis, the citrate cycle, and the oxidative pentose phosphate cycle, were observed, with only a slight correlation between mRNA and protein levels. Still, some common conclusion could be made. In Arabidopsis roots, transcription of sequences corresponding to enzymes of anaerobic respiration was found induced. This correlates with our observations of increased protein levels of several glycolytic enzymes, such as glyceraldehyde-3-phosphate dehydrogenase, pyruvate dehydrogenase, fructose-1,6-bisphosphate aldolase, etc. Thus, it seems likely that the energy demand of the roots required for the Fe-deficiency response exceeded the capacity of oxidative phosphorylation, and an increase in anaerobic respiration was required to maintain metabolism.

5. Discussion

It is important to consider that in our case, tomato plants were grown hydroponically under different Fe-supply conditions for 8 days before harvesting. For the transcriptomic study, Arabidopsis plants were grown hydroponically for 1, 3 or 7 days under Fe deficiency. Generally, Thimm et al. observed maximum levels of response at 3 days of treatment, whereas at 1 and 7 days the mRNA levels were relatively low. Interestingly, there was somewhat higher level of correlation between our 2 sets of data when comparing with the 3 days of Fe-deficiency treatment. A possible explanation may be that at 3 days under low Fe supply the mRNA levels peak in order to create a pool of the respective protein. At 7 (or 8) days after the onset of Fe deficiency, the protein pool is already established (observed as high levels of protein expression), and only a basal level of mRNA expression is needed to support it.

Several metabolic enzymes were previously shown to respond to Fe deficiency on the level of enzyme activity, which allowed us to compare the reported changes with our protein expression data. For five enzymes, activity levels under Fe deficiency correlated well with protein expression levels. The glycolytic enzyme glyceraldehyde-3-phosphate dehydrogenase, for example, was shown to have an increased activity in cucumber (*Cucumis sativus*) (Espen et al., 2000), as well as in tomato roots (Herbik et al., 1996). The same was true for the activity of H^+-ATPase (Dell'Orto et al., 2000). Reduced enzyme activity of several Fe-containing enzymes correlated with decreased protein expression, as it was shown for catalase (Machold, 1968), aconitase (De Vos et al., 1986), and Fe-superoxide dismutase (Sevilla et al., 1984). For three enzymes, protein expression and enzyme activity levels differed – formate dehydrogenase (Herbik et al., 1996; Suzuki et al., 1998) and ascorbate peroxidase (Herbik et al., 1996) had increased enzyme activity under Fe deficiency but no increase in protein expression was observed in our study. Peroxidase showed increased protein levels but a decrease in enzyme activity (Machold, 1968), although in this case the comparison is more difficult due to the large number of different peroxidases and peroxidase isoforms. In conclusion, relatively high correlation between protein expression and activity levels was observed. An exception may be represented in some cases by Fe-containing enzymes, where overproduction of the apoproteins probably attemps to counteract the loss of activity.

6. Perspectives

Tomato is a valuable crop species, whose importance as a model plant has increased in the recent years. Molecular biology techniques available for Arabidopsis have also been successfully applied in tomato, and a genome sequencing initiative is currently under way.

The work presented here has aimed to contribute to our understanding of the regulation and underlying molecular mechanisms of an important physiological process for the plant – the uptake of the micronutrient Fe.

The screening for putative interaction partners of LeFER yielded several promising candidates, which could be involved in signal transduction and modification of LeFER function. The interaction of these proteins with LeFER has to be further verified in planta. Several techiques are available. One possibility would be to perform bimolecular fluorescence complementation (BiFC) (Bracha-Drori et al., 2004) by transient expression in protoplasts, in bombarded leaves, or in stably transformed tomato plants. The functional relevance of the interactions could be investigated through a RNAi antisense approach (Vaucheret et al., 2001) or by observing transient downregulation in tomato through virus induced gene silencing (Lindbo et al., 1993; Kumagai et al., 1995).

The proteomics approach presented here has suggested the existence of a network of metabolic pathways under the control of Fe supply and/or LeFER presence/activity. An important information on the extent of posttranscriptional regulation triggered by Fe deficiency could be provided by a complementary transcriptomic study on a tomato microarray chip which has recently become available (Alba et al., 2004).

Additional level of regulation in response to Fe deficiency may be investigated by performing phosphoproteomics studies with the aim to identify activated proteins. This would provide an even more specific picture of underlying events and possibly hint towards new targets of LeFER action.

7. Summary

Iron (Fe) deficiency in humans is the most prevalent nutritional disorder in the world, causing illness, premature death and economic losses. Since plants serve as the primary source of dietary Fe, improving the Fe content of crops could represent an important step towards a better public health. However, to achieve this, a deep understanding of the mechanisms controlling the uptake and distribution of Fe inside the plant is of major importance.

Tomato is a Strategy I-type Fe-efficient plant. Its response to low Fe availability in the environment is characterized by an increase in the amount of FeII in the rhizosphere due to an enhanced proton extrusion from the root and an upregulation of the root FeIII-chelate reductase (LeFRO1) and FeII transporter (LeIRT1). As a result, more Fe is rendered soluble and thus accessible for the plant. Previous work in our group has identified the tomato *LeFER* gene, encoding a bHLH transcription factor protein, as one of the major regulators controlling Fe uptake in the roots under Fe-deficiency conditions.

The aim of the presented study was to investigate the mechanism and regulation of *LeFER* action, and to discover additional components of the Fe-deficiency response in tomato roots, which would allow us to identify the involved pathways and their interconnections.

We analyzed the upstream regulation of the *LeFER* gene and LeFER protein, which is essential for the onset of Fe-mobilization responses at low Fe supply. Our experiments showed a dependence of *LeFER* gene expression on Fe availability. Using the generated affinity purified polyclonal antisera and several tomato transgenic lines constitutively overexpressing *LeFER*, we could demonstrate an Fe-dependent posttranscriptional level of regulation on LeFER protein abundance, which ensures its increased stability (and possibly activity) upon Fe starvation. Thus, LeFER protein action was found to be controlled through transcriptional regulation at the mRNA level and posttranscriptional regulation at the protein level, depending on the Fe nutritional status. The action of LeFER is suppressed by high Fe, whereas at low Fe LeFER exerts positive control over Fe-mobilization responses.

7. Summary

By the use of Arabidopsis protoplasts and tomato root nuclear extracts, we demonstrated the nuclear localization of the LeFER protein. This observation, along with the fact that LeFER can activate transription on its own in a heterologous yeast system, and its role in upregulating a number of Fe-mobilization genes, allowed us to conclude a transcription factor function for LeFER. A transcription activation domain was found to be shared between the N-terminal part and the basic part of the bHLH domain of the protein, which is rather unconventional, considering the fact that most of the demonstrated activation domains are strongly acidic or contain acidic residues among hydrophobic ones (Kotak et al., 2004).

We used non-activating deletion constructs to perform Yeast Two-Hybrid library screens with a generated cDNA library from Fe-deficient tomato roots, which yielded several putative LeFER binding partners. Of special interest is an uncharacterised bHLH protein, since BHLHs are known to function as homo- or heterodimers. Another interesting candidate, identified by this approach, is a protein phosphatase, which hints towards possible regulation of LeFER by phosphorylation, adding a third level of control over its action – the level of protein activity.

A central question in studying Fe homeostasis in plants, and their response to insufficient Fe in the environment, is to unreavel the underlying key metabolic pathways and their interconnections. To address this, and to estimate the role of LeFER in the crosstalk of involved processes, we have used proteomics tools to investigate the changes occurring at protein level when different genotypes (wild type, *fer* mutant, *LeFER* overexpressing line) were grown under different Fe-supply conditions (0.1, 10, 100 µM FeNaEDTA). Our comprehensive study on the identity and expression patterns of selected proteins yielded a network of metabolic pathways regulated by Fe supply and/or LeFER presence/activity, allowing us to pinpoint specific functional groups of proteins with shared types of regulation. Fe deficiency was found to trigger major changes in the plant proteome, ranging from energy balance and stress response to phytohormone signaling. Furthermore, we could reveal an important additional function of LeFER – protecting the plant from hypersensitive response by fine-tunning the control of different stress responses of the plant.

7. Summary

Zusammenfassung

Eisenmangel ist die häufigste Ernährungskrankheit von Menschen, die zu Folgekrankheiten, vorzeitigem Tod und ökonomischen Verlusten führt. Da Pflanzen die primäre Quelle von Eisen (Fe) in unserer Ernährung sind, sind Kulturpflanzen mit verbessertem Eisengehalt ein wichtiger Schritt in Richtung einer besseren Gesundheit der Bevölkerung. Um dies zu erreichen ist es notwendig, die Mechanismen zu kennen, welche die Aufnahme und Verteilung von Fe in der Pflanze kontrollieren.

Tomate ist eine Strategie I Fe-effiziente Pflanze. Tomatenpflanzen reagieren auf niedrige Eisenverfügbarkeit mit Erhöhung der FeII Konzentration in der Wurzelumgebung aufgrund der erhöhten Protonenausscheidung und der Induktion der FeIII-Chelatreduktase (LeFRO1) und des FeII Transporters (LeIRT1). Infolgedessen wird mehr Fe löslich gemacht und steht der Pflanze zur Verfügung. Vorangegangene Arbeiten der Arbeitsgruppe haben *LeFER* als hauptsächliches Regulatorgen identifziert, welches die Eisenaufnahme in Wurzeln bei Eisenmangel kontrolliert. *LeFER* kodiert für einen Transkriptionsfaktor der basischen Helix-Loop-Helix Familie.

Ziel der vorliegenden Arbeit war es, den Mechanismus und die Regulation von *LeFER* näher zu untersuchen, sowie weitere Komponenten der Eisenmangelantwort zu entdecken. Dadurch sollen die beteiligten Wege und Verbindungen der Antworten gefunden werden.

Wir analysierten die oberhalb liegende Regulation von *LeFER* Gen und LeFER Protein, welches für das Anschalten von Eisenmobilisierungsantworten bei niedriger Eisenverabreichung essentiell ist. Unsere Experimente zeigten eine Abhängigkeit der *LeFER* Genexpression von der Eisenverfügbarkeit. Mittels des generierten Affinitäts-gereinigten polyklonalen Antiserums und verschiedener *LeFER* überexprimierender transgener Tomatenlinien konnten wir zeigen, dass LeFER Protein auch durch Fe-abhängige posttranslationale Mechanismen kontrolliert wird. Hierdurch wird eine größere Stabilität des FER Proteins (und dadurch vermutlich höhere Aktivität) erreicht. Das heißt, LeFER Proteinaktion wird durch transkriptionelle Regulation auf mRNA Ebene kontrolliert sowie durch posttranskriptionelle Regulation auf Proteinebene, in Abhängigkeit von der Eisenverfügbarkeit. Die Handlung von LeFER wird durch viel Fe

7. Summary

unterdrückt, während LeFER bei wenig Fe eine insgesamt positive Kontrolle über Eisenmobilisierungsantworten ausübt.

Mit Hilfe von Arabidopsis Protoplasten und Tomatenwurzelkernextrakten konnten wir nukleäre Lokalisation von LeFER Protein zeigen. LeFER konnte die Transkription im heterologen Hefesystem stimulieren. Aufgrund seiner Aktivität in Pflanzen, verschiedene Eisenmobilisierungsgene zu aktivieren, folgerten wir auf eine Funktion als Transkriptionsfaktor, wie es auch für andere bHLH Proteine gezeigt wurde. Eine Transkriptions-aktivierende Domäne wurde geteilt zwischen N-terminalem Teil und basischer Domäne, was eher ungewöhnlich ist. Die meisten Aktivierungsdomänen sind sauer oder enthalten saure und hydrophobe Aminosäuren.

Wir verwendeten nicht-aktivierende Deletionskonstrukte, um eine cDNA Hefe 2-Hybridbank zu screenen, welche aus Eisenmangel-ausgesetzten Tomatenwurzeln präpariert worden war. Mehrere LeFER Bindepartner wurden gefunden. Von besonderem Interesse war ein bislang uncharakterisiertes bHLH Protein, denn bHLH Proteine agieren als Homo- oder Heterodimere. Eine Proteinphosphatase war ein weiterer interessanter Kandidat, der auf eine mögliche Beteiligung von Phosphorylierung bei der LeFER Regulation hindeuten könnte.

Eine zentrale Frage bei der Untersuchung der Eisenhomöostase in Pflanzen ist es, die metabolischen Wege und Verbindungen zu entfädeln. Um dies zu untersuchen und um die Rolle von LeFER bei den Verbindungen der verschiedenen metabolischen Prozesse abzuschätzen, haben wir einen Proteomics Ansatz gewählt und die Veränderungen des Wurzelproteoms in verschiedenen Tomatengenotypen (Wildtyp, *fer* Mutante, LeFER Überexpressionslinie) bei verschiedenen Eisenbedingungen (0.1, 10, 100 µM Fe) analysiert. Diese umfangreiche Studie über die Identifizierung und Expressionsmuster von ausgewählten Proteinspots zeigte ein Netzwerk von metabolischen Wegen auf, welche von Fe und/oder LeFER kontrolliert werden. Diese Proteine konnten in Klassen mit gemeinsamen Funktionen eingeordnet werden. Eisenmangel induzierte Proteomveränderungen, welche den Energiehaushalt, Stressantworten bis hin zu Phytohormonantworten betrafen. Desweiteren konnten wir eine neue Funktion für LeFER vorschlagen, nämlich den Schutz von Pflanzen vor hypersensitiver Antwort durch feinregulierte Kontrolle von Stressantworten der Pflanzen.

8. Abbreviations

2-DE – two-dimensional gel electrophoresis

ACN – acetonitrile

AMP – adenosine monophosphate

ATP – adenosine triphosphate

BCIP – 5-bromo-4-chloro-3-indolyl-phosphate toluidine salt

bp – base pair(s)

bHLH – basic Helix-Loop-Helix

β-ME – β-mercaptoethanol

BPDS – sodium bathophenanthrolinedisulfonate

BSA – bovine serum albumin

CaMV – cauliflower mosaic virus

CBB – Coomassie Brilliant Blue

cDNA – complementary DNA

cfu – colony forming units

CHAPS – 3-[(3-cholamidopropyl)dimethylamonio]-1-propanesulfonate

CHCA – α-cyano-4-hydroxycinnamic acid

Da – dalton (molecular mass)

DAPI – 4',6'-Diamidino-2-phenylindole

DIC – differential interference contrast

DMA – 2'-deoxymugenic acid

dsDNA – double-stranded DNA

DTT – dithiothreitol

ECL – enhanced chemiluminescence

EDTA – ethylenediaminetetraacetic acid

epi-HDMA – 3-epihydroxy-2'-deoxymugenic acid

epi-HMA – 3-epihydroxymugenic acid

ESI – electrospray ionization

EST – expressed sequence tag

Fe – iron

FeII – ferrous iron

FeIII – ferric Fe

GFP – green fluorescent protein

GUS – β-glucuronidase

HEPES – N-(2-hydroxyethyl)-piperazine-2'-(2-ethanesulfonic acid)

IEF – isoelectric focusing

IPG - immobilized pH gradient

IPTG – isopropylthio-β-galactoside

LiAc – lithium acetate

MA – mugineic acid

MALDI-TOF – matrix-assisted laser desorption ionization time-of-flight

MBB – Metal Binding buffer

mRNA – messenger RNA

MS – mass spectrometry

MS/MS – tandem mass spectrometry

m/z – mass-to-charge ratio

N – nitrogen

NA – nicotianamine

8. Abbreviations

NBT – nitroblue tetrazolium chloride

OD – optical density

PEG – polyethyleneglycol

Pi – inorganic phosphate

pI – isoelectric point

ppm – parts per million

PS – phytosiderophore

RGU – relative grayscale units

RP – reversed phase

RT-PCR – reverse transcriptase-PCR

SD – standard deviation

SDS – sodium dodecyl sulfate

ssDNA – single-stranded DNA

SSP – sample spot number

TCA – trichloroacetic acid

T-DNA – transferred DNA

TFA – trifluoroacetic acid

TM – transmembrane domain

Vh – volt6hours

WT – wild type

9. References

Alba R, Fei Z, Payton P, Liu Y, Moore SL, Debbie P, Cohn J, D'Ascenzo M, Gordon JS, Rose JK, Martin G, Tanksley SD, Bouzayen M, Jahn MM, Giovannoni J (2004) ESTs, cDNA microarrays, and gene expression profiling: tools for dissecting plant physiology and development. Plant J **39:** 697-714

Altschul, Stephen F, Madden T, Schaeffer A, Zhang J, Zhang Z, Miller W, Lipman D (1997) Gapped BLAST and PSI-BLAST: a new generation of protein database search programs. Nucleic Acids Res **25:** 3389-3402

Amme S, Rutten T, Melzer M, Sonsmann G, Vissers JP, Schlesier B, Mock HP (2005) A proteome approach defines protective functions of tobacco leaf trichomes. Proteomics **5:** 2508-2518

Bailey-Serres J (1999) Selective translation of cytoplasmic mRNAs in plants. Trends Plant Sci **4:** 142-148

Bauer P, Bereczky Z, Brumbarova T, Klatte M, Wang HY (2004a) Molecular regulation of iron uptake in the dicot species *Lycopersicon esculentum* and *Arabidopsis thaliana*. Soil Sci Plant Nutr **50:** 997-1001

Bauer P, Thiel T, Klatte M, Bereczky Z, Brumbarova T, Hell R, Grosse I (2004b) Analysis of sequence, map position, and gene expression reveals conserved essential genes for iron uptake in *Arabidopsis* and tomato. Plant Physiol **136:** 4169-4183

Beinert H, Kennedy MC, Stout CD (1996) Aconitase as Iron-Sulfur Protein, Enzyme, and Iron-Regulatory Protein. Chem Rev **96:** 2335-2374

Benfey PN, Weigel D (2001) Transcriptional networks controlling plant development. Plant Physiol **125:** 109-111

Bereczky Z, Wang HY, Schubert V, Ganal M, Bauer P (2003) Differential regulation of *nramp* and *irt* metal transporter genes in wild type and iron uptake mutants of tomato. J Biol Chem **278:** 24697-24704

Bienfait HF (1985) Regulated redox processes at the plasmalemma of plant root cells and their function in iron uptake. J Bioenerg Biomembr **17:** 73-83

Bienfait HF (1988) Proteins under the control of the gene for Fe efficiency in tomato. Plant Physiol **88:** 785-787

Bienfait HF, van den Briel W, Mesland-Mul NT (1985) Free Space Iron Pools in Roots: Generation and Mobilization. Plant Physiol **78:** 596-600

Boyd J, Oza MN, Murphy JR (1990) Molecular cloning and DNA sequence analysis of a diphtheria tox iron-dependent regulatory element (dtxR) from Corynebacterium diphtheriae. Proc Natl Acad Sci U S A **87:** 5968-5972

Bracha-Drori K, Shichrur K, Katz A, Oliva M, Angelovici R, Yalovsky S, Ohad N (2004) Detection of protein-protein interactions in plants using bimolecular fluorescence complementation. Plant J **40:** 419-427

Briat JF, Fobis-Loisy I, Grignon N, Lobréaux S, Pascal N, Savino G, Thoiron S, Von Wiren N, Wuytswinkel OV (1995) Cellular and molecular aspects of iron metabolism in plants. Biol Cell **84:** 69-81

9. References

Briat JF, Lobreaux S (1997) Iron transport and storage in plants. Trends Plant Sci **2:** 187-193

Brown JC, Ambler JE (1974) Iron-stress response in tomato (*Lycopersicon esculentum*). 1. Sites of Fe reduction, absorption and transport. Physiol Plant **31:** 221-224

Brown JC, Chaney RL, Ambler JE (1971) A New Tomato Mutant Inefficient in the Transport of Iron. Physiol Plant **25:** 48-53

Brüggemann W, Maas-Kantel K, Moog PR (1993) Iron uptake by leaf mesophyll cells: The role of the plasma membrane-bound ferric-chelate reductase. Planta **190:** 151 - 155

Buckhout TJ, Bell PF, Luster DG, Chaney RL (1989) Iron-stress induced redox activity in tomato (*Lycopersicon esculentum* Mill.) is localized on the plasma membrane. Plant Physiol **90:** 151-156

Burger AM, Seth AK (2004) The ubiquitin-mediated protein degradation pathway in cancer: therapeutic implications. Eur J Cancer **40:** 2217-2229

Byrne ME, Simorowski J, Martienssen RA (2002) ASYMMETRIC LEAVES1 reveals knox gene redundancy in Arabidopsis. Development **129:** 1957-1965

Callis J, Vierstra RD (2000) Protein degradation in signaling. Curr Opin Plant Biol **3:** 381-386

Canovas FM, Dumas-Gaudot E, Recorbet G, Jorrin J, Mock HP, Rossignol M (2004) Plant proteome analysis. Proteomics **4:** 285-298

Casas C, Aldea M, Espinet C, Gallego C, Gil R, Herrero E (1997) The AFT1 transcriptional factor is differentially required for expression of high-affinity iron uptake genes in *Saccharomyces cerevisiae*. Yeast **13:** 621-637

Chaney RL, Brown JC, Tiffin LO (1972) Obligatory reduction of ferric chelates in iron uptake by soybeans. Plant Physiol **50:** 208-213

Chen Y (1997) Remedy of iron deficiency - present and future. 9th International Symposium on Iron Nutrition and Interactions in Plants**:** p 51

Clemens S, Palmgren MG, Kramer U (2002) A long way ahead: understanding and engineering plant metal accumulation. Trends Plant Sci **7:** 309-315

Cockman ME, Masson N, Mole DR, Jaakkola P, Chang GW, Clifford SC, Maher ER, Pugh CW, Ratcliffe PJ, Maxwell PH (2000) Hypoxia inducible factor-alpha binding and ubiquitylation by the von Hippel-Lindau tumor suppressor protein. J Biol Chem **275:** 25733-25741

Cohen CK, Fox TC, Garvin DF, Kochian LV (1998) The role of iron-deficiency stress responses in stimulating heavy-metal transport in plants. Plant Physiol **116:** 1063-1072

Colangelo EP, Guerinot ML (2004) The essential basic helix-loop-helix protein FIT1 is required for the iron deficiency response. Plant Cell **16:** 3400-3412

Colangelo EP, Guerinot ML (2006) Put the metal to the petal: metal uptake and transport throughout plants. Curr Opin Plant Biol **9:** 322-330

Connolly EL, Campbell NH, Grotz N, Prichard CL, Guerinot ML (2003) Overexpression of the FRO2 ferric chelate reductase confers tolerance to growth on low iron and uncovers posttranscriptional control. Plant Physiol **133:** 1102-1110

9. References

Connolly EL, Fett JP, Guerinot ML (2002) Expression of the IRT1 metal transporter is controlled by metals at the levels of transcript and protein accumulation. Plant Cell **14:** 1347-1357

Curie C, Alonso JM, Le Jean M, Ecker JR, Briat JF (2000) Involvement of NRAMP1 from *Arabidopsis thaliana* in iron transport. Biochem J **347 Pt 3:** 749-755

Curie C, Panaviene Z, Loulergue C, Dellaporta SL, Briat JF, Walker EL (2001) Maize *yellow stripe1* encodes a membrane protein directly involved in Fe(III) uptake. Nature **409:** 346-349

de Napoles M, Mermoud JE, Wakao R, Tang YA, Endoh M, Appanah R, Nesterova TB, Silva J, Otte AP, Vidal M, Koseki H, Brockdorff N (2004) Polycomb group proteins Ring1A/B link ubiquitylation of histone H2A to heritable gene silencing and X inactivation. Dev Cell **7:** 663-676

De Vos CR, Lubberding HJ, Bienfait HF (1986) Rhizosphere acidification as a response to iron deficiency in bean plants. Plant Physiol **81:** 842–846

Delhaize E (1996) A metal-accumulator mutant of *Arabidopsis thaliana*. Plant Physiol **111:** 849-855

Dell'Orto M, Santi S, De Nisi P, Cesco S, Varanini Z, Zocchi G, Pinton R (2000) Development of Fe-deficiency responses in cucumber (*Cucumis sativus* L.) roots: involvement of plasma membrane $H^{(+)}$-ATPase activity. J Exp Bot **51:** 695–701

Deshaies RJ (1999) SCF and Cullin/Ring H2-based ubiquitin ligases. Annu Rev Cell Dev Biol **15:** 435-467

DiDonato RJ, Jr., Roberts LA, Sanderson T, Eisley RB, Walker EL (2004) *Arabidopsis Yellow Stripe-Like2* (*YSL2*): a metal-regulated gene encoding a plasma membrane transporter of nicotianamine-metal complexes. Plant J **39:** 403-414

Downes B, Vierstra RD (2005) Post-translational regulation in plants employing a diverse set of polypeptide tags. Biochem Soc Trans **33:** 393-399

Durrett T, Gassmann W, Rogers E (2006) Functional characterization of FRD3, a novel organic acid effluxer involved in iron homeostasis. *In* 13th international symposium on iron nutrition and interactions in plants, Montpellier, France

Eckhardt U, Mas Marques A, Buckhout TJ (2001) Two iron-regulated cation transporters from tomato complement metal uptake-deficient yeast mutants. Plant Mol Biol **45:** 437-448

Eide D, Broderius M, Fett J, Guerinot ML (1996) A novel iron-regulated metal transporter from plants identified by functional expression in yeast. Proc Natl Acad Sci U S A **93:** 5624-5628

Eide DJ (1998) The molecular biology of metal ion transport in *Saccharomyces cerevisiae*. Annu Rev Nutr **18:** 441-469

Eng BH, Guerinot ML, Eide D, Saier MH, Jr. (1998) Sequence analyses and phylogenetic characterization of the ZIP family of metal ion transport proteins. J Membr Biol **166:** 1-7

Escobar C, Aristizabal, F., Navas, A., Del Campo, F.F., and Fenoll, C. (2001) Plant Mol. Biol. Reporter **19:** 375a-375h

Espen L, Dell'Orto M, De Nisi P, Zocchi G (2000) Metabolic responses in cucumber (*Cucumis sativus* L.) roots under Fe-deficiency: a ^{31}P-nuclear magnetic resonance in-vivo study. Planta **210:** 985–992

9. References

Figueroa C, Taylor J, Vojtek AB (2001) Prenylated Rab acceptor protein is a receptor for prenylated small GTPases. J Biol Chem **276:** 28219-28225

Fox TC, Guerinot ML (1998) Molecular Biology of Cation Transport in Plants. Annu Rev Plant Physiol Plant Mol Biol **49:** 669-696

Frary A, Nesbitt TC, Grandillo S, Knaap E, Cong B, Liu J, Meller J, Elber R, Alpert KB, Tanksley SD (2000) *fw2.2*: a quantitative trait locus key to the evolution of tomato fruit size. Science **289:** 85-88

Gietz D, St Jean A, Woods RA, Schiestl RH (1992) Improved method for high efficiency transformation of intact yeast cells. Nucleic Acids Res **20:** 1425

Gitan RS, Eide DJ (2000) Zinc-regulated ubiquitin conjugation signals endocytosis of the yeast ZRT1 zinc transporter. Biochem J **346 Pt 2:** 329-336

Gitan RS, Luo H, Rodgers J, Broderius M, Eide D (1998) Zinc-induced inactivation of the yeast ZRT1 zinc transporter occurs through endocytosis and vacuolar degradation. J Biol Chem **273:** 28617-28624

Graves PR, Haystead TA (2002) Molecular biologist's guide to proteomics. Microbiol Mol Biol Rev **66:** 39-63; table of contents

Gray WM, del Pozo JC, Walker L, Hobbie L, Risseeuw E, Banks T, Crosby WL, Yang M, Ma H, Estelle M (1999) Identification of an SCF ubiquitin-ligase complex required for auxin response in *Arabidopsis thaliana*. Genes Dev **13:** 1678-1691

Gray WM, Kepinski S, Rouse D, Leyser O, Estelle M (2001) Auxin regulates SCF^{TIR1}-dependent degradation of AUX/IAA proteins. Nature **414:** 271-276

Green LS, Rogers EE (2004) FRD3 controls iron localization in *Arabidopsis*. Plant Physiol **136:** 2523-2531

Grotewold E, Sainz MB, Tagliani L, Hernandez JM, Bowen B, Chandler VL (2000) Identification of the residues in the Myb domain of maize C1 that specify the interaction with the bHLH cofactor R. Proc Natl Acad Sci U S A **97:** 13579-13584

Grusak MA, Pezeshgi S (1996) Shoot-to-Root Signal Transmission Regulates Root Fe(III) Reductase Activity in the *dgl* Mutant of Pea. Plant Physiol **110:** 329-334

Grusak MA, Welch RM, Kochian LV (1990) Physiological characterization of a single-gene mutant of Pisum sativum exhibiting excess iron accumulation: I. Root iron reduction and iron uptake. Plant Physiol **93:** 976-981

Guerinot ML (2000) The ZIP family of metal transporters. Biochim Biophys Acta **1465:** 190-198

Guerinot ML, Yi Y (1994) Iron: Nutritious, Noxious, and Not Readily Available. Plant Physiol **104:** 815-820

Gunshin H, Mackenzie B, Berger UV, Gunshin Y, Romero MF, Boron WF, Nussberger S, Gollan JL, Hediger MA (1997) Cloning and characterization of a mammalian proton-coupled metal-ion transporter. Nature **388:** 482-488

Guo B, Phillips JD, Yu Y, Leibold EA (1995) Iron regulates the intracellular degradation of iron regulatory protein 2 by the proteasome. J Biol Chem **270:** 21645-21651

Guo HS, Xie Q, Fei JF, Chua NH (2005) MicroRNA directs mRNA cleavage of the transcription factor *NAC1* to downregulate auxin signals for arabidopsis lateral root development. Plant Cell **17:** 1376-1386

9. References

Gupta AK, Kaur N (2005) Sugar signalling and gene expression in relation to carbohydrate metabolism under abiotic stresses in plants. J Biosci **30:** 761–776

Hantke K (1981) Regulation of ferric iron transport in *Escherichia coli* K12: isolation of a constitutive mutant. Mol Gen Genet **182:** 288-292

Hantke K (2001) Iron and metal regulation in bacteria. Curr Opin Microbiol **4:** 172-177

Harper JW, Adami GR, Wei N, Keyomarsi K, Elledge SJ (1993) The p21 Cdk-interacting protein Cip1 is a potent inhibitor of G1 cyclin-dependent kinases. Cell **75:** 805-816

Harrison PM, Arosio P (1996) The ferritins: molecular properties, iron storage function and cellular regulation. Biochim Biophys Acta **1275:** 161-203

Hatakeyama S, Nakayama KI (2003) Ubiquitylation as a quality control system for intracellular proteins. J Biochem (Tokyo) **134:** 1-8

Hatakeyama S, Yada M, Matsumoto M, Ishida N, Nakayama KI (2001) U box proteins as a new family of ubiquitin-protein ligases. J Biol Chem **276:** 33111-33120

Heim MA, Jakoby M, Werber M, Martin C, Weisshaar B, Bailey PC (2003) The basic helix-loop-helix transcription factor family in plants: a genome-wide study of protein structure and functional diversity. Mol Biol Evol **20:** 735-747

Heintzen C, Nater M, Apel K, Staiger D (1997) AtGRP7, a nuclear RNA-binding protein as a component of a circadian-regulated negative feedback loop in Arabidopsis thaliana. Proc Natl Acad Sci U S A **94:** 8515-8520

Hell R, Stephan UW (2003) Iron uptake, trafficking and homeostasis in plants. Planta **216:** 541-551

Henriques R, Jasik J, Klein M, Martinoia E, Feller U, Schell J, Pais MS, Koncz C (2002) Knock-out of *Arabidopsis* metal transporter gene IRT1 results in iron deficiency accompanied by cell differentiation defects. Plant Mol Biol **50:** 587-597

Hentze MW, Kühn LC (1996) Molecular control of vertebrate iron metabolism: mRNA-based regulatory circuits operated by iron, nitric oxide, and oxidative stress. Proc Natl Acad Sci U S A **93:** 8175-8182

Hentze MW, Muckenthaler MU, Andrews NC (2004) Balancing acts: molecular control of mammalian iron metabolism. Cell **117:** 285-297

Herbik A, Giritch A, Horstmann C, Becker R, Balzer HJ, Bäumlein H, Stephan UW (1996) Iron and copper nutrition-dependent changes in protein expression in a tomato wild type and the nicotianamine-free mutant chloronerva. Plant Physiol **111:** 533-540

Hobo T, Kowyama Y, Hattori T (1999) A bZIP factor, TRAB1, interacts with VP1 and mediates abscisic acid-induced transcription. Proc Natl Acad Sci U S A **96:** 15348-15353

Hofius D, Hajirezaei MR, Geiger M, Tschiersch H, Melzer M, Sonnewald U (2004) RNAi-mediated tocopherol deficiency impairs photoassimilate export in transgenic potato plants. Plant Physiol **135:** 1256-1268

Houben A, Wako T, Furushima-Shimogawara R, Presting G, Kunzel G, Schubert II, Fukui K (1999) Short communication: the cell cycle dependent phosphorylation of histone H3 is correlated with the condensation of plant mitotic chromosomes. Plant J **18:** 675-679

9. References

Iliopoulos O, Levy AP, Jiang C, Kaelin WG, Jr., Goldberg MA (1996) Negative regulation of hypoxia-inducible genes by the von Hippel-Lindau protein. Proc Natl Acad Sci U S A **93:** 10595-10599

Itai RN, Nakanishi H, Inoue H, Ogo Y, Kobayashi T, Takahashi M, Mori S, Nishizawa NK (2004) Isolation of the Fe deficiency inducible gene encoding a basic leucine zipper protein. *In* 12th international symposium on iron nutrition and interactions in plants, Tokyo, Japan

Iwakawa H, Ueno Y, Semiarti E, Onouchi H, Kojima S, Tsukaya H, Hasebe M, Soma T, Ikezaki M, Machida C, Machida Y (2002) The ASYMMETRIC LEAVES2 gene of Arabidopsis thaliana, required for formation of a symmetric flat leaf lamina, encodes a member of a novel family of proteins characterized by cysteine repeats and a leucine zipper. Plant Cell Physiol **43:** 467-478

Jakoby M, Wang HY, Reidt W, Weisshaar B, Bauer P (2004) *FRU* (*BHLH029*) is required for induction of iron mobilization genes in *Arabidopsis thaliana*. FEBS Lett **577:** 528-534

James P, Halladay J, Craig EA (1996) Genomic libraries and a host strain designed for highly efficient two-hybrid selection in yeast. Genetics **144:** 1425-1436

Jolley VD, Brown JC, Davies TD, Walser RH (1986) Increased iron efficiency in soybeans (Glycine max) through plant breeding related to increased response to iron deficiency stress. I. Iron stress response. J Plant Nutr **9:** 373-386

Kanazawa K, Higuchi K, Nishizawa NK, Fushiya S, Mitsuo C, Mori S (1994) Nicotianamine aminotransferase activities are correlated to the phytosiderophore secretions under Fe-deficient conditions in Gramineae. J Exp Bot **45:** 1903-1906

Kanazawa K, Higuchi K, Nishizawa NK, Fushiya S, Mori S (1995) Detection of two distinct isozymes of nicotianamine aminotransferases in Fe-deficient barley roots. J Exp Bot **46:** 1241-1244

Kang DK, Jeong J, Drake SK, Wehr NB, Rouault TA, Levine RL (2003) Iron regulatory protein 2 as iron sensor. Iron-dependent oxidative modification of cysteine. J Biol Chem **278:** 14857-14864

Kazan K (2003) Alternative splicing and proteome diversity in plants: the tip of the iceberg has just emerged. Trends Plant Sci **8:** 468-471

Kepinski S, Leyser O (2002) Ubiquitination and auxin signaling: a degrading story. Plant Cell **14 Suppl:** S81-95

Klausner RD, Rouault TA, Harford JB (1993) Regulating the fate of mRNA: the control of cellular iron metabolism. Cell **72:** 19-28

Kneen BE, LaRue TA, Welch RM, Weeden NF (1990) Pleiotropic effects of brz: A mutation ir Pisum sativum (L.) cv 'sparkle' conditioning decreased modulation and increased iron uptake and leaf necrosis. Plant Physiol **93:** 717-722

Kobayashi T, Nakayama Y, Itai RN, Nakanishi H, Yoshihara T, Mori S, Nishizawa NK (2003) Identification of novel cis-acting elements, IDE1 and IDE2, of the barley IDS2 gene promoter conferring iron-deficiency-inducible, root-specific expression in heterogeneous tobacco plants. Plant J **36:** 780-793

Korshunova YO, Eide D, Clark WG, Guerinot ML, Pakrasi HB (1999) The IRT1 protein from *Arabidopsis thaliana* is a metal transporter with a broad substrate range. Plant Mol Biol **40:** 37-44

9. References

Kotak S, Port M, Ganguli A, Bicker F, von Koskull-Doring P (2004) Characterization of C-terminal domains of Arabidopsis heat stress transcription factors (Hsfs) and identification of a new signature combination of plant class A Hsfs with AHA and NES motifs essential for activator function and intracellular localization. Plant J **39:** 98-112

Krueger C, Berkowitz O, Stephan UW, Hell R (2002) A Metal-binding Member of the Late Embryogenesis Abundant Protein Family Transports Iron in the Phloem of *Ricinus communis* L. J Biol Chem **277:** 25062-25069

Kumagai MH, Donson J, della-Cioppa G, Harvey D, Hanley K, Grill LK (1995) Cytoplasmic inhibition of carotenoid biosynthesis with virus-derived RNA. Proc Natl Acad Sci U S A **92:** 1679-1683

Lafuse WP, Alvarez GR, Zwilling BS (2000) Regulation of Nramp1 mRNA stability by oxidants and protein kinase C in RAW264.7 macrophages expressing Nramp1(Gly169). Biochem J **351 Pt 3:** 687-696

Lanquar V, Lelievre F, Bolte S, Hames C, Alcon C, Neumann D, Vansuyt G, Curie C, Schroder A, Kramer U, Barbier-Brygoo H, Thomine S (2005) Mobilization of vacuolar iron by AtNRAMP3 and AtNRAMP4 is essential for seed germination on low iron. Embo J **24:** 4041-4051

Le Jean M, Schikora A, Mari S, Briat JF, Curie C (2005) A loss-of-function mutation in *AtYSL1* reveals its role in iron and nicotianamine seed loading. Plant J **44:** 769-782

Lemon B, Tjian R (2000) Orchestrated response: a symphony of transcription factors for gene control. Genes Dev **14:** 2551-2569

Li L, Cheng X, Ling HQ (2004) Isolation and characterization of Fe(III)-chelate reductase gene *LeFRO1* in tomato. Plant Mol Biol **54:** 125-136

Lidder P, Gutierrez RA, Salome PA, McClung CR, Green PJ (2005) Circadian control of messenger RNA stability. Association with a sequence-specific messenger RNA decay pathway. Plant Physiol **138:** 2374-2385

Lindbo JA, Silva-Rosales L, Proebsting WM, Dougherty WG (1993) Induction of a Highly Specific Antiviral State in Transgenic Plants: Implications for Regulation of Gene Expression and Virus Resistance. Plant Cell **5:** 1749-1759

Ling HQ, Bauer P, Bereczky Z, Keller B, Ganal M (2002) The tomato *fer* gene encoding a bHLH protein controls iron-uptake responses in roots. Proc Natl Acad Sci U S A **99:** 13938-13943

Ling HQ, Koch G, Baumlein H, Ganal MW (1999) Map-based cloning of *chloronerva*, a gene involved in iron uptake of higher plants encoding nicotianamine synthase. Proc Natl Acad Sci U S A **96:** 7098-7103

Ling HQ, Pich A, Scholz G, Ganal MW (1996) Genetic analysis of two tomato mutants affected in the regulation of iron metabolism. Mol Gen Genet **252:** 87-92

Litwin CM, Calderwood SB (1993) Role of iron in regulation of virulence genes. Clin Microbiol Rev **6:** 137-149

Lopez-Millan AF, Morales F, Abadia A, Abadia J (2000) Effects of iron deficiency on the composition of the leaf apoplastic fluid and xylem sap in sugar beet. Implications for iron and carbon transport. Plant Physiol **124:** 873-884

9. References

Maas FM, van de Wetering DAM, van Beusichem ML, Bienfait HF (1988) Characterization of Phloem Iron and Its Possible Role in the Regulation of Fe-Efficiency Reactions. Plant Physiol **87:** 167-171

Machold O (1968) Einfluss der Ernaehrungsbedingungen auf den Zustand des Eisens in den Blaettern, den Chlorophyllgehalt und die Katalase-, sowie Peroxidaseaktivitaet. Flora **159:** 1–25

Magee AI, Seabra MC (2003) Are prenyl groups on proteins sticky fingers or greasy handles? Biochem J **376:** e3-4

Mallory AC, Bartel DP, Bartel B (2005) MicroRNA-directed regulation of Arabidopsis *AUXIN RESPONSE FACTOR17* is essential for proper development and modulates expression of early auxin response genes. Plant Cell **17:** 1360-1375

Marschner H, Römheld V (1994) Strategies of plants for acquisition of iron. Plant Soil **165:** 375-388

Maser P, Thomine S, Schroeder JI, Ward JM, Hirschi K, Sze H, Talke IN, Amtmann A, Maathuis FJ, Sanders D, Harper JF, Tchieu J, Gribskov M, Persans MW, Salt DE, Kim SA, Guerinot ML (2001) Phylogenetic relationships within cation transporter families of Arabidopsis. Plant Physiol **126:** 1646-1667

McKie AT, Marciani P, Rolfs A, Brennan K, Wehr K, Barrow D, Miret S, Bomford A, Peters TJ, Farzaneh F, Hediger MA, Hentze MW, Simpson RJ (2000) A novel duodenal iron-regulated transporter, IREG1, implicated in the basolateral transfer of iron to the circulation. Mol Cell **5:** 299-309

Meyron-Holtz EG, Ghosh MC, Iwai K, LaVaute T, Brazzolotto X, Berger UV, Land W, Ollivierre-Wilson H, Grinberg A, Love P, Rouault TA (2004a) Genetic ablations of iron regulatory proteins 1 and 2 reveal why iron regulatory protein 2 dominates iron homeostasis. Embo J **23:** 386-395

Meyron-Holtz EG, Ghosh MC, Rouault TA (2004b) Mammalian tissue oxygen levels modulate iron-regulatory protein activities in vivo. Science **306:** 2087-2090

Miller RO, Olsen RA (1986) Changes in the roots of sunflower under iron stress. J Plant Nutr **9:** 815-822

Moghaieb RE, Saneoka H, Fujita K (2004) Shoot regeneration from GUS-transformed tomato (Lycopersicon esculentum) hairy root. Cell Mol Biol Lett **9:** 439-449

Mukherjee I, Campbell NH, Ash JS, Connolly EL (2006) Expression profiling of the Arabidopsis ferric chelate reductase (*FRO*) gene family reveals differential regulation by iron and copper. Planta **223:** 1178-1190

Murre C, Bain G, van Dijk MA, Engel I, Furnari BA, Massari ME, Matthews JR, Quong MW, Rivera RR, Stuiver MH (1994) Structure and function of helix-loop-helix proteins. Biochim Biophys Acta **1218:** 129-135

Nakamura S, Lynch TJ, Finkelstein RR (2001) Physical interactions between ABA response loci of Arabidopsis. Plant J **26:** 627-635

Nakanishi H, Okumura N, Umehara Y, Nishizawa NK, Chino M, Mori S (1993) Expression of a gene specific for iron deficiency (Ids3) in the roots of Hordeum vulgare. Plant Cell Physiol **34:** 401-410

Nakanishi H, Yamaguchi H, Sasakuma T, Nishizawa NK, Mori S (2000) Two dioxygenase genes, Ids3 and Ids2, from *Hordeum vulgare* are involved in the

9. References

       biosynthesis of mugineic acid family phytosiderophores. Plant Mol Biol **44:** 199-207

Neilands JB (1981) Iron absorption and transport in microorganisms. Annu Rev Nutr **1:** 27-46

Ogo Y, Itai RN, Nakanishi H, Inoue H, Kobayashi T, Suzuki M, Takahashi M, Mori S, Nishizawa NK (2006) Isolation and characterization of IRO2, a novel iron-regulated bHLH transcription factor in graminaceous plants. *In* 13th international symposium on iron nutrition and interactions in plants, Montpellier, France

Ohata T, Mihashi S, Nishizawa NK, Fushiya S, Nozoe S, Chino M, Mori S (1993) Biosynthetic pathway of phytosiderophores in iron-deficient gramineous plants. Soil Sci Plant Nutr **39:** 745-749

Okumura N, Nishizawa NK, Umehara Y, Ohata T, Nakanishi H, Yamaguchi T, Chino M, Mori S (1994) A dioxygenase gene (*Ids2*) expressed under iron deficiency conditions in the roots of *Hordeum vulgare*. Plant Mol Biol **25:** 705-719

Passmore LA, Barford D (2004) Getting into position: the catalytic mechanisms of protein ubiquitylation. Biochem J **379:** 513-525

Pelletier B, Beaudoin J, Mukai Y, Labbe S (2002) Fep1, an iron sensor regulating iron transporter gene expression in *Schizosaccharomyces pombe*. J Biol Chem **277:** 22950-22958

Pelletier B, Beaudoin J, Philpott CC, Labbe S (2003) Fep1 represses expression of the fission yeast *Schizosaccharomyces pombe* siderophore-iron transport system. Nucleic Acids Res **31:** 4332-4344

Peng J, Richards DE, Hartley NM, Murphy GP, Devos KM, Flintham JE, Beales J, Fish LJ, Worland AJ, Pelica F, Sudhakar D, Christou P, Snape JW, Gale MD, Harberd NP (1999) 'Green revolution' genes encode mutant gibberellin response modulators. Nature **400:** 256-261

Petit JM, van Wuytswinkel O, Briat JF, Lobreaux S (2001) Characterization of an iron-dependent regulatory sequence involved in the transcriptional control of AtFer1 and ZmFer1 plant ferritin genes by iron. J Biol Chem **276:** 5584-5590

Pich A, Manteuffel R, Hillmer S, Scholz G, Schmidt W (2001) Fe homeostasis in plant cells: does nicotianamine play multiple roles in the regulation of cytoplasmic Fe concentration? Planta **213:** 967-976

Pich A, Scholz G (1996) Translocation of copper and other micronutrients in tomato plants (*Lycopersicon esculentum* Mill.): nicotianamine-stimulated copper transport in the xylem. J Exp Bot **47:** 41-47

Price J, Laxmi A, Martin SK, Jang JC (2004) Global transcription profiling reveals multiple sugar signal transduction mechanisms in *Arabidopsis*. Plant Cell **16:** 2128–2150

Puig S, Askeland E, Thiele DJ (2005) Coordinated remodeling of cellular metabolism during iron deficiency through targeted mRNA degradation. Cell **120:** 99-110

Ratledge C, Dover LG (2000) Iron metabolism in pathogenic bacteria. Annu Rev Microbiol **54:** 881-941

Reidt W, Wohlfarth T, Ellerstrom M, Czihal A, Tewes A, Ezcurra I, Rask L, Baumlein H (2000) Gene regulation during late embryogenesis: the RY motif of

9. References

maturation-specific gene promoters is a direct target of the FUS3 gene product. Plant J **21:** 401-408

Riechmann JL, Heard J, Martin G, Reuber L, Jiang C, Keddie J, Adam L, Pineda O, Ratcliffe OJ, Samaha RR, Creelman R, Pilgrim M, Broun P, Zhang JZ, Ghandehari D, Sherman BK, Yu G (2000) Arabidopsis transcription factors: genome-wide comparative analysis among eukaryotes. Science **290:** 2105-2110

Roberts LA, Pierson AJ, Panaviene Z, Walker EL (2004) Yellow stripe1. Expanded roles for the maize iron-phytosiderophore transporter. Plant Physiol **135:** 112-120

Robinson NJ, Procter CM, Connolly EL, Guerinot ML (1999) A ferric-chelate reductase for iron uptake from soils. Nature **397:** 694-697

Rogers EE, Eide DJ, Guerinot ML (2000) Altered selectivity in an *Arabidopsis* metal transporter. Proc Natl Acad Sci U S A **97:** 12356-12360

Rogers EE, Guerinot ML (2002) FRD3, a member of the multidrug and toxin efflux family, controls iron deficiency responses in *Arabidopsis*. Plant Cell **14:** 1787-1799

Römheld V (1987) Different strategies for iron acquisition in higher plants. Physiol Plant **70:** 231-234

Römheld V, Marschner H (1983) Mechanisms of iron uptake by peanut plant. I. Fe^{III} reduction, chelate splitting, and release of phenolics. Plant Physiol **71:** 949-954

Römheld V, Marschner H (1986) Evidence for a specific uptake system for iron phytosiderophore in roots of grasses. Plant Physiol **80:** 175-180

Rouault T, Klausner R (1997) Regulation of iron metabolism in eukaryotes. Curr Top Cell Regul **35:** 1-19

Ruegger M, Dewey E, Gray WM, Hobbie L, Turner J, Estelle M (1998) The TIR1 protein of *Arabidopsis* functions in auxin response and is related to human SKP2 and yeast grr1p. Genes Dev **12:** 198-207

Sambrook J, Fritsch EF, Maniatis T (1989) Molecular cloning. A laboratory manual, Ed 2. Cold Spring Harbor Laboratory Press

Savolainen V, Chase MW, Hoot SB, Morton CM, Soltis DE, Bayer C, Fay MF, de Bruijn AY, Sullivan S, Qiu YL (2000) Phylogenetics of flowering plants based on combined analysis of plastid atpB and rbcL gene sequences. Syst Biol **49:** 306-362

Schaaf G, Honsbein A, Meda AR, Kirchner S, Wipf D, von Wiren N (2006) *AtIREG2* encodes a tonoplast transport protein involved in iron-dependent nickel detoxification in *Arabidopsis thaliana* roots. J Biol Chem

Schaaf G, Ludewig U, Erenoglu BE, Mori S, Kitahara T, von Wiren N (2004) ZmYS1 functions as a proton-coupled symporter for phytosiderophore- and nicotianamine-chelated metals. J Biol Chem **279:** 9091-9096

Schaaf G, Schikora A, Haberle J, Vert G, Ludewig U, Briat JF, Curie C, von Wiren N (2005) A putative function for the arabidopsis Fe-Phytosiderophore transporter homolog AtYSL2 in Fe and Zn homeostasis. Plant Cell Physiol **46:** 762-774

Schlesier B, Mock HP (2004) Protein Isolation and 2-D Electrophoretic Separation. *In* J Salinas, ed, Arabidopsis protocols,

Schlesier B, Mock HP (2006) Protein isolation and second-dimension electrophoretic separation. Methods Mol Biol **323:** 381-391

9. References

Schmidt W (1999) Mechanisms and regulation of reduction-based iron uptake in plants. New Phytol **141:** 1-26

Schmidt W, Boomgaarden B, Ahrens V (1996) Reduction of root iron in Plantago lanceolata during recovery from Fe deficiency. Physiol Plant **98:** 587-593

Schmitt MP, Holmes RK (1991) Iron-dependent regulation of diphtheria toxin and siderophore expression by the cloned Corynebacterium diphtheriae repressor gene dtxR in C. diphtheriae C7 strains. Infect Immun **59:** 1899-1904

Schneider BD, Leibold EA (2000) Regulation of mammalian iron homeostasis. Curr Opin Clin Nutr Metab Care **3:** 267-273

Schofield CJ, Ratcliffe PJ (2004) Oxygen sensing by HIF hydroxylases. Nat Rev Mol Cell Biol **5:** 343-354

Scholz G, Becker R, Pich A, Stephan UW (1992) Nicotianamine - A common constituent of Strategies I and II of iron acquisition in plants. Rev J Plant Nutr **15:** 1649-1665

Schurr U (1999) Dynamics of nutrient transport from the root to the shoot. Prog Bot **60:** 234-253

Scrimshaw NS (1991) Iron deficiency. Sci Am **265:** 46-52

Sevilla F, del Rio LA, Hellin E (1984) Superoxide dismutases from a citrus plant: presence of two iron-containing isoenzymes in leaves of lemon trees (*Citrus limonum* L.). J Plant Physiol **116:** 381–387

Shi H, Xiong L, Stevenson B, Lu T, Zhu JK (2002) The *Arabidopsis salt overly sensitive 4* mutants uncover a critical role for vitamin B6 in plant salt tolerance. Plant Cell **14:** 575-588

Shojima S, Nishizawa NK, Fushiya S, Nozoe S, Irifune T, Mori S (1990) Biosynthetic pathway of phytosiderophores in iron-deficient gramineous plants. Plant Physiol **93:** 1497-1503

Smith LG, Greene B, Veit B, Hake S (1992) A dominant mutation in the maize homeobox gene, Knotted-1, causes its ectopic expression in leaf cells with altered fates. Development **116:** 21-30

Sorin C, Bussell JD, Camus I, Ljung K, Kowalczyk M, Geiss G, McKhann H, Garcion C, Vaucheret H, Sandberg G, Bellini C (2005) Auxin and light control of adventitious rooting in Arabidopsis require ARGONAUTE1. Plant Cell **17:** 1343-1359

Stephan UW, Grün M (1989) Physiological disorders of the nicotianamine auxotroph tomato mutant chloronerva at different levels of iron nutrition. II. Iron deficiency response and heavy metal metabolism. Biochem Physiol Pflanzen **185:** 189-200

Stephan UW, Prochazka Z (1989) Physiological disorders of the nicotianamine-auxotroph tomato mutant *chloronerva* at different levels of iron nutrition. I. Growth characteristics and physiological abnormalities related to iron and nicotianamine supply. Acta Bot Neerl **38:** 147-153

Stephan UW, Schmidke I, Pich A (1994) Phloem translocation of Fe, Cu, Mn, and Zn in *Ricinus* seedlings in relation to the concentrations of nicotianamine, an endogenous chelator of divalent metal ions, in different seedling parts. Plant Soil **165:** 181 - 188

9. References

Stephan UW, Schmidke I, Stephan VW, Scholz G (1996) The nicotianamine molecule is made-to-measure for complexation of metal micronutrients in plants. Biometals **9:** 84 - 90

Stephan UW, Scholz G (1993) Nicotianamine: mediator of transport of iron and heavy metals in the phloem? Physiol Plant **88:** 522-529

Stringer KF, Ingles CJ, Greenblatt J (1990) Direct and selective binding of an acidic transcriptional activation domain to the TATA-box factor TFIID. Nature **345:** 783-786

Sussman MR (1994) Molecular analysis of proteins in the plant plasma membrane. Ann Rev Plant Physiol Plant Mol Biol **45:** 211-234

Sussman MR (1999) Pumping iron. Nat Biotech **17:** 230-231

Suzuki K, Itai R, Suzuki K, Nakanishi H, Nishizawa NK, Yoshimura E, Mori S (1998) Formate Dehydrogenase, an Enzyme of Anaerobic Metabolism, Is Induced by Iron Deficiency in Barley Roots. Plant Physiol **116:** 725-732

Takagi S (1976) Naturally occuring iron-chelating compounds in oat- and rice-root washing. I. Soil Sci Plant Nutr **22:** 423-433

Takagi S (1993) Production of phytosiderophores. *In* L Barton, B Hemming, eds, Iron chelation in plants and soil microorganisms. Academic, pp 111-131

Takahashi M, Terada Y, Nakai I, Nakanishi H, Yoshimura E, Mori S, Nishizawa NK (2003) Role of nicotianamine in the intracellular delivery of metals and plant reproductive development. Plant Cell **15:** 1263-1280

Tautz D (2000) Evolution of transcriptional regulation. Curr Opin Genet Dev **10:** 575-579

Thimm O, Essigmann B, Kloska S, Altmann T, Buckhout TJ (2001) Response of Arabidopsis to iron deficiency stress as revealed by microarray analysis. Plant Physiol **127:** 1030-1043

Thomine S, Lelievre F, Debarbieux E, Schroeder JI, Barbier-Brygoo H (2003) AtNRAMP3, a multispecific vacuolar metal transporter involved in plant responses to iron deficiency. Plant J **34:** 685-695

Thomine S, Wang R, Ward JM, Crawford NM, Schroeder JI (2000) Cadmium and iron transport by members of a plant metal transporter family in *Arabidopsis* with homology to *Nramp* genes. Proc Natl Acad Sci U S A **97:** 4991-4996

Tiffin LO (1966) Iron Translocation I. Plant Culture, Exudate Sampling, Iron-Citrate Analysis. Plant Physiol **41:** 510-514

Toledo-Ortiz G, Huq E, Quail PH (2003) The Arabidopsis basic/helix-loop-helix transcription factor family. Plant Cell **15:** 1749-1770

Triezenberg SJ, Kingsbury RC, McKnight SL (1988) Functional dissection of VP16, the trans-activator of herpes simplex virus immediate early gene expression. Genes Dev **2:** 718-729

van de Donk NW, Lokhorst HM, Nijhuis EH, Kamphuis MM, Bloem AC (2005) Geranylgeranylated proteins are involved in the regulation of myeloma cell growth. Clin Cancer Res **11:** 429-439

Varotto C, Maiwald D, Pesaresi P, Jahns P, Salamini F, Leister D (2002) The metal ion transporter IRT1 is necessary for iron homeostasis and efficient photosynthesis in *Arabidopsis thaliana*. Plant J **31:** 589-599

9. References

Vaucheret H, Beclin C, Fagard M (2001) Post-transcriptional gene silencing in plants. J Cell Sci **114:** 3083-3091

Vert G, Briat JF, Curie C (2001) *Arabidopsis* IRT2 gene encodes a root-periphery iron transporter. Plant J **26:** 181-189

Vert G, Grotz N, Dedaldechamp F, Gaymard F, Guerinot ML, Briat JF, Curie C (2002) IRT1, an *Arabidopsis* transporter essential for iron uptake from the soil and for plant growth. Plant Cell **14:** 1223-1233

Vert GA, Briat JF, Curie C (2003) Dual regulation of the Arabidopsis high-affinity root iron uptake system by local and long-distance signals. Plant Physiol **132:** 796-804

Von Wiren N (2004) Progress in research on iron nutrition and interactions in plants. Soil Sci Plant Nutr **50:** 955-964

von Wiren N, Klair S, Bansal S, Briat JF, Khodr H, Shioiri T, Leigh RA, Hider RC (1999) Nicotianamine chelates both FeIII and FeII. Implications for metal transport in plants. Plant Physiol **119:** 1107-1114

Von Wiren N, Mori S, Marschner H, Romheld V (1994) Iron Inefficiency in Maize Mutant *ys1* (*Zea mays* L. cv Yellow-Stripe) Is Caused by a Defect in Uptake of Iron Phytosiderophores. Plant Physiol **106:** 71-77

Voronova A, Baltimore D (1990) Mutations that disrupt DNA binding and dimer formation in the E47 helix-loop-helix protein map to distinct domains. Proc Natl Acad Sci U S A **87:** 4722-4726

Wang GL, Jiang BH, Rue EA, Semenza GL (1995) Hypoxia-inducible factor 1 is a basic-helix-loop-helix-PAS heterodimer regulated by cellular O2 tension. Proc Natl Acad Sci U S A **92:** 5510-5514

Wang GL, Semenza GL (1995) Purification and characterization of hypoxia-inducible factor 1. J Biol Chem **270:** 1230-1237

Wang RL, Stec A, Hey J, Lukens L, Doebley J (1999) The limits of selection during maize domestication. Nature **398:** 236-239

Wang YH, Garvin DF, Kochian LV (2002) Rapid induction of regulatory and transporter genes in response to phosphorus, potassium, and iron deficiencies in tomato roots. Evidence for cross talk and root/rhizosphere-mediated signals. Plant Physiol **130:** 1361-1370

Waters BM, Blevins DG, Eide DJ (2002) Characterization of FRO1, a pea ferric-chelate reductase involved in root iron acquisition. Plant Physiol **129:** 85-94

Welch RM, Kochian LV (1992) Regulation of iron accumulation in food crops: studies using single gene pea mutants. *In* DD Bills, S-D Kung, eds, Biotechnology and Nutrition. Butterworth-Heinemann, Boston, MA, pp 325-344

White MC, Baker FD, Chaney RL, Decker AM (1981) Metal complexation in xylem fluid. II. Theoretical equilibrium model and computational computer program. Plant Physiol **67:** 301-310

Wilusz CJ, Wilusz J (2004) Bringing the role of mRNA decay in the control of gene expression into focus. Trends Genet **20:** 491-497

Wu H, Li L, Du J, Yuan Y, Cheng X, Ling HQ (2005) Molecular and biochemical characterization of the Fe(III) chelate reductase gene family in *Arabidopsis thaliana*. Plant Cell Physiol **46:** 1505-1514

Yamaguchi-Iwai Y, Dancis A, Klausner RD (1995) AFT1: a mediator of iron regulated transcriptional control in *Saccharomyces cerevisiae*. Embo J **14:** 1231-1239

9. References

Yamaguchi-Iwai Y, Stearman R, Dancis A, Klausner RD (1996) Iron-regulated DNA binding by the AFT1 protein controls the iron regulon in yeast. Embo J **15:** 3377-3384

Yamaguchi-Iwai Y, Ueta R, Fukunaka A, Sasaki R (2002) Subcellular localization of Aft1 transcription factor responds to iron status in *Saccharomyces cerevisiae*. J Biol Chem **277:** 18914-18918

Yamanaka K, Ishikawa H, Megumi Y, Tokunaga F, Kanie M, Rouault TA, Morishima I, Minato N, Ishimori K, Iwai K (2003) Identification of the ubiquitin-protein ligase that recognizes oxidized IRP2. Nat Cell Biol **5:** 336-340

Yen MR, Tseng YH, Saier MH, Jr. (2001) Maize Yellow Stripe1, an iron-phytosiderophore uptake transporter, is a member of the oligopeptide transporter (OPT) family. Microbiology **147:** 2881-2883

Yi Y, Guerinot ML (1996) Genetic evidence that induction of root Fe(III) chelate reductase activity is necessary for iron uptake under iron deficiency. Plant J **10:** 835-844

Yuan YX, Zhang J, Wang DW, Ling HQ (2005) AtbHLH29 of Arabidopsis thaliana is a functional ortholog of tomato FER involved in controlling iron acquisition in strategy I plants. Cell Res **15:** 613-621

Zhao H, Eide D (1996) The yeast ZRT1 gene encodes the zinc transporter protein of a high-affinity uptake system induced by zinc limitation. Proc Natl Acad Sci U S A **93:** 2454-2458

10. Appendix

Appendix A

SSP	Protein	NCBI	SwissProt	TIGR_LeEST	Functional Cat.
0005	ni				ni
0006	similar to AF295775S2 ral guanine nucleotide dissociation stimulator [H. sapiens], partial (9%)			TC153570	signal transduction
0008	RSI-1 protein precursor [Le]		P47926		root morphology
0302	ni				ni
0303	late embryogenesis like protein [Prunus armeniaca] (100% probability)	gi I 3264769		TC138013	abiotic stress
0502	ni				ni
0601	similar to UP|O81340 26S proteasome regulatory subunit S5A, partial (90%)	gi I 3202042		TC149782	protein degradation
0705	ni				ni
0706	similar to AY070475 AT3g04610/F7O18_9 [At] putative RNA-binding protein, partial (54%)			TC138171	regulation
0803	similar to UP|Q9FF55 Protein disulphide isomerase-like protein (At5g60640), partial (80%)			TC149519	protein folding & stability
1106	putative chloroplast inorganic pyrophosphatase [Os] gi 46805453	gi I 46805453		TC142544	energy metabolism
1202	Ran binding protein-1 [Le]	gi	14091665			nuclear transport
1203	1. histone deacetylase [S. chacoense]	gi I 33667906		TC136749	chromatin remodelling
	2. low temperature induced cysteine proteinase precursor [Le] (Fragment)	gi I 5917765	CYSPL_LYCES		protein degradation
1204	auxin-responsive protein IAA6 [At]		Q38824		hormone response
1209	ni				ni
1302	ubiquitin-specific protease 6 [At]	gi	11993465		TC137019	protein degradation
1303	similar to TIGR_Ath1|At5g03300.1 adenosine kinase 2 (ADK2), partial (98%)			TC137019	signal transduction
1501	similar to UP|Q93YR3 HSP associated protein like, partial (80%)			TC137767	protein folding & stability
1502	vacuolar H ATPase B subunit [Nt] (100% probability)	gi	6715512		TC142318	energy metabolism
1503	alpha-tubulin [Nt]	gi	17402471			structural protein
1604	DS2 protein [S. tuberosum]	gi	23095773		TC149088	abiotic stress
1606	protein disulfide isomerase [Ipomoea batatas] (100% probability)	gi	47933777		TC136590	protein folding & stability
1607	DS2 protein [S. tuberosum] (100% probability)	gi	23095773		TC149088	abiotic stress
1608	metacaspase 1 [Le]	gi	23343885			cell death
1702	similar to TIGR_Ath1|At5g19320.1 RAN GTPase activating protein 2 (RanGAP2), partial (51%)			TC148679	nuclear transport
1710	phytochrome kinase substrate 1 [At]		Q9SWI1		signal transduction
1807	At5g43420, zinc finger (C3HC4-type RING finger) family protein	gi	30725342			regulation
1808	weakly similar to TIGR_Ath1|At4g39690.1 expressed protein , partial (50%)			TC142936	unknown
2001	putative mitochondrial ATP synthase [S. demissum]	gi	48209968			energy metabolism
2003	thioredoxin peroxidase 1 [Le]	gi	30841938			oxidative stress
2102	1. low temperature induced cysteine proteinase precursor tomato fragment, thiol protease (20.8%	JA0159	CYSPL_LYCES		protein degradation
	2. DREPP2 protein Nicotiana tabacum (50% probability)	gi	7801129		TC142756	unknown
2201	1. COG1123 ATPase components of various ABC type transport systems contain duplicated	gi I 45520931			unknown
	ATPase [Methylobacillus flagellatus]				/
	2. 60S acidic ribosomal protein P0 [Zm]	gi	1550814			protein synthesis
2304	glutamine synthetase GS58 [N. attenuata] (100% probability)	gi	40457328		TC137243	nitrogen metabolism
2401	alpha-tubulin [Nt]	gi	17402471			structural protein
2402	homologue to UP|Q84UV7 SGT1, complete			TC143027	protein degradation
2405	SET domain protein putative [Plasmodium berghei]	gi I 56497407		TC137402	chromatin remodelling
2407	actin 51 [Le]	gi	3219772			structural protein
2603	nitrite reductase [Capsicum annuum] (100% probability)	gi	3152717		TC142802	nitrogen metabolism
2701	heat shock protein cognate 70 [Le]	gi	19258			protein folding & stability
2702	glucose-regulated protein 78 [Le]	gi	170386			protein folding & stability
2704	heat shock protein cognate 70 [Le]	gi	19258			protein folding & stability
2709	vacuolar H+ATPase A1 subunit isoform [Le]	gi	27883932			energy metabolism
3002	similar to UP|GRP2_NICSY (P27484) Glycine-rich protein 2, partial (66%)			TC147731	abiotic stress
3003	Similar to Glycine-rich protein 2 [N. sylvestris]			TC147731	abiotic stress
3004	TSI 1 protein [Le]	gi I 2887310		TC148096	biotic stress
3005	citrate lyase synthetase [Le]		CITC_LEUMC		metabolism
3008	eukaryotic translation initiation factor 5A-4 [Le]	gi	12407793			protein synthesis
3009	eukaryotic translation initiation factor 5A-2 [Le]	gi	12407789			protein synthesis
3010	ni				ni
3105	remorin 1 [Le]	gi	4731573			unknown
3204	putative lactoylglutathione lyase [At] (50% probability)	gi	15810219		TC148187	carbohydrate metabolism
3301	succinyl CoA ligase beta subunit [Le]	gi	27803873			energy metabolism
3302	actin 51 [Le]	gi	3219772			structural protein
3304	1. hypothetical protein CBG20549 [Caenorhabditis briggsae]	gi	39581078		TC143310	unknown
	2. similar to UP|Q8GT65 (Q8GT65) Serpin-like protein (Fragment), partial (34%)			TC136954	protein degradation
3305	stem cambial region actin protein [Eucommia ulmoides]	gi	55820068			structural protein
3308	glutamine synthetase GS1 [S. tuberosum] (100% probability)	gi	11761907		TC136294	nitrogen metabolism
3401	putative RNA-binding protein 45 [At]	gi	30682335		TC136953	regulation
3402	S-adenosylmethionine synthase 2 [Le]	gi	429106			amino acid metabolism
3501	xylose isomerase [At]	gi I 62319619		TC136577	carbohydrate metabolism
3508	ni				ni

10. Appendix

SSP	Protein	NCBI	SwissProt	TIGR_LeEST	Functional Cat.
4101	carbonic anhydrase [Le]	gi | 56562175			carbohydrate metabolism
4102	ascorbate peroxidase [Le]	gi | 6066418			oxidative stress
4103	ascorbate peroxidase [Le]	gi | 21039134			oxidative stress
4104	ascorbate peroxidase [Le]	gi | 6066418			oxidative stress
4204	unknown protein [Os]	gi | 50933415			unkown
4303	ascorbate free radical reductase [Le]	gi | 832876			oxidative stress
4304	UDP-glucose:protein transglucosylase-like protein SlUPTG1 [Le]	gi | 48478827			metabolism
4305	probable cinnamyl alcohol dehydrogenase [Le]	S72477			metabolism
4307	mitochondrial malate dehydrogenase [Le]	gi | 52139816			energy metabolism
4308	ni				ni
4407	G/HBF-1 [Glycine max]	gi | 1905785			regulation
4408	S-adenosylmethionine synthase 3 [Le]	P43282			amino acid metabolism
4505	cytochrome c reductase-processing peptidase subunit II [potatoes]	gi | 410634			protein degradation
4506	enolase [Le]	gi | 19281			energy metabolism
4513	S-adenosyl-L-methionine synthetase 3 [Le]	gi | 429108			amino acid metabolism
4611	26S proteasome AAA-ATPase subunit RPT2a [At]	gi | 6652880			protein degradation
5002	glutathione S transferase class phi [S. commersonii] gi 7434067	gi | 2290782		TC142134	metabolism
5003	homologue to UP|SODM_NICPL (P11796) Superoxide dismutase [Mn], mitochondrial precursor , complete			TC148838	oxidative stress
5101	ascorbate peroxidase [Le]	gi | 62526498			oxidative stress
5201	cytosolic malate dehydrogenase [Triticum aestivum]	gi | 37928995		TC142327	metabolism
5301	1. probable cynnamyl-alcohol dehydrogenase [Le]	S72477		TC137923	metabolism
	2. phosphoglycerate kinase PGK [Nt] gi 7434547 pir T03661 (100% probability)	gi | 1161602	PGKY_TOBAC	TC136272	signal transduction
5302	1. probable cynnamyl-alcohol dehydrogenase [Le]	S72477		TC137923	metabolism
	2. phosphoglycerate kinase PGK [Nt] gi 7434547 pir T03661 (100% probability)	gi | 1161602	PGKY_TOBAC	TC136272	signal transduction
5306	glucan endo-1,3-beta-glucosidase A precursor [Le]		Q01412		biotic stress
5401	S-adenosyl-L-methionine synthetase [Le]	gi | 429108			amino acid metabolism
5405	similar to UP|O22523 DNA-binding protein GBP16, partial (58%)			TC148531	regulation
5410	2-oxoglutarate-dependent dioxygenase [Le]	gi | 66730858			metabolism
5501	UDP-glucose pyrophosphorylase [S. tuberosum]	gi | 1388021			carbohydrate metabolism
5504	enolase [Le]	gi | 1161573			energy metabolism
5506	subtilisin-like protease [Le]	gi | 6723681			protein degradation
5605	DnaJ protein homolog DNAJ 1 (100% probability)		DNJH_CUCSA	BG642987	protein folding & stability
5701	transketolase 1 [Capsicum annuum] gi 7433617, chloroplast (100% probability)	gi | 3559814		TC143726	metabolism
5804	aconitase [L. penellii]	gi | 30407706		TC136898	energy metabolism
6005	ni				ni
6101	1PRCI [Nt]	gi | 4539545			protein degradation
6103	ni				ni
6104	ni				ni
6107	ni				ni
6108	Osmotin like protein OSML13 precursor PA13 (34.2% probability)		OS13_SOLCO		stress response
6201	glyceraldehyde 3-phosphate dehydrogenase [Le]	gi | 2078298			metabolism
6202	glyceraldehyde 3-phosphate dehydrogenase [Le]	gi | 2078298			metabolism
6205	weakly similar to TIGR_Ath1|At3g14750.1expressed protein Septation ring formation regulator (O34894)			TC148752	unknown
	[Bacillus subtilis], partial (47%)				/
6301	NADP-dependent isocitrate dehydrogenase-like protein [Le]	gi | 3687404			energy metabolism
6304	pyruvate dehydrogenase [Le]	gi | 12003246			energy metabolism
6307	UDP-D-glucuronat carboxy-lyase [Ps]	gi | 13591616			metabolism
6401	alcohol dehydrogenase [Le]	gi | 623249			metabolism
6402	S-adenosyl-L-methionine synthetase [Le]	gi | 429108			amino acid metabolism
6406	nuclear RNA binding protein B [Spinacia oleracea]	gi | 6492268		TC137225	regulation
6407	isocytrate dehydrogenase (NADP+) [Nt]	gi | 1617198			energy metabolism
6506	polyphenol oxidase precursor [Le]	gi | 22725	PPOA_LYCES	TC136351	amino acid metabolism
6507	DnaJ like protein [Le] (100% probability)	gi | 6782421		BG642987	protein folding & stability
6508	dihydrolipoamide dehydrogenase precursor [Le]	gi | 372802			metabolism
6603	ferredoxin-nitrite reductase [Nt]	gi | 861065			nitrogen metabolism
7010	ni				ni
7011	Osmotin like protein OSML13 precursor PA13 (34.2% probability)		OS13_SOLCO		stress response
7101	chitinase [Le]	gi | 19191			biotic stress
7102	putative vacuolar proton ATPase subunit E [Le]	gi | 9652289			energy metabolism
7110	putative adenilate kinase [S. tuberosum]	gi | 14599412			signal transduction
7111	Proteasome subunit alpha type 7 EC 3 4 25 1, 20S proteasome alpha subunit D (100% probability)	gi | 2315211	PSA7_LYCES	TC143445	protein degradation
7113	Osmotin like protein OSML13 precursor PA13 (34.2% probability)		OS13_SOLCO		stress response
7115	ni				ni

10. Appendix

SSP	Protein	NCBI	SwissProt	TIGR_LeEST	Functional Cat.
7201	putative plastidic aldolase [Os] gi 14090214	gi I 34895322		TC136285	metabolism
7203	ni				ni
7301	formate dehydrogenase [Le]	gi	56562181			metabolism
7403	ni				ni
7404	citrate synthase [Nt] (100% probability)	gi I 1556429	CISY_ARATH	TC149617	energy metabolism
7501	similar to UP|O23254 Serine hydroxymethyltransferase (Glycine hydroxymethyltransferase), complete			TC136258	amino acid metabolism
7502	similar to PIR|B86367 protein F26F24.16 [A. thaliana], partial (97%)			TC137392	amino acid metabolism
7503	hydroxymethyltransferase [At] gi 2244749	gi I 7268097		TC136258	amino acid metabolism
7509	catalase 2 [Le]	gi	5257185			oxidative stress
7603	catalase isozyme 1 [Le] gi 170398	CAT1_LYCES		TC136551	oxidative stress
7604	catalase [S. tuberosum]	gi	57339044			oxidative stress
7707	subtilisin like protease [Le] (100% probability)	gi I 6723683		TC137552	protein degradation
7711	subtilisin like protease [Le] (100% probability)	gi I 6723683		TC137552	protein degradation
7801	similar to TIGR_Ath1|At1g26110.1 expressed protein , partial (23%)			TC149809	unknown
8001	probable germin protein [Le] gi 2979494	T04361		TC144812	stress response
8003	putative beta5 proteasome subunit [Nt] (100% probability)	gi I 14594931		TC143384	protein degradation
8005	rotamase (cyclophilin) (cyclosporin A-binding protein) [Le]	CYPH_LYCES		TC147993	protein folding & stability
8010	probable germine protein [Le]	gi I 7447345			stress response
8102	homologue to PRF|1302305A.0|225412|1302305A chitinase [Nicotiana sp.] , partial (96%)			TC136491	biotic stress
8107	germin like protein [S. tuberosum] gi 7447341 pir T07004 (50.5% probability)	gi I 3171251		TC138076	stress response
8108	germin like protein [S. tuberosum] gi 7447341 pir T07004 (50.5% probability)	gi I 3171251		TC138076	stress response
8203	Ferredoxin NADP reductase root type isozyme chloroplast precursor FNR [Nt] gi 2190038	FENR2_TOBAC	O04397	TC142862	energy metabolism
8204	Similar to Peroxidase [Nt]			TC136771	oxidative stress
8205	similar to UP|Q07445 Peroxidase precursor , partial (64%)			TC137953	oxidative stress
8212	Similar to Peroxidase [Nt]			TC136771	oxidative stress
8303	peroxidase [Le]	gi I 678547		TC142656	oxidative stress
8309	fructose-1,6-bisphosphate aldolase [Le]	gi I 927505		TC136283	metabolism
8401	nuclear RNA binding protein B [Spinacia oleracea] (15.3% probability)	gi I 6492268		TC137225	regulation
8403	1. nuclear RNA binding protein B [Spinacia oleracea] (15.3% probability)	gi I 6492268		TC137225	regulation
	2. Ethylene insensitive protein 2 EIN 2 AtEIN2 Cytokinin resistant protein AtCKR1 (100% probability)		EIN2_ARATH		hormone response
8405	peroxidase [Le]	gi I 678547		TC142656	oxidative stress
8407	Fructose bisphosphate aldolase cytoplasmic isozyme EC 4 1 2 13 (17% probability)		ALF_MAIZE	TC146083	metabolism
8409	26S proteasome AAA-ATPase subunit RPT4a [S. tuberosum]	gi	24745880			protein degradation
8502	phospho-2-dehydro-3-deoxyheptonate aldolase [Le]	gi	410488			metabolism
8503	phospho-2-dehydro-3-deoxyheptonate aldolase [Le]	gi	410488			metabolism
9001	rotamase (cyclophilin) (cyclosporin A-binding protein) [Le]	gi	118103			protein folding & stability

10. Appendix

Appendix B

0.1 µM FeNaEDTA

A	B	C	D	E	F	G
1202	0601	2402	2701	0005	0705	1106
1607	0803	3304	2704	1203	1209	1502
3402	1501	3305	5410	1204	1303	1604
3508	1503	4304	5701	1302	2001	2405
4204	1710	5101		2201	3004	2702
5002	1807	6304		3005	3008	3010
5003	2401	7101		4305	3009	6108
5306	2407	7110		4308	3401	6307
6107	3003	7203		5405	4408	7115
6401	3501	8001		5605	4611	7201
6406	4303			6104	5302	7403
7010	4506			6507	6005	7502
7111	5201			7102	6103	7801
8403	5506			7113	6402	8107
	6201			7301	6506	8108
	6202			8003	7011	8203
	6304			8102	7404	8204
	7707			8303	7503	8205
	8005			8409		8212
				8502		8309
				8503		8401
						8407
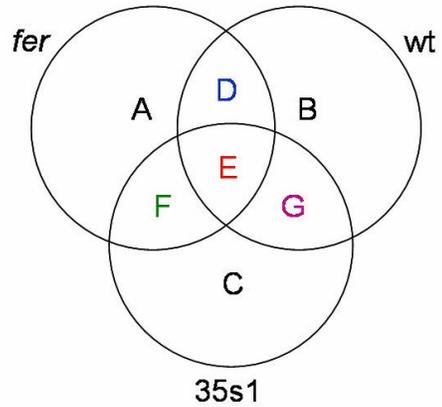
10 µM FeNaEDTA

A	B	C	D	E	F	G
1302	0803	0705	6301	0006	1209	0008
3204	1202	1608	6304	1503	4407	1606
4204	1501	2402		4307	7111	2304
5003	2102	3008		6603	7604	5410
5401	3003	3301		7011	8502	7502
5701	3308	3302		8001		
6506	6104	3308				
7102	7403	4101				
7115	7707	4513				
7503	7711	6103				
8102		6402				
8204		6507				
8205		7101				
8303		7203				

8309		7301			
8407		7404			
8409		7509			
		9001			

100 μM FeNaEDTA

A	B	C	D	E	F	G
0302	1202	1808	2402	0006	0601	0008
0303	1209	3301		2102	0803	1608
1106	3105	4307		2304	1501	2003
2709	4103	4506		4101	1503	3308
3204	5003	7501		4104	2401	5804
3305	6005			7509	3302	8010
4304	6103			7603	4102	8403
6108	6406			7604	5301	9001
6307	6603			7711	5401	
6407	7101					
7110	7111					
7403	7203					
8001						
8204						
8212						

10. Appendix

Appendix C
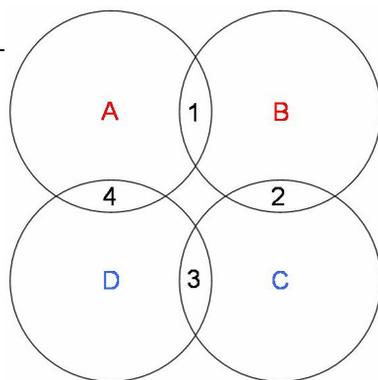
A: - Fe upregulated (WT)
B: *fer* mutant upregulated
C: - Fe downregulated (WT)
D: *fer* mutant downregulated

A		B		C	D	1 (A:B)	2 (B:C)	3 (C:D)	4 (D:A)
0005	6104	0006	7503	0006	0008	1203	0006	0008	0601
0601	6108	1203	7603	0008	0303	1204	1607	2304	1503
0803	6201	1204	7711	1202	0601	1302	1608	4102	2702
1106	6202	1302	7801	1209	0706	2201	6406	4104	4506
1203	6304	1607	8003	1607	1503	3005	7101	4307	5201
1204	6307	1608	8102	1608	1710	3010	7203	5804	6202
1302	6507	2201	8203	2003	2304	4308	7603	6603	6507
1501	7102	3004	8204	2102	2702	6108	7711	7509	8107
1502	7113	3005	8205	2304	3305	7113		7604	8108
1503	7115	3009	8303	2402	4102	7115		8010	
1604	7201	3010	8309	3105	4104	7301		9001	
1807	7301	3204	8407	3308	4307	7403			
2201	7403	3402	8502	4101	4407	7502			
2401	7502	3508	8503	4102	4506	7801			
2405	7707	4308		4103	5101	8003			
2407	7801	4408		4104	5201	8102			
2701	8003	5302		4307	5401	8203			
2702	8005	5306		5003	5804	8204			
2704	8102	5504		5804	6202	8205			
3003	8107	6108		6005	6402	8303			
3005	8108	6401		6103	6507	8309			
3010	8203	6406		6406	6603	8502			
3501	8204	6506		6603	7509	8503			
4303	8205	7010		7101	7604				
4305	8212	7011		7111	8010				
4308	8303	7101		7203	8107				
4506	8309	7113		7509	8108				
5201	8401	7115		7603	9001				
5405	8407	7203		7604					
5410	8409	7301		7711					
5506	8502	7403		8010					
5605	8503	7501		8403					
5701		7502		9001					

Appendix D

I.
a. 4611, 5405, 5410, 5605, 6507, 7102, 8409, 8503

b. 2102, 2304, 4101, 7509, 7603, 7711

II.
 8107, 8108

III.
a. 4407, 5201, 6402, 6603, 7509

b. 0008, 3308, 4307, 5804, 7604, 9001

c. 8010

IV.
 0601, 3305, 4102, 4104

V.
a. 2201, 7113, 7115, 8003, 8203, 8204, 8205, 8303, 8309, 8401, 8502

b. 1203, 4308

c. 1204, 3005, 3010, 7801, 8407

d. 0006

e. 5504, 7101, 7110, 7203, 7403, 7502

f. 1607, 3004, 3402, 5302, 6401, 7301, 8102
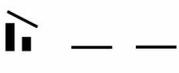
g. 3508, 4408, 5306, 7010

h. 1106, 6108, 8212

VI.
 2402

Acknowledgements

Last, but not least I want to thank my husband Rumen Ivanov for the endless help (especially with radioactivity), support and discussions, and to my family, and especially my father, Krassimir Brumbarov, for helping me to become what I am both as a scientist and as a person.

Curriculum Vitae

Name:	Tzvetina Brumbarova
Date and place of birth:	5 April 1979, Sofia, Bulgaria
Marial status:	Married
Nationality:	Bulgarian

Education:

Current position:	PhD student
7.10.2002-15.07.2006	Leibniz Institute of Plant Genetics and Crop Plant Research (IPK), Gatersleben, Germany (2002 – 2005)
	University of Saarland, Saarbruecken, Germany (2005 – 2006)
	Supervisor: Prof. Dr. Petra Bauer
	Thesis title: Functional Characterization of the bHLH Transcription Factor LeFER Essential for Upregulation of Iron Responses in Tomato Roots

Higher Education:

1997-2002	"St. Kliment Ohridski" University of Sofia, Bulgaria Faculty of Biology
	Master of Biology, Speciality **Molecular Biology**, Specialization **Biochemistry**

Masters Degree:

2002	St. Kliment Ohridski" University of Sofia, Bulgaria
	Master thesis: Leibniz Institute of Plant Genetics and Crop Plant Research (IPK), Gatersleben, Germany
	Supervisor: Prof. Dr. Petra Bauer
	Topic: Cloning and Expression of the *LeFER* Gene – Putative Regulator of Iron Homeostasis in Plants
	Defended: September 2002, with the maximal score of 6.00

Secondary Education:

1992-1997   "Akad. Liubomir Chakalov" National Secondary School for
                       Natural Sciences and Mathematics, Sofia, Bulgaria
                       Profile **Biology and Biotechnology with extensive**
                       English language study
                       Average grade award: Excellent (5.95)
                       (in a six scale awarding system, wherein the highest grade is
                       6.00 and the lowest positive – 3.00)

Practical Activities:

1999-2000   Faculty of Biology, University of Sofia, Bulgaria
                       Supervisor: Dr. Magdalena Chorbadjieva
                       Practical activity – **Laboratory of Enzymology**

July 2000-Sept 2000   Leibniz Institute of Plant Genetics and Crop Plant Research
                          (IPK), Gatersleben, Germany
                          Supervisor: Dr. habil. Helmut Baeumlein
                          Topic: Training on basic molecular genetics techniques

Fellowships:

1998, 1999, 2000, 2001   Fellowships from the Sofia University for excellent results
                             in education

Languages: Bulgarian, Russian, German, and English (Cambridge
                        Advanced Certificate, Grade A)

Publication List

Publications:

Petra Bauer, Thomas Thiel, Marco Klatte, Zsolt Bereczky, **Tzvetina Brumbarova**, Ruediger Hell, and Ivo Grosse (2004) Analysis of Sequence, Map Position, and Gene Expression Reveals Conserved Essential Genes for Iron Uptake in Arabidopsis and Tomato **Plant Physiol** (136) 4169-4183.

Petra Bauer, Zsolt Bereczky, **Tzvetina Brumbarova**, Marco Klatte, and Hong-Yu Wang (2004) Molecular Regulation of Iron Uptake in the Dicot Species *Lycopersicon esculentum* and *Arabidopsis thaliana* **Soil Sci Plant Nutr** 50 (7) 997-1001.

Tzvetina Brumbarova and Petra Bauer (2005) Iron-Mediated Control of the Basic Helix-Loop-Helix Protein FER, a Regulator of Iron Uptake in Tomato **Plant Physiol** (137) 1018-1026.

Tzvetina Brumbarova, Andrea Matros, Udo Seiffert, Hans-Peter Mock, and Petra Bauer; A Comprehensive Proteomics Study on the Effects of Iron Deficiency and FER Presence in Tomato Roots (Manuscript in Preparation).

Tzvetina Brumbarova and Petra Bauer (2006) Iron Uptake and Transport, *In* P K Jaiwal, ed, Plant Genetic Engineering (9): Plant Membrane and Vacuolar Transporters (Book in Preparation)

Personal Presentations at Meetings:

4th International Biometals Symposium, Sept 2004, Garmisch-Partenkirchen, Germany
Regulation of The Regulator: Role of FER in Root Iron Mobilization (Oral Presentation)
Tzvetina Brumbarova and Petra Bauer

13th International Symposium on Iron Nutrition and Interactions in Plants, July 2006, Montpellier, France

A Comprehensive Proteomics Study on the Effects of Iron Deficiency and FER Presence in Tomato Roots (Poster)

Tzvetina Brumbarova, Andrea Matros, Udo Seiffert, Hans-Peter Mock, and Petra Bauer

XV FESPB Congress "Plant, People, Ecosystems and Applications", July 2006, Lyon, France

A Comprehensive Proteomics Study on the Effects of Iron Deficiency and FER Presence in Tomato Roots (Poster)

Tzvetina Brumbarova, Andrea Matros, Udo Seiffert, Hans-Peter Mock, and Petra Bauer

Eidesstattliche Versicherung

Hiermit versichere ich an Eides statt, dass ich die vorliegende Arbeit selbständig und ohne Benutzung anderer als der angegebenen Hiflsmittel angefertigt habe. Die aus anderen Quellen oder indirekt übernommenen Daten und Konzepte sind unter Angabe der Quelle gekennzeichnet.

Die Arbeit wurde bisher weder im In- noch im Ausland in gleicher oder ähnlicher Form in einem Verfahren zur Erlangung eines akademischen Grades vorgelegt.

Tzvetina Brumbarova

Saarbruecken, August 2006